変形した原子核の構造・崩壊・反応

東北大学　　萩野浩一

hagino@nucl.phys.tohoku.ac.jp

www.nucl.phys.tohoku.ac.jp/~hagino

東北大学

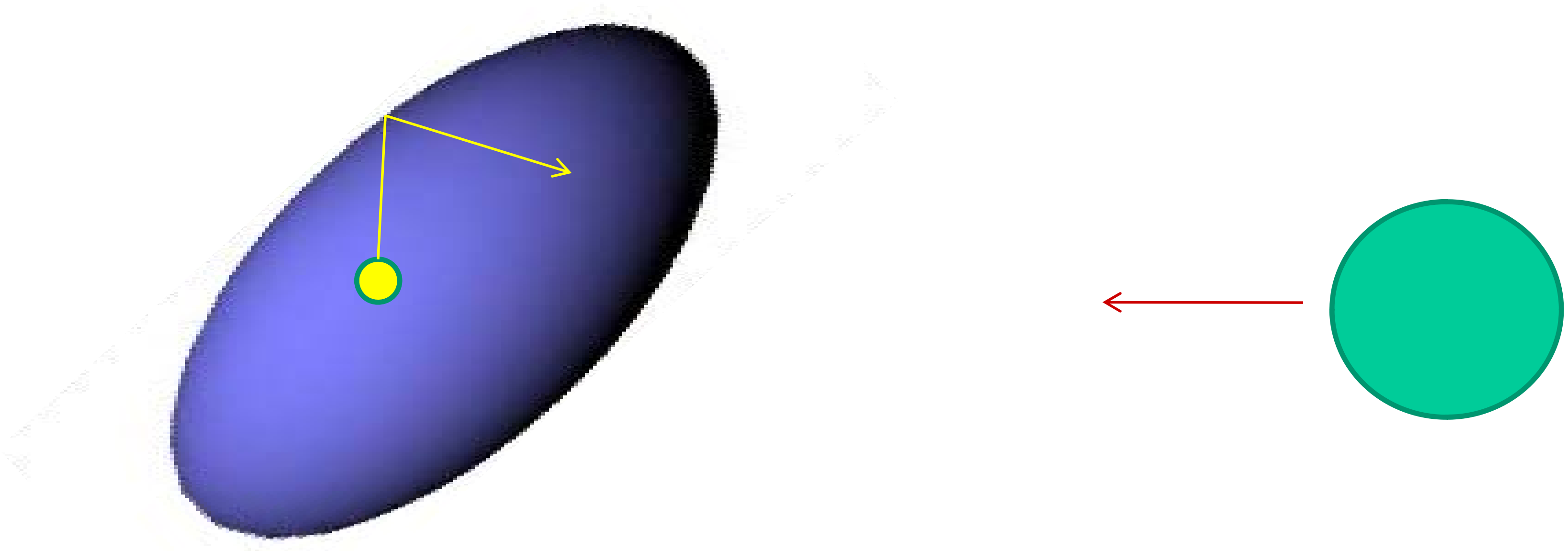

講義の内容（予定）

１．原子核の変形：液滴模型と殻補正
２．対称性の自発的破れ
３．平均場近似と変形核
４．回転運動と結合チャンネル法
５．変形した原子核の一粒子共鳴
６．変形核の陽子放出崩壊及びα崩壊
７．変形核の重イオン反応

原子核の変形:液滴模型と殻補正

原子核の束縛エネルギー

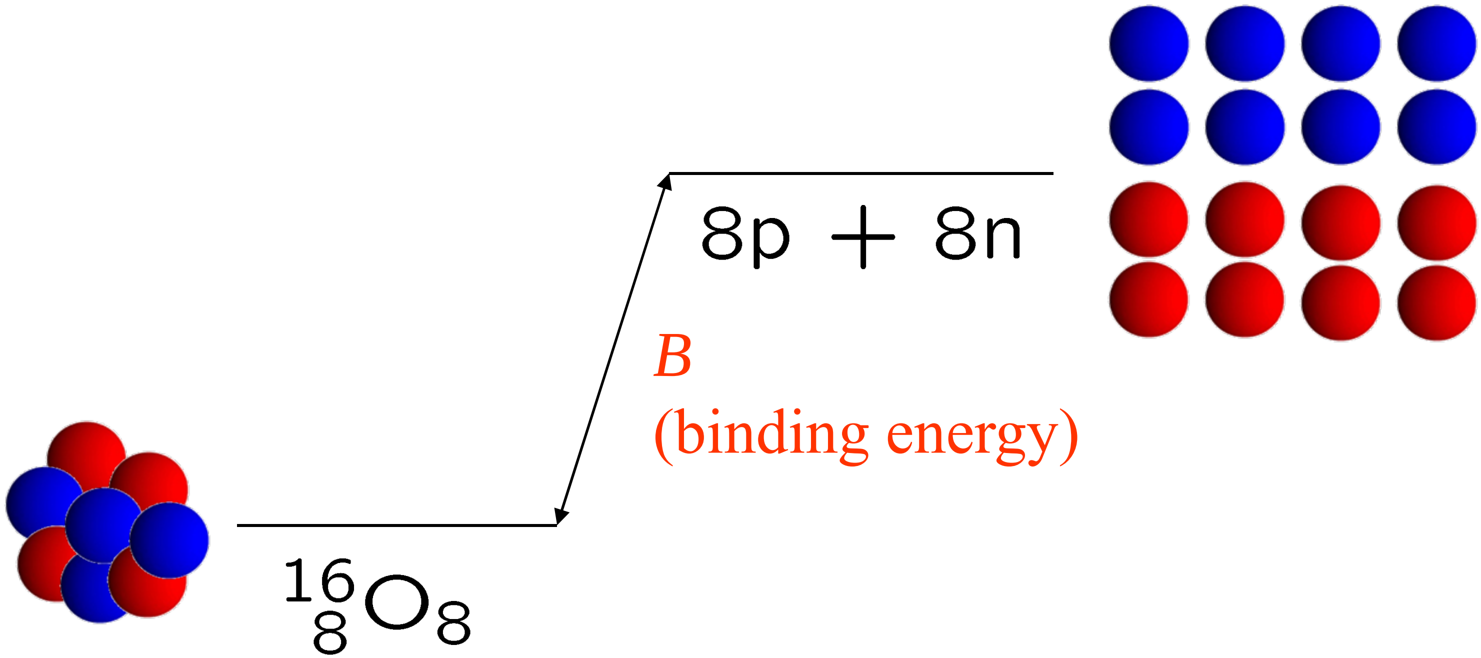

$$m(N,Z)c^2 = Zm_pc^2 + Nm_nc^2 - B$$

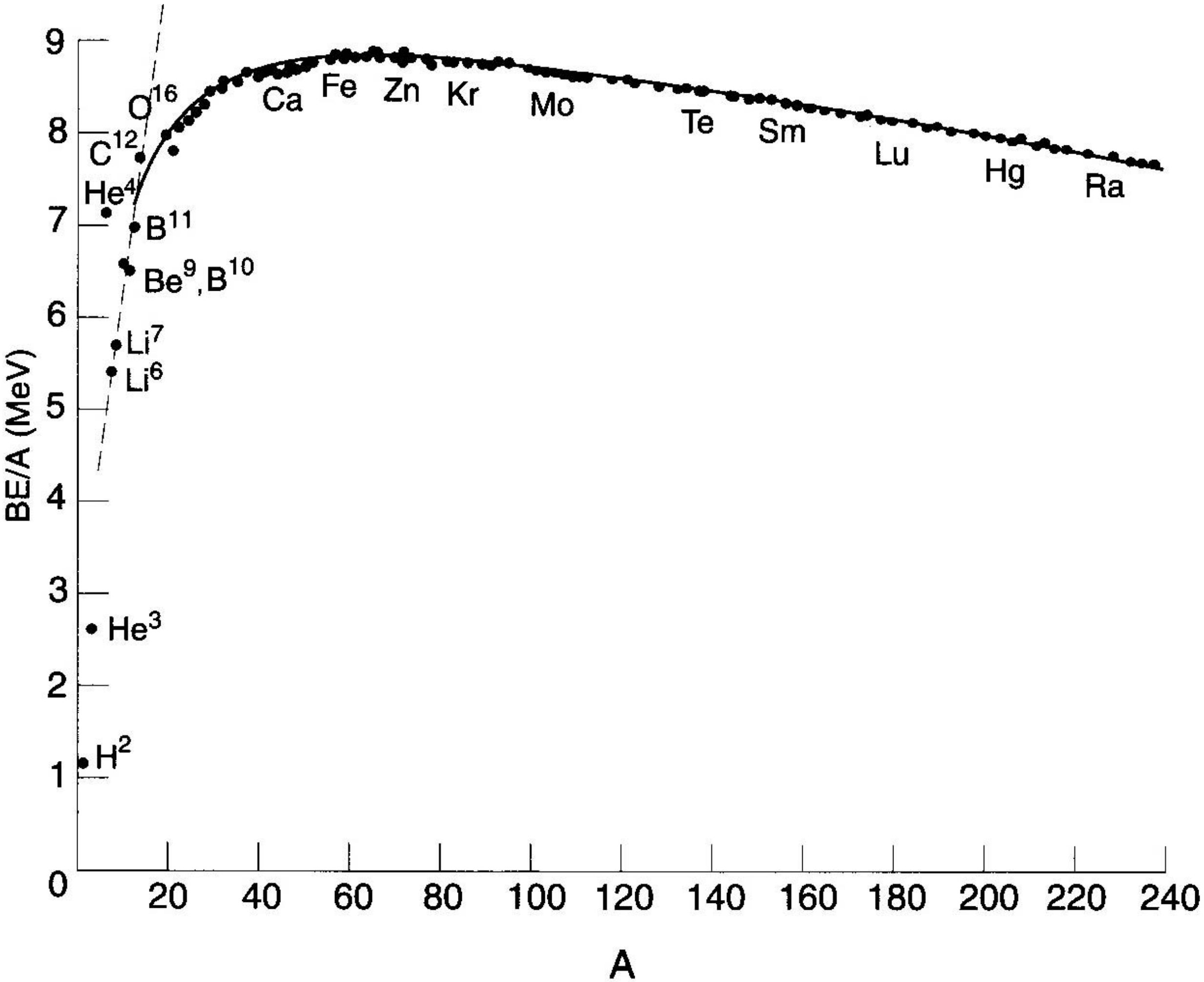

半経験的質量公式（液滴模型）

$$\boxed{B(N,Z) = a_v A - a_s A^{2/3} - a_C \frac{Z^2}{A^{1/3}} - a_{\mathrm{sym}} \frac{(N-Z)^2}{A}}$$

核分裂障壁

$$B(N,Z) = a_v A - a_s A^{2/3} - a_C \frac{Z^2}{A^{1/3}} - a_{\mathrm{sym}} \frac{(N-Z)^2}{A}$$

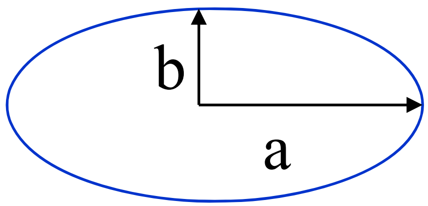

$$\begin{aligned} a &= R\cdot(1+\epsilon) \\ b &= R\cdot(1+\epsilon)^{-1/2} \end{aligned}$$

$$\begin{aligned} E_{\mathrm{surf}} &= E^{(0)}_{\mathrm{surf}}\,(1+2\epsilon^2/5+\cdots) \\ E_C &= E^{(0)}_C\,(1-\epsilon^2/5+\cdots) \end{aligned}$$

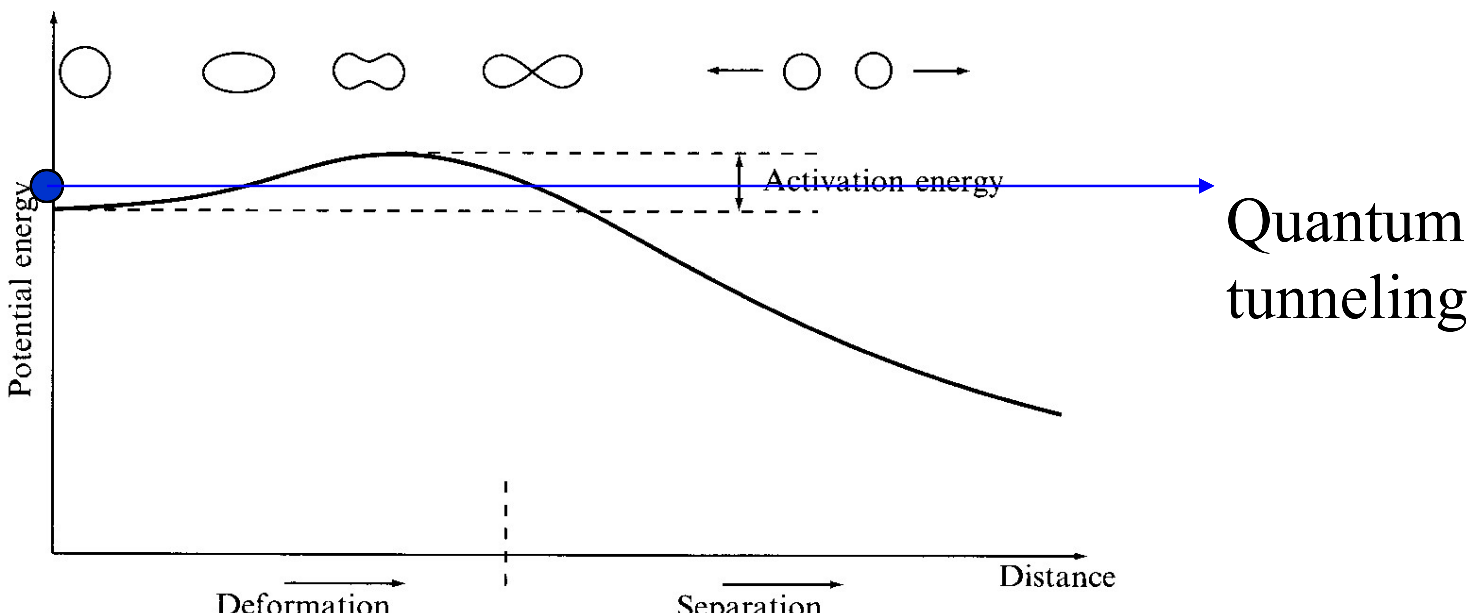

原子核の変形

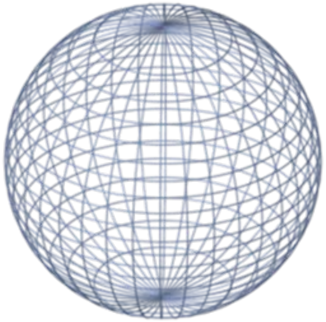

球形

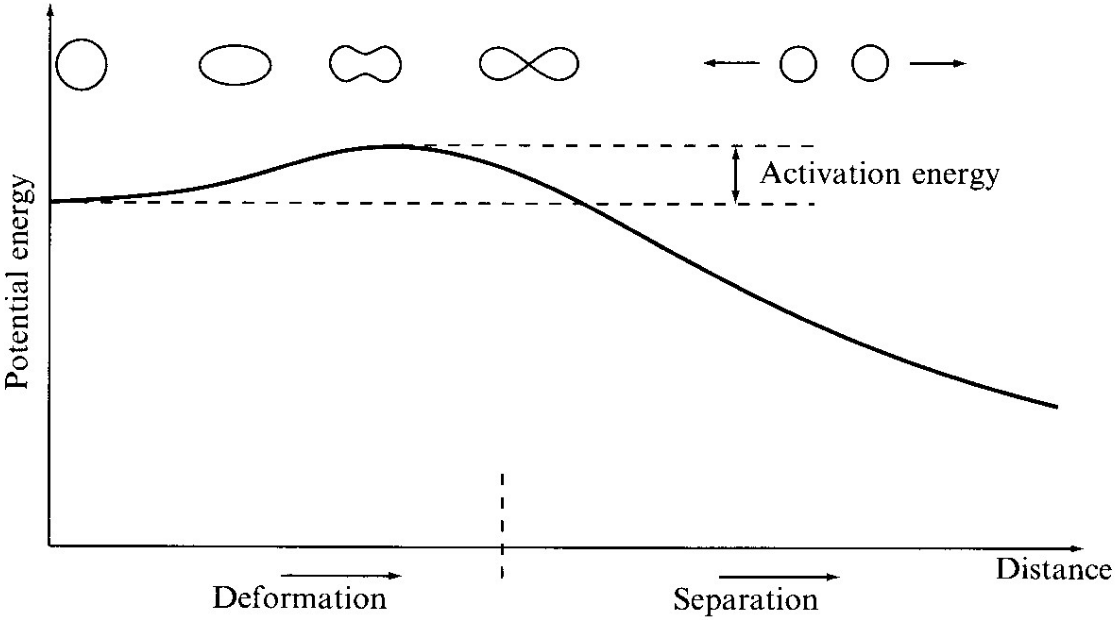
Activation energy
Potential energy
Deformation
Separation
Distance

Shell Energy

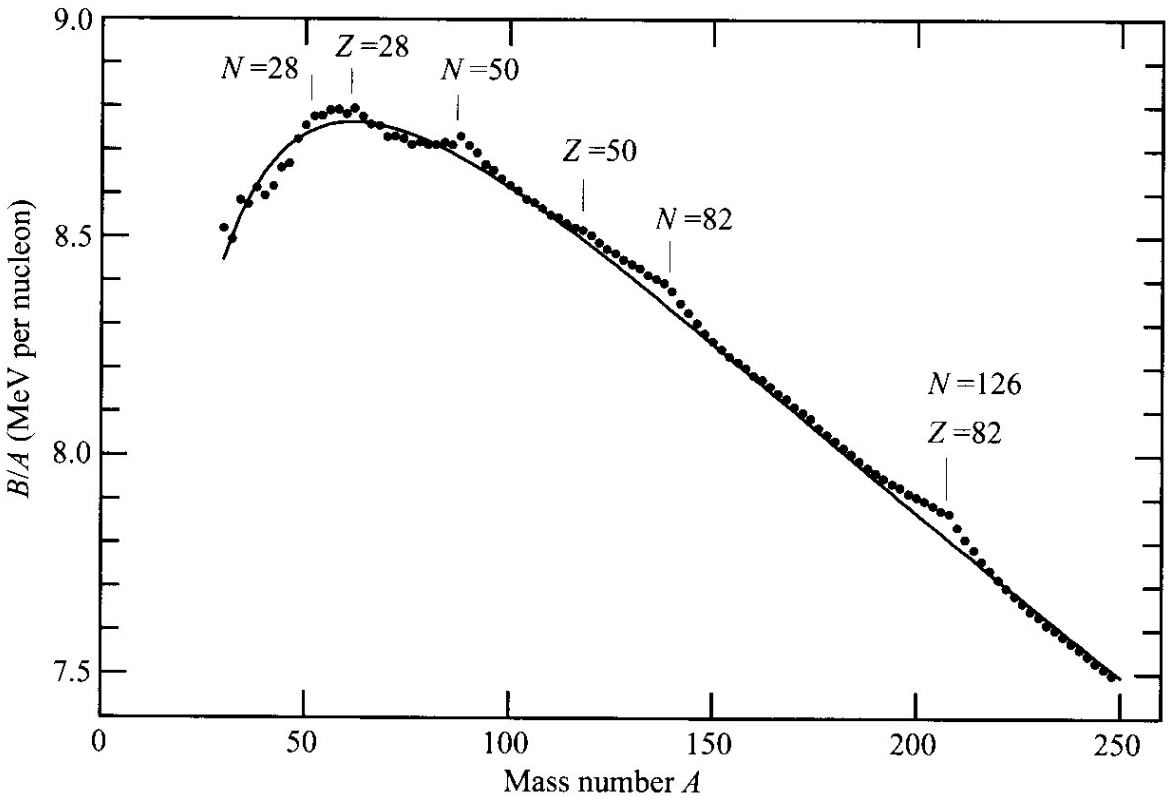

Extra binding for N,Z = 2, 8, 20, 28, 50, 82, 126 (magic numbers)

⇒ Very stable

$^{4}_{2}He_{2}, ^{16}_{8}O_{8}, ^{40}_{20}Ca_{20}, ^{48}_{20}Ca_{28}, ^{208}_{82}Pb_{126}$

(note) Atomic magic numbers (Noble gas)

He (Z=2), Ne (Z=10), Ar (Z=18), Kr (Z=36), Xe (Z=54), Rn (Z=86)

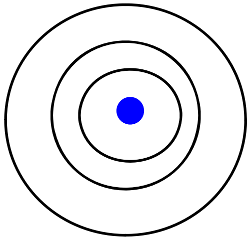

Shell structure

Similar attempt in nuclear physics: independent particle motion in a potential well

Woods-Saxon potential

$$V(r) = -V_0/[1 + \exp((r - R_0)/a)]$$

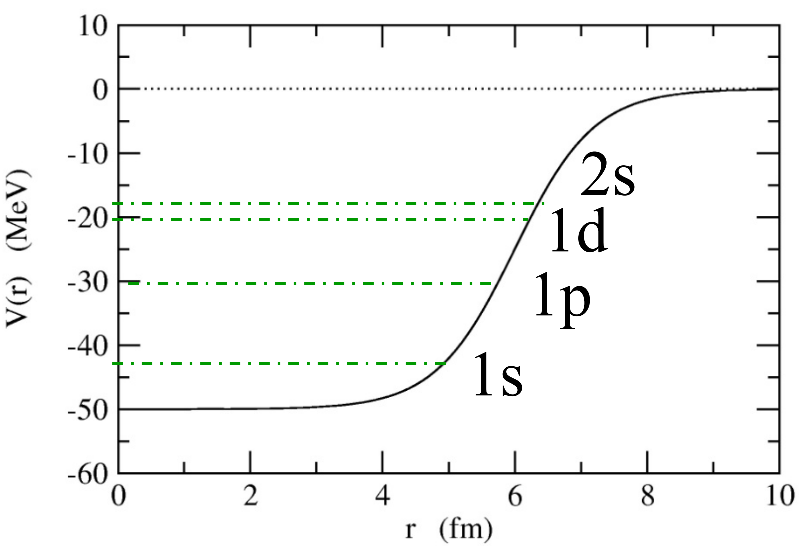

$$\left[-\frac{\hbar^2}{2m}\nabla^2 + V(r) - \epsilon\right]\psi(\boldsymbol{r}) = 0$$

$$\psi(\boldsymbol{r}) = \frac{u_l(r)}{r} Y_{lm}(\hat{\boldsymbol{r}}) \cdot \chi_{m_s}$$

彦坂忠義(1902 – 1989)

1934 年
殻模型の考えに基づき
計算を行う

⇩

中性子の分離エネルギー、
原子核の安定領域、
磁気モーメント

など当時測定されていた
実験データをきれいに説明

（ただし、当時、殻模型の
考えは受け入れられなかった。）

Phys. Rev. に論文を reject をされる。
独語に書き直し、東北大紀要に発表。

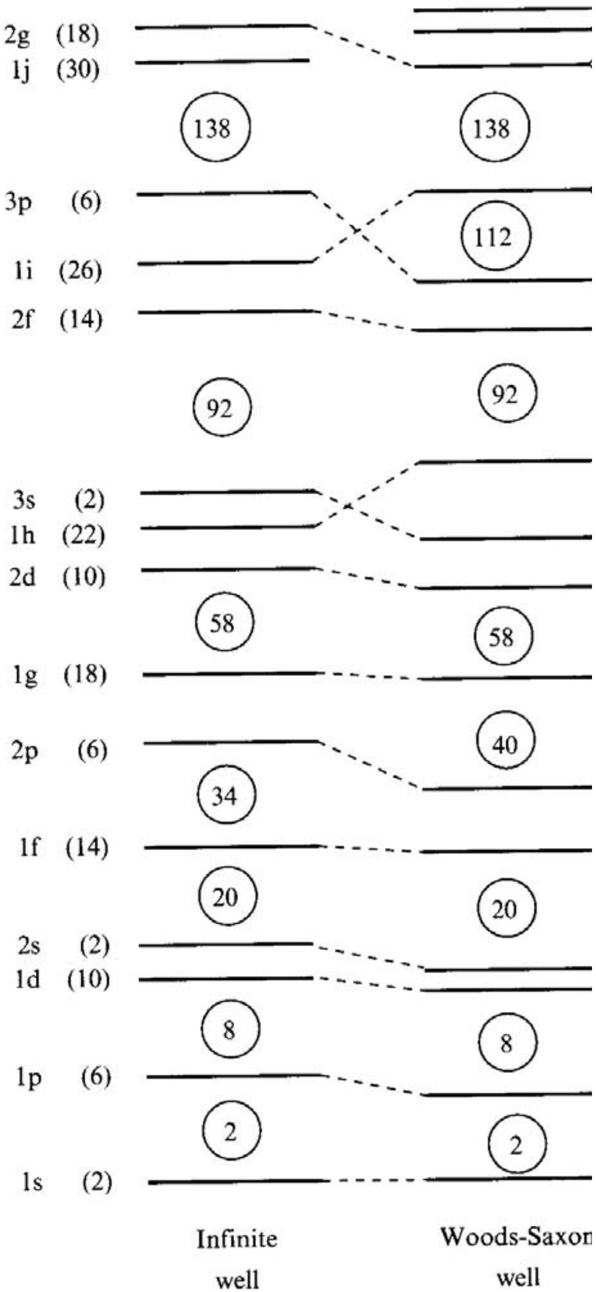

Woods-Saxon itself does not provide the correct magic numbers (2,8,20,28, 50,82,126).

Meyer and Jensen (1949):

Strong spin-orbit interaction

$$\left[-\frac{\hbar^2}{2m}\nabla^2 + V(r) + V_{ls}(r)\boldsymbol{l}\cdot\boldsymbol{s} - \epsilon\right]\psi(\boldsymbol{r}) = 0$$

$$V_{ls}(r) \sim -\lambda\frac{1}{r}\frac{dV}{dr} \qquad (\lambda\ >\ 0)$$

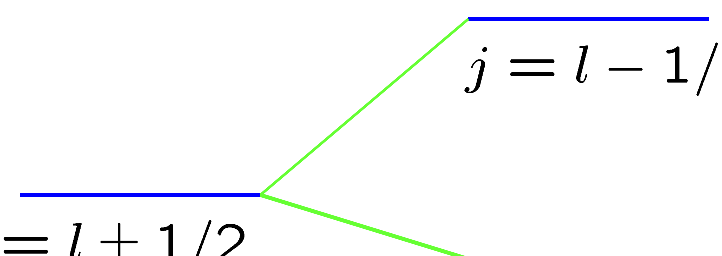

$-(l+1)/2\cdot\langle V_{ls}\rangle$

$j = l - 1/2$

$j = l \pm 1/2$

$l/2\cdot\langle V_{ls}\rangle$

$j = l + 1/2$

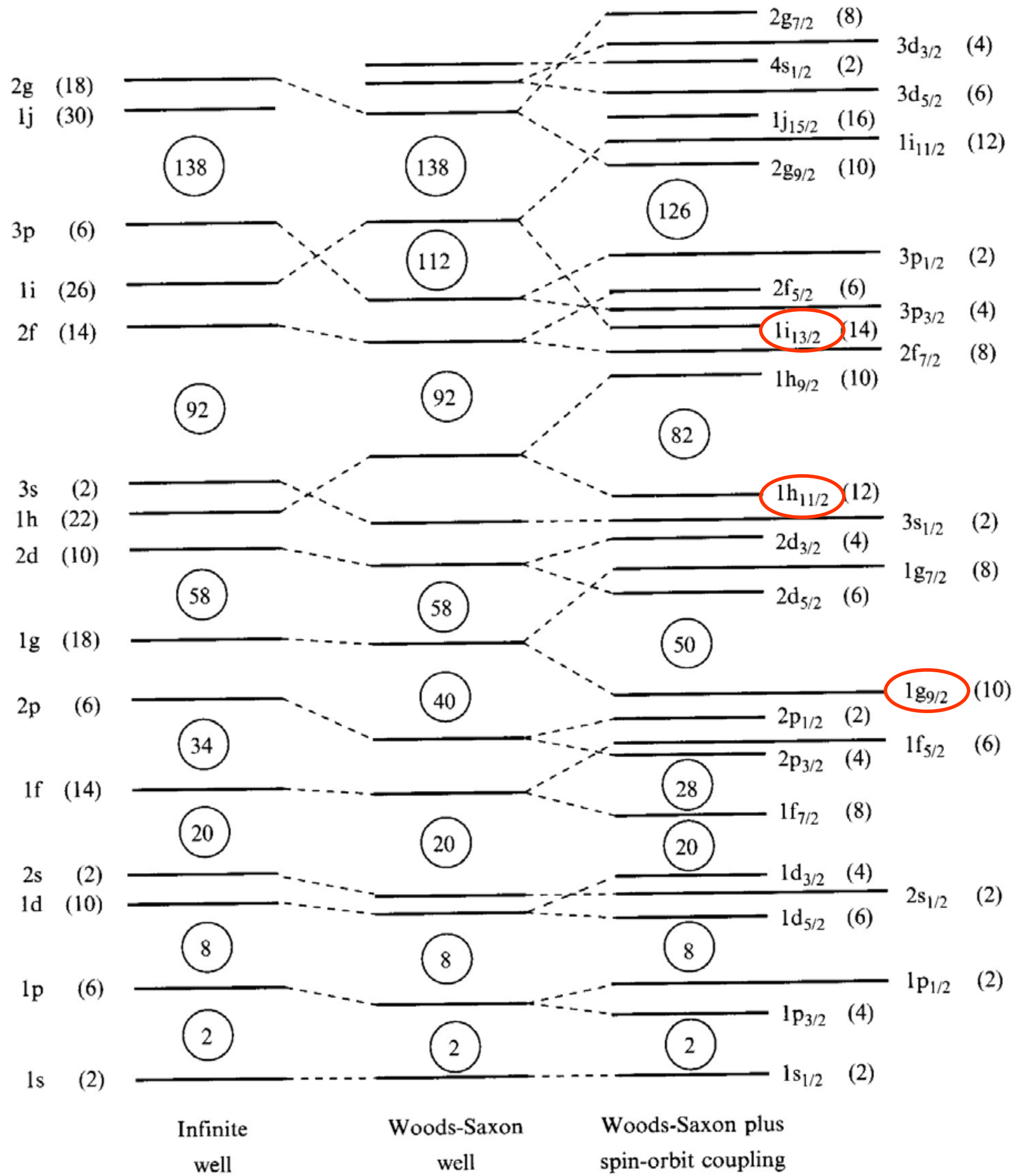

intruder states

unique parity states

Nuclear Deformation

Deformed energy surface for a given nucleus

$$E(\beta) = E_{LDM}(\beta) + E_{\text{shell}}(\beta)$$

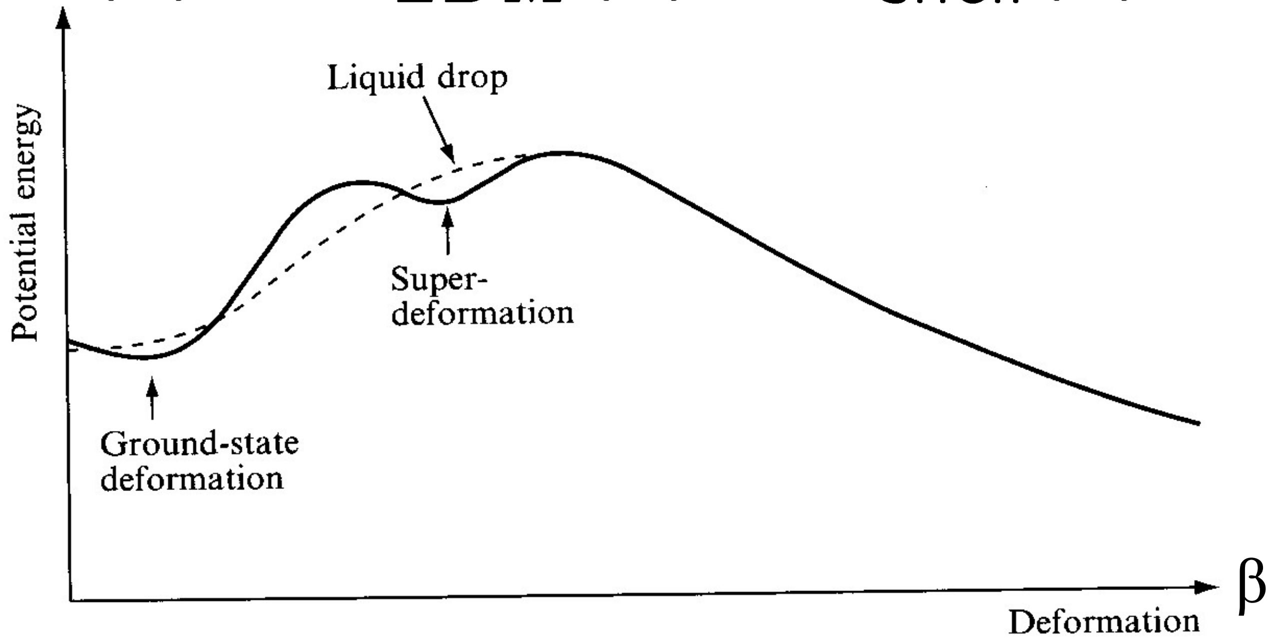

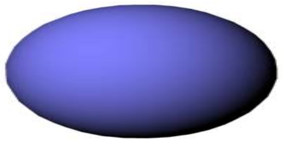

LDM only → always spherical ground state

Shell correction → may lead to a deformed g.s.

* Spontaneous Symmetry Breaking

回転楕円体

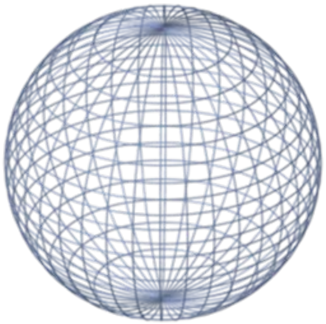

球形

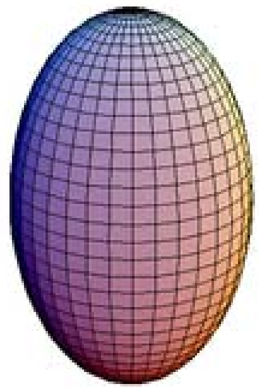

プロレート

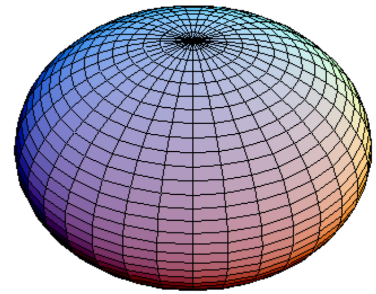

オブレート

三軸非対称

殻効果

$$B_{\mathrm{micro}} = B_{\mathrm{pair}} + B_{\mathrm{shell}}$$

Nuclear Deformation

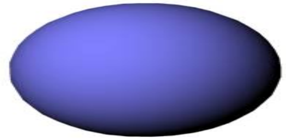

cf. Rotational energy of a rigid body
(Classical mechanics)

$$E = \frac{1}{2}\mathcal{J}\omega^2 = \frac{I^2}{2\mathcal{J}}$$

$$(I = \mathcal{J}\omega, \;\; \omega = \dot{\theta})$$

Excitation spectra of ^{154}Sm

(MeV)	
0.903	8^+
0.544	6^+
0.267	4^+
0.082	2^+
0	0^+

^{154}Sm

$$\boxed{E_I \sim \frac{I(I+1)\hbar^2}{2\mathcal{J}}}$$

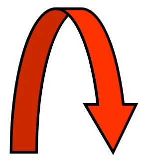

^{154}Sm is deformed

(note) What is 0^+ state (Quantum Mechanics)?

0^+: no preference of direction (spherical)

→ Mixing of all orientations with an equal probability

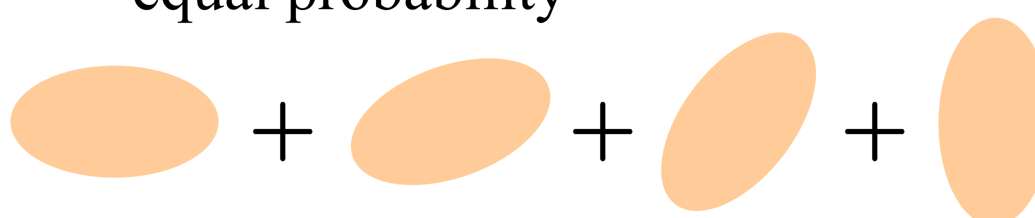

c.f. HF + Angular Momentum Projection

Evidences for nuclear deformation

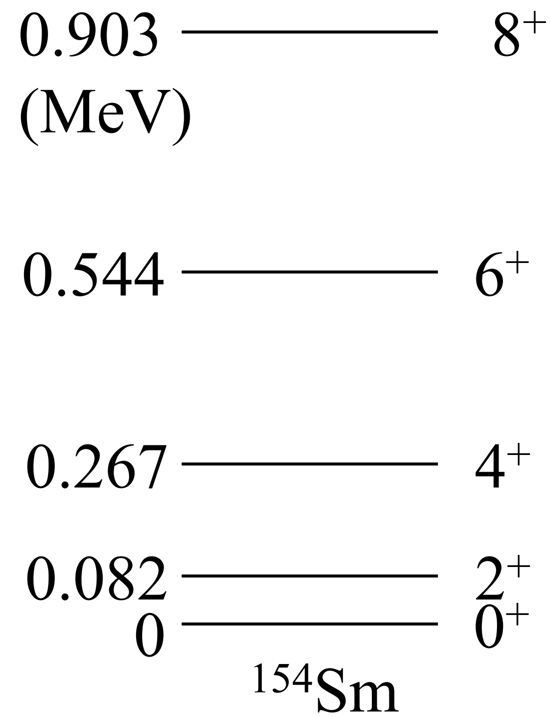

- The existence of rotational bands

$$E_I = \frac{I(I+1)\hbar^2}{2\mathcal{J}}$$

- Very large quadrupole moments
  (for odd-A nuclei)

$$Q = e\sqrt{\frac{16\pi}{5}}\langle\Psi_{II}|r^2Y_{20}|\Psi_{II}\rangle$$

- Strongly enhanced quadrupole transition probabilities
- Hexadecapole matrix elements $\longleftrightarrow$ β_4
- Single-particle structure
- Fission isomers

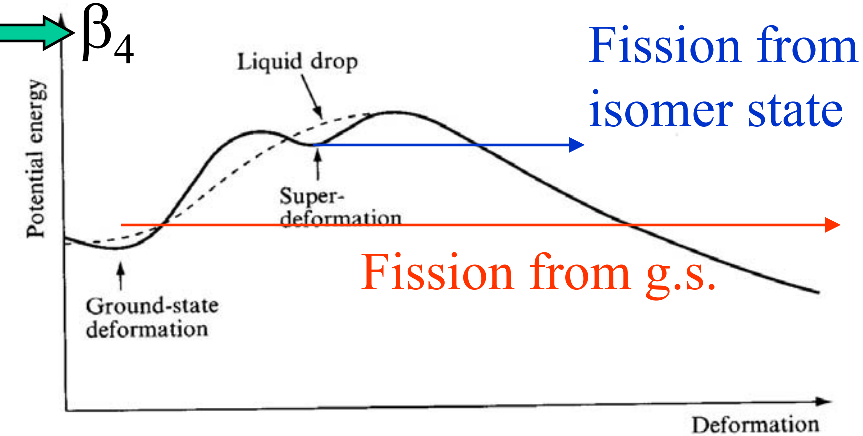

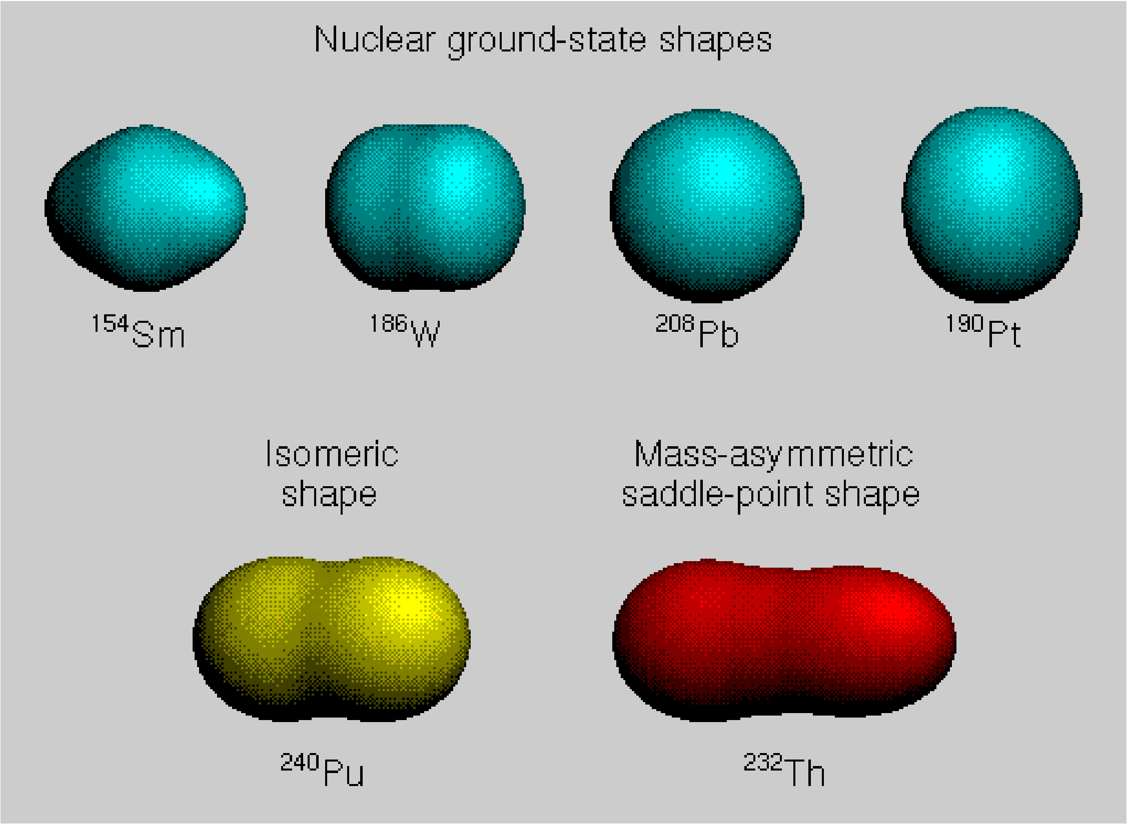

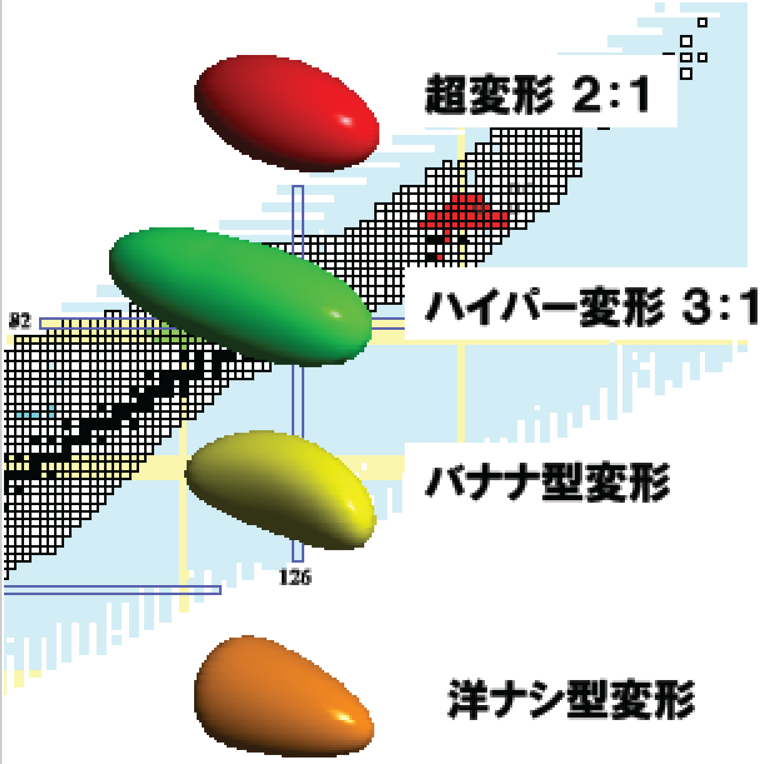

http://t2.lanl.gov/tour/sch001.html

原子核は陽子と中性子の組み合わせの仕方によって様々な形をとり得る！

Nobel Prize in Physics 2008

“for the discovery of the mechanism of spontaneous broken symmetry in subatomic physics”

Yoichiro Nambu

“for the discovery of the origin of the broken symmetry which predicts the existence of at least three families of quarks in nature”

Kobayashi-Maskawa

対称性の自発的破れ

ハミルトニアンが持つ対称性を、真空が持たない（破る）。

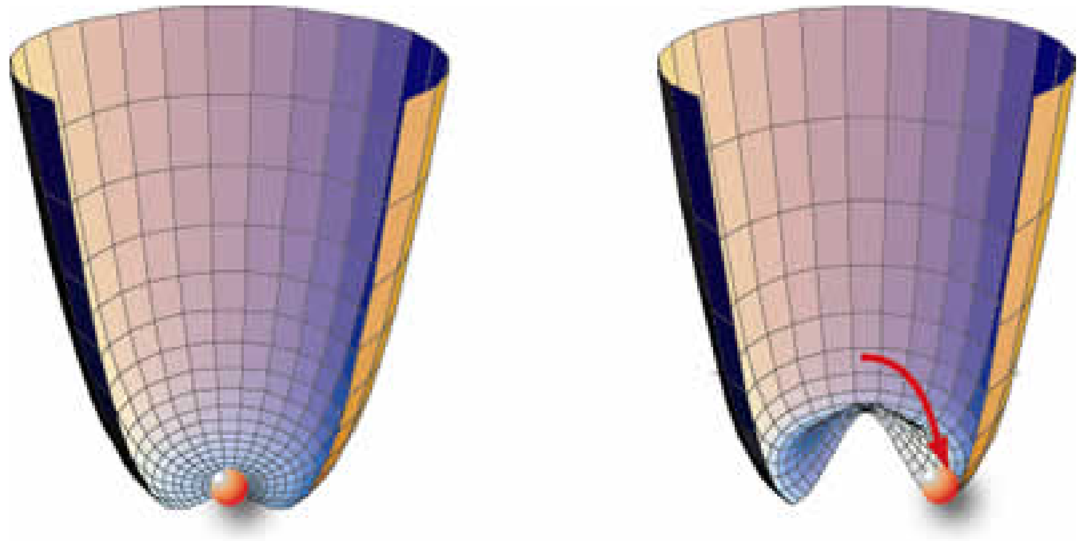

対称性を回復するように
南部・ゴールドストン・モード（ゼロ・モード）
が発生

(note) rigid rotation of mechanical systems

E.R. Marshalek, Ann. of Phys. 53('69) 569

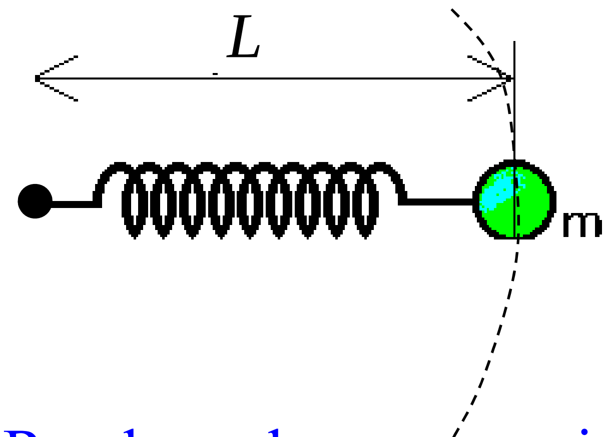

$$H = \frac{p_x^2}{2m} + \frac{p_y^2}{2m} + \frac{1}{2}k(\sqrt{x^2+y^2} - L)^2$$

Random phase approximation:

- Small oscillation around equillibrium

$$V(x,y) \sim V(x_0,y_0) + \frac{1}{2}\sum_{i,j}(\partial_i\partial_j V)(x_i - x_{i0})(x_j - x_{j0})$$

- All degrees of freedom are treated equally

⇨ Treat *x* and *y* on the same footing
(work with the Cartesian coordinate)

i) "Spherical" case (L=0)

$$H=\frac{p_x^2}{2m}+\frac{p_y^2}{2m}+\frac{1}{2}k(x^2+y^2)$$

$$\Longrightarrow \quad \omega_x=\omega_y=\sqrt{k/m}$$

ii) "Deformed" case ($L\neq 0$)

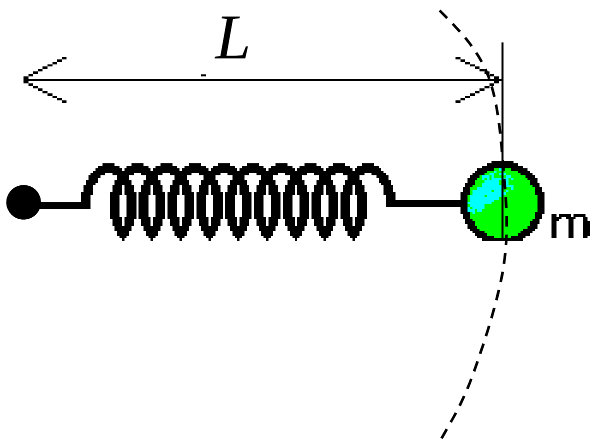

$$x_0=L,\;\; y_0=0$$

$\Longleftarrow$ Spontaneous Symm. Breaking

(note) $$\frac{\partial^2}{\partial x^2}(r-L)^2 = \frac{2}{r^3}(r^3-Ly^2)$$
$$\frac{\partial^2}{\partial y^2}(r-L)^2 = \frac{2}{r^3}(r^3-Lx^2)$$

$$H\sim\frac{p_x^2}{2m}+\frac{1}{2}kx^2+\frac{p_y^2}{2m}$$

$$\omega_x=\sqrt{k/m},\;\; \underline{\underline{\omega_y=0}}$$

A warm up

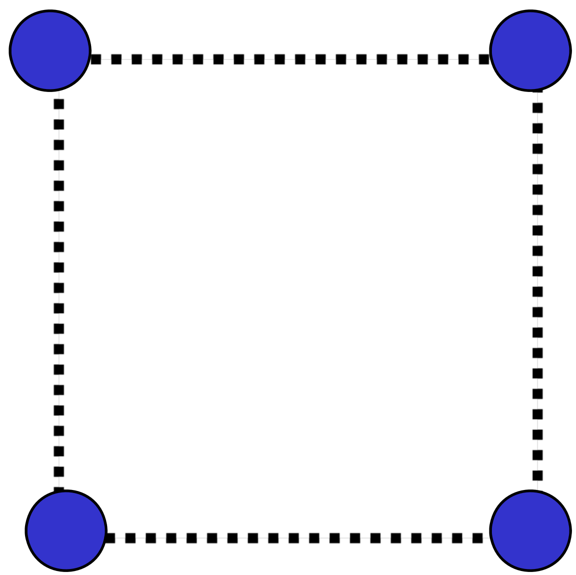

正方形の4頂点を全長が最小になるように線で結ぶには？

スライド：小池武志氏（東北大学）

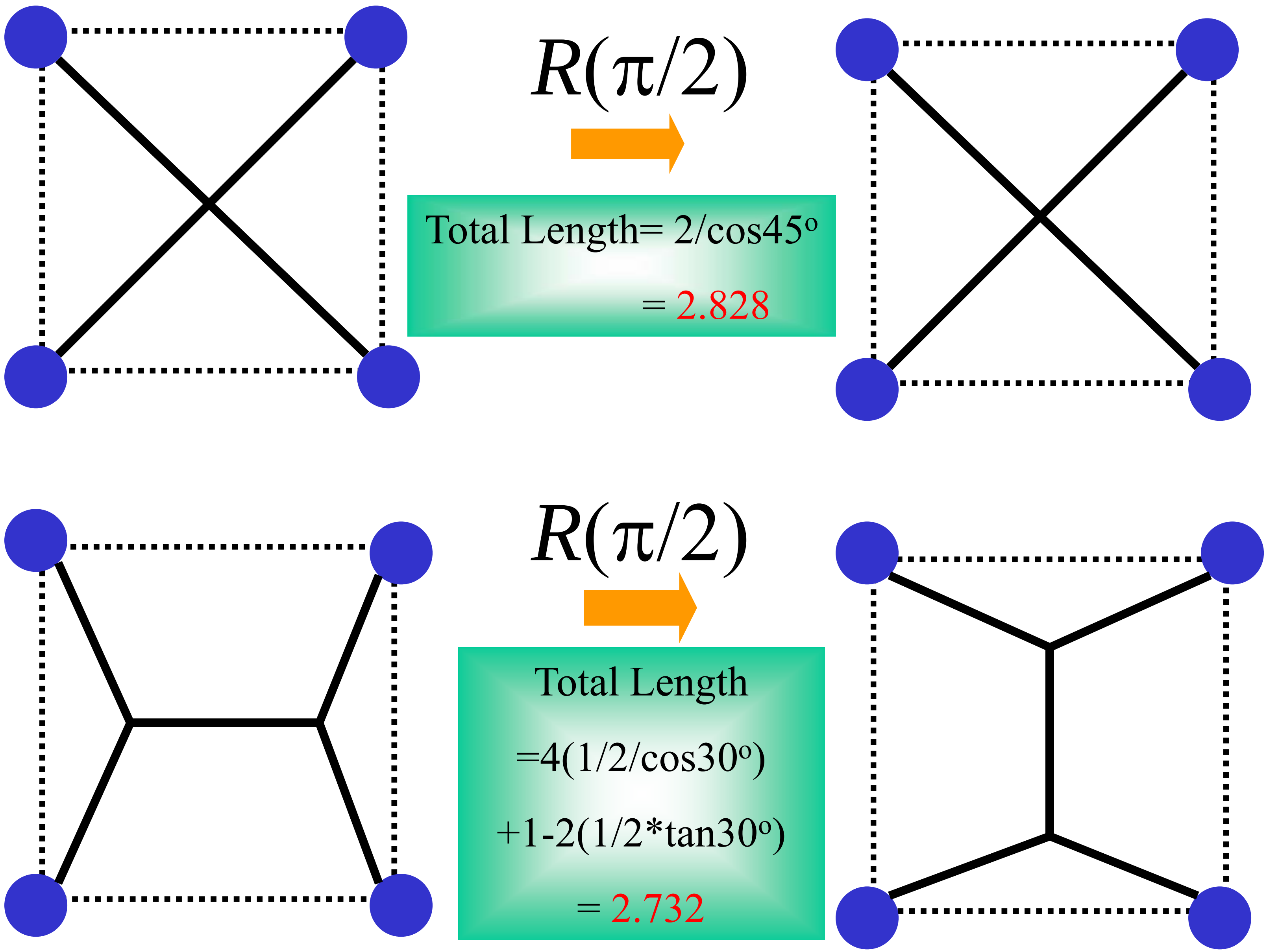

スライド：小池武志氏（東北大学）

平均場近似と変形核

2 body problem

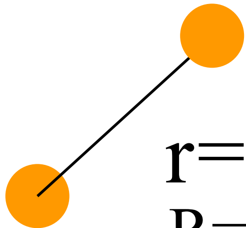

$\mathbf{r}=\mathbf{r}_1-\mathbf{r}_2$

$\mathrm{R}=(\mathrm{m}_1\mathrm{r}_1+\mathrm{m}_2\mathrm{r}_2)/(\mathrm{m}_1+\mathrm{m}_2)$

3 body problem

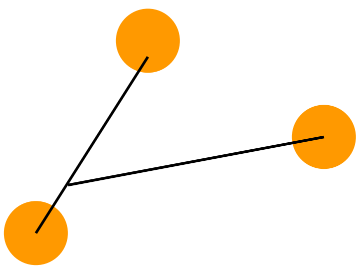

4 body problem

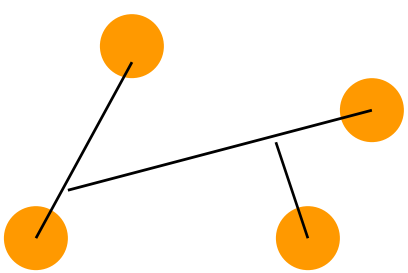

N body problem: necessitates an approximate method

Mean Field Approach

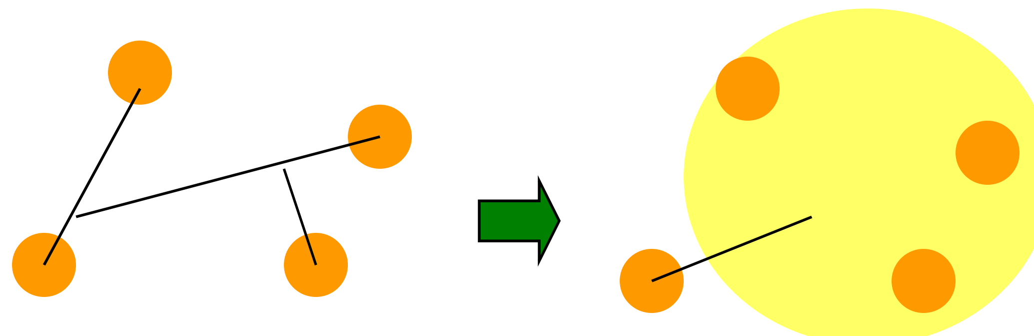

treat the interaction with other particles on average

→ independent particle motion in an *effective one-body potential*

Variational principle

Variational Principle (Rayleigh-Ritz method)

$$\boxed{\frac{\langle\Psi|H|\Psi\rangle}{\langle\Psi|\Psi\rangle} \geq E_{\mathrm{g.s.}}}$$

(note)

$$|\Psi\rangle = \sum_n C_n\,|\phi_n\rangle \Longrightarrow \mathrm{lhs} = \frac{\sum_n C_n^2\,E_n}{\sum_n C_n^2} \geq E_0$$

(note)

$$\frac{\delta}{\delta\,\Psi^*}\left(\langle\Psi|H|\Psi\rangle - E\langle\Psi|\Psi\rangle\right) = 0$$

$\Longrightarrow$ Schrodinger equation: $H|\Psi\rangle = E|\Psi\rangle$

Example: find an approximate solution for AHV

$$H = -\frac{\hbar^2}{2m}\frac{d^2}{dx^2} + \frac{1}{2}m\omega^2 x^2 + \beta x^4$$

Trial wave function:

$$\Psi(x) = (\pi b^2)^{-1/4}\,\mathrm{exp}(-x^2/2b^2)$$

(note) $\text{if } \beta = 0, \quad b = \sqrt{\hbar/m\omega}$

$$\frac{\langle\Psi|H|\Psi\rangle}{\langle\Psi|\Psi\rangle} = \frac{\hbar^2}{4mb^2} + \frac{m\omega^2 b^2}{4} + \frac{3\beta b^4}{4} \equiv F(b)$$

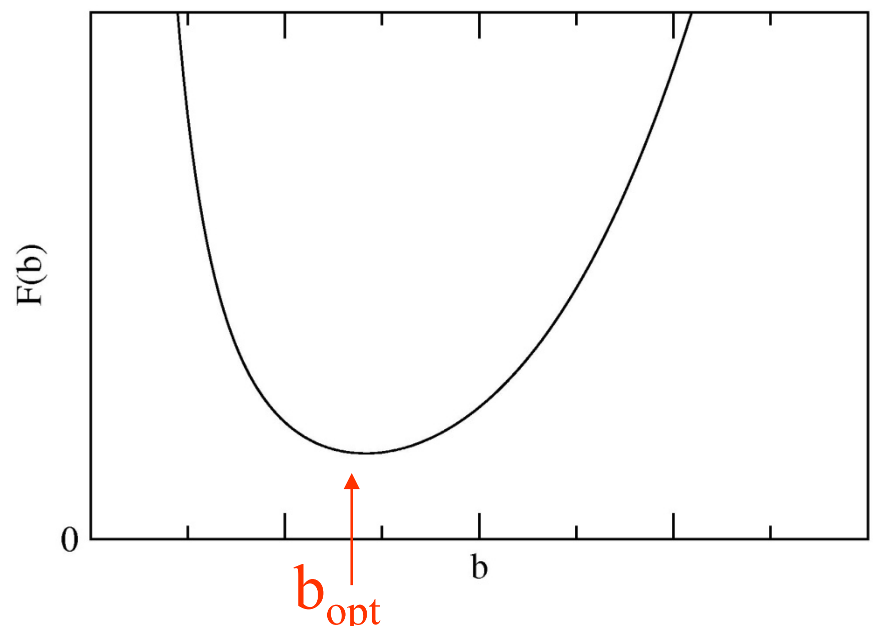

Hartree-Fock Method

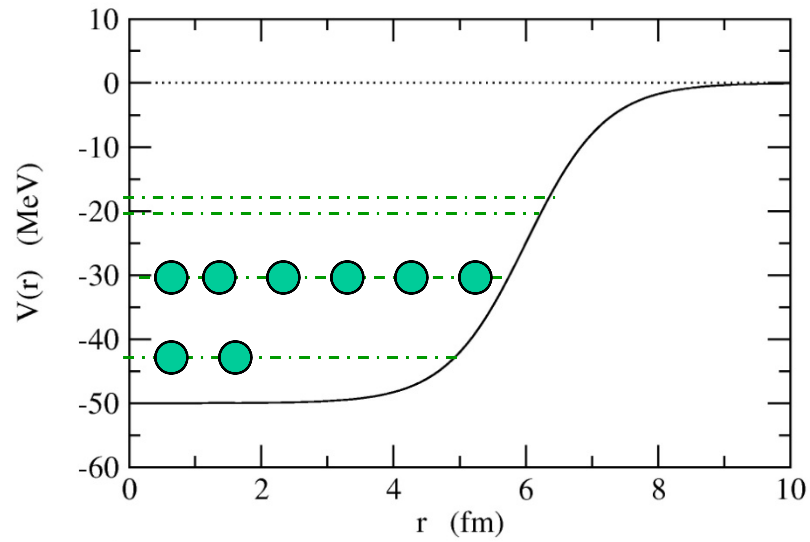

independent particle motion
in a potential well

$$
\begin{aligned}
\Psi(1,2,\cdots,A) &= \mathcal{A}[\psi_1(1)\psi_2(2)\cdots\psi_A(A)] \\
&= \frac{1}{\sqrt{A!}}\begin{vmatrix} \psi_1(1) & \psi_2(1) & \cdots & \psi_A(1) \\ \psi_1(2) & \psi_2(2) & \cdots & \psi_A(2) \\ \vdots & & & \\ \psi_1(A) & \psi_2(A) & \cdots & \psi_A(A) \end{vmatrix}
\end{aligned}
$$

Slater determinant: antisymmetrization due to the Pauli principle

(note)

$$\Psi(1,2) = (\psi_1(1)\psi_2(2) - \psi_1(2)\psi_2(1))/\sqrt{2}$$

many-body Hamiltonian: $$H = -\sum_{i=1}^{A} \frac{\hbar^2}{2m} \boldsymbol{\nabla}_i^2 + \frac{1}{2} \sum_{i,j}^{A} v(\boldsymbol{r}_i, \boldsymbol{r}_j)$$

$$\begin{aligned}
\langle \Psi | H | \Psi \rangle \;=\; & -\frac{\hbar^2}{2m} \sum_{i=1}^{A} \int \psi_i^*(\boldsymbol{r}) \boldsymbol{\nabla}^2 \psi_i(\boldsymbol{r}) \, d\boldsymbol{r} \\
& + \frac{1}{2} \sum_{i,j}^{A} \int \psi_i^*(\boldsymbol{r}) \psi_j^*(\boldsymbol{r}') v(\boldsymbol{r}, \boldsymbol{r}') \psi_i(\boldsymbol{r}) \psi_j(\boldsymbol{r}') \, d\boldsymbol{r} d\boldsymbol{r}' \\
& - \frac{1}{2} \sum_{i,j}^{A} \int \psi_i^*(\boldsymbol{r}) \psi_j^*(\boldsymbol{r}') v(\boldsymbol{r}, \boldsymbol{r}') \psi_i(\boldsymbol{r}') \psi_j(\boldsymbol{r}) \, d\boldsymbol{r} d\boldsymbol{r}'
\end{aligned}$$

Variation with respect to ψ_i^*

Hartree-Fock equation:

$$\boxed{\begin{aligned}
& -\frac{\hbar^2}{2m} \boldsymbol{\nabla}^2 \psi_i(\boldsymbol{r}) + \sum_j \int \psi_j^*(\boldsymbol{r}') v(\boldsymbol{r}, \boldsymbol{r}') \psi_j(\boldsymbol{r}') \psi_i(\boldsymbol{r}) \, d\boldsymbol{r}' \\
& \quad - \sum_j \int \psi_j^*(\boldsymbol{r}') v(\boldsymbol{r}, \boldsymbol{r}') \psi_j(\boldsymbol{r}) \psi_i(\boldsymbol{r}') \, d\boldsymbol{r}' = \epsilon_i \psi_i(\boldsymbol{r})
\end{aligned}}$$

$$\boxed{\begin{aligned}&-\frac{\hbar^2}{2m}\nabla^2\psi_i(\boldsymbol{r})+\int v(\boldsymbol{r},\boldsymbol{r}')\rho_{\mathsf{HF}}(\boldsymbol{r}')d\boldsymbol{r}'\psi_i(\boldsymbol{r})\\&\qquad-\int\rho_{\mathsf{HF}}(\boldsymbol{r},\boldsymbol{r}')v(\boldsymbol{r},\boldsymbol{r}')\psi_i(\boldsymbol{r}')\,d\boldsymbol{r}'=\epsilon_i\,\psi_i(\boldsymbol{r})\end{aligned}}$$

Density matrix:

$$\boxed{\begin{aligned}\rho_{\mathsf{HF}}(\boldsymbol{r},\boldsymbol{r}') &= \sum_i\psi_i^*(\boldsymbol{r}')\psi_i(\boldsymbol{r})\\ \rho_{\mathsf{HF}}(\boldsymbol{r}) &= \sum_i\psi_i^*(\boldsymbol{r})\psi_i(\boldsymbol{r})=\rho_{\mathsf{HF}}(\boldsymbol{r},\boldsymbol{r})\end{aligned}}$$

1. Single-particle Hamiltonian:

$$\hat{h}=\hat{T}+\hat{V}_H+\hat{V}_F$$

$$V_H(\boldsymbol{r}) = \int v(\boldsymbol{r},\boldsymbol{r}')\rho_{\mathsf{HF}}(\boldsymbol{r}')d\boldsymbol{r}$$ Direct (Hartree) term

$$\hat{V}_F(\boldsymbol{r},\boldsymbol{r}') = -\rho_{\mathsf{HF}}(\boldsymbol{r},\boldsymbol{r}')v(\boldsymbol{r},\boldsymbol{r}')$$ Exchange (Fock) term

[non-local pot.]

2. Iteration

V_{HF}: depends on ψ_i $\longleftarrow$ non-linear problem

Iteration: $\{\psi_i\}\rightarrow\rho_{\mathsf{HF}}\rightarrow V_{\mathsf{HF}}\rightarrow\{\psi_i\}\rightarrow\cdots$

Hartree-Fock Method and Symmetries

$$\begin{aligned} H &= -\sum_{i=1}^{A}\frac{\hbar^2}{2m}\boldsymbol{\nabla}_i^2 + \frac{1}{2}\sum_{i,j}^{A} v(\boldsymbol{r}_i,\boldsymbol{r}_j) \\ &= \underbrace{\sum_{i=1}^{A}\left(-\frac{\hbar^2}{2m}\boldsymbol{\nabla}_i^2 + V_{\mathrm{HF}}(i)\right)}_{h_{\mathrm{HF}}} + \underbrace{\frac{1}{2}\sum_{i,j}^{A} v(\boldsymbol{r}_i,\boldsymbol{r}_j) - \sum_i V_{\mathrm{HF}}(i)}_{V_{\mathrm{res}}} \end{aligned}$$

Slater determinant

$$\Psi_{\mathrm{HF}}(1,2,\cdots,A) = \mathcal{A}[\psi_1(1)\psi_2(2)\cdots\psi_A(A)]$$

$\Leftarrow$ Eigen-state of h_{HF}, but not of H

$\boxed{\Psi_{\mathrm{HF}} \text{: does not necessarily possess the symmetries that } H \text{ has.}}$

"Symmetry-broken solution"

"Spontaneous Symmetry Broken"

Ψ_{HF} : does not necessarily possess the symmetries that H has.

Typical Example

➢ Translational symmetry: always broken in nuclear systems

$$H = -\sum_{i=1}^{A}\frac{\hbar^2}{2m}\boldsymbol{\nabla}_i^2 + \frac{1}{2}\sum_{i,j}^{A} v(\boldsymbol{r}_i - \boldsymbol{r}_j) \rightarrow \sum_{i=1}^{A}\left(-\frac{\hbar^2}{2m}\boldsymbol{\nabla}_i^2 + \underline{\underline{V_{\mathrm{HF}}(\boldsymbol{r}_i)}}\right)$$

(cf.) atoms

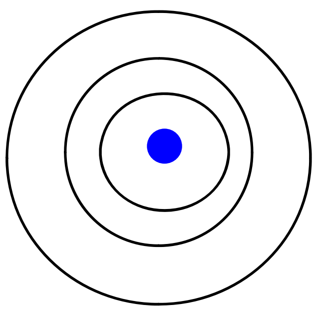

nucleus in the center

⟶ translational symmetry: broken from the begining

Symmetry Breaking

Advantage: a large part of many-body correlation can be taken into account without losing the independent particle picture

Disadvantage: a need to restore the symmetry (in principle) to compute experimental observables

➢ Rotational symmetry

Deformed solution

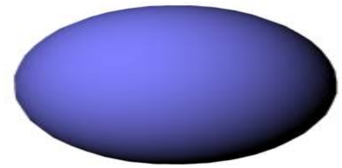

Constrained Hartree-Fock method

$\langle \Psi_{\mathrm{CHF}} | H | \Psi_{\mathrm{CHF}} \rangle$

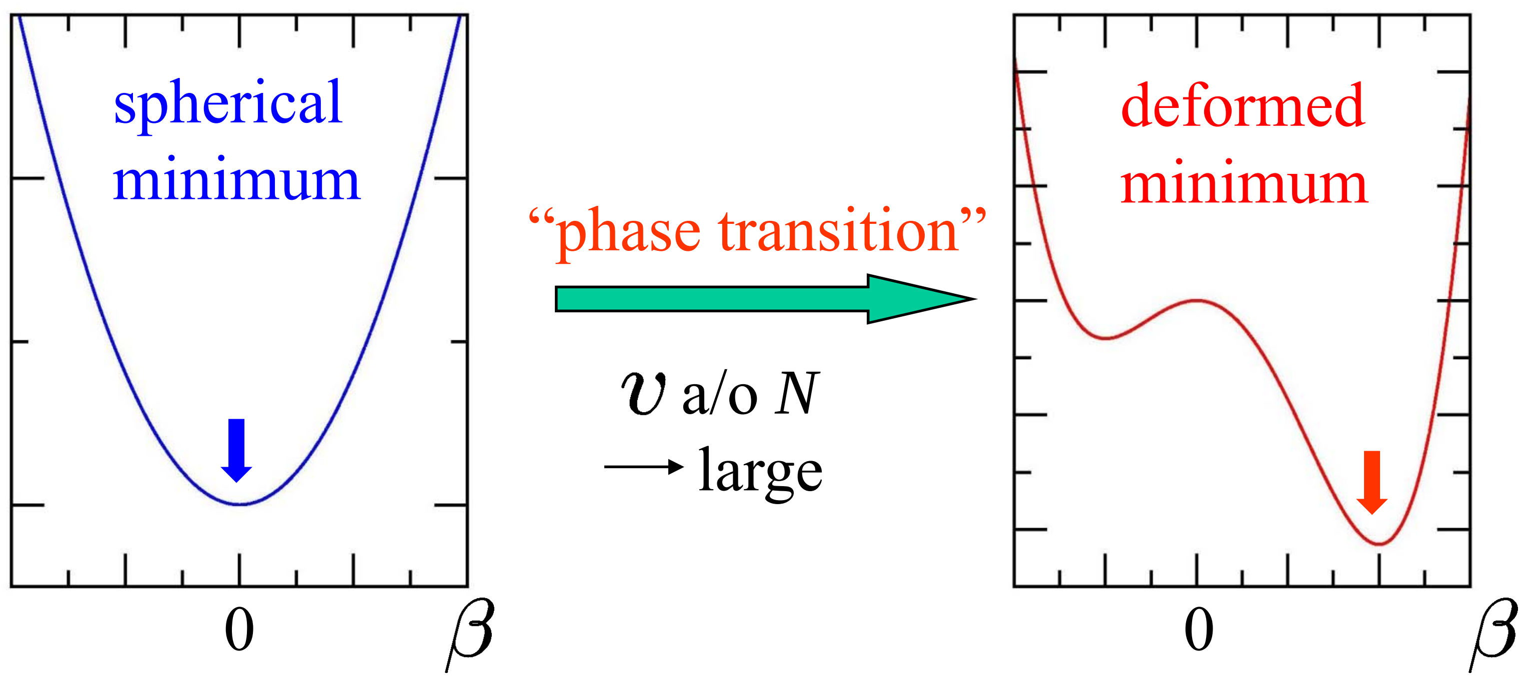

応用例：RMF for deformed hypernuclei

ハイパー核：
原子核＋Λ粒子
Λ粒子の影響は？

self-consistent solution (iteration)

→ (intrinsic) Quadrupole moment

$$\boxed{Q=\sqrt{\frac{16\pi}{5}}\int d\boldsymbol{r}\,[\rho_v(\boldsymbol{r})+\psi^\dagger_\Lambda(\boldsymbol{r})\psi_\Lambda(\boldsymbol{r})]\,r^2Y_{20}(\hat{\boldsymbol{r}})}$$

- Λ particle: the lowest s.p. level ($K^\pi=1/2^+$)
- Deformation parameter:

$$\begin{aligned} Q &= \sqrt{\frac{16\pi}{5}}\frac{3}{4\pi}(A_c+1)R_0^2\beta \\ R_0 &= 1.2\,A_c^{1/3}\quad (\mathrm{fm}) \end{aligned}$$

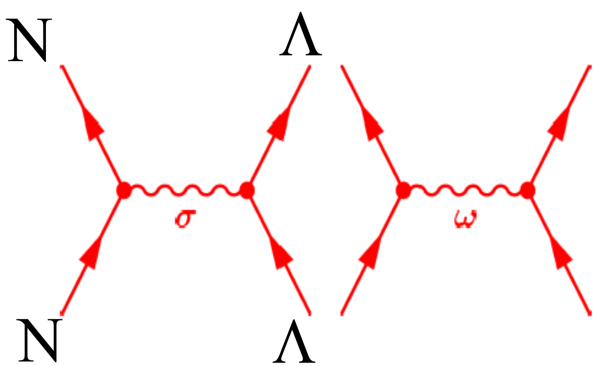

Λσ and Λω couplings

Ne isotopes

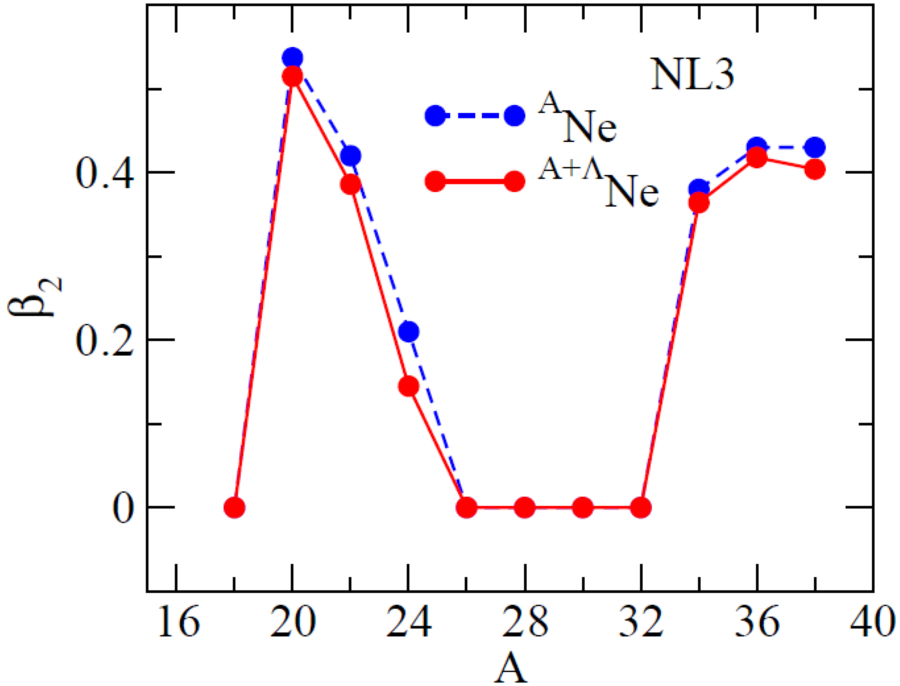

Si isotopes

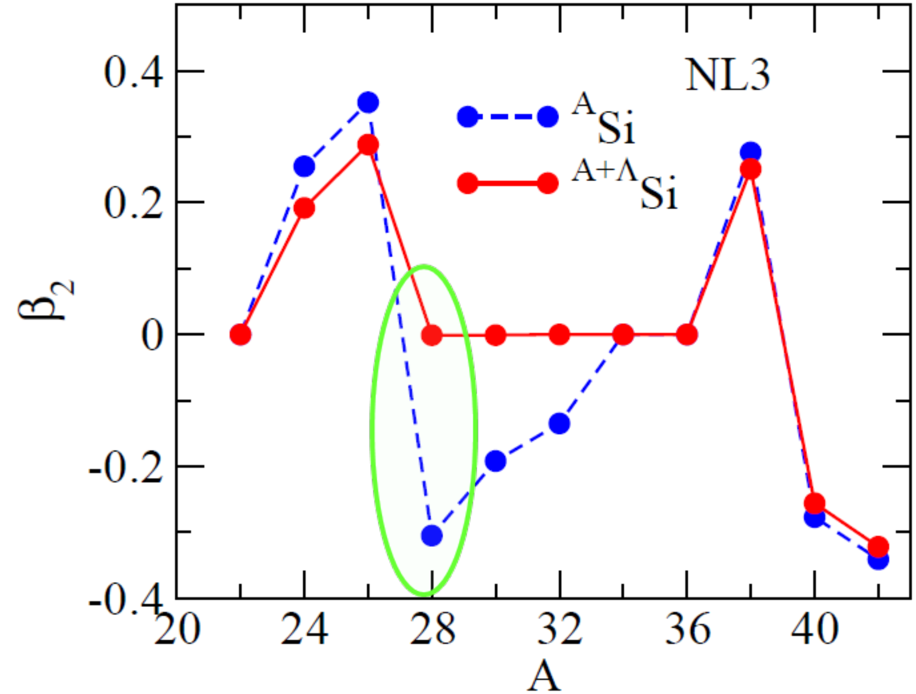

- in most cases, similar deformation between the core and the hypernuclei
- hypernuclei: slightly smaller deformation than the core

$\longrightarrow$ conclusions similar to Skyrme-Hartree-Fock (Zhou *et al.*)

Exception: $^{29}{}_{\Lambda}$Si oblate (^{28}Si) $\xrightarrow{\Lambda}$ spherical ($^{29}{}_{\Lambda}$Si)

Myaing Thi Win and K.H., PRC78('08)054311

density distribution (RMF)

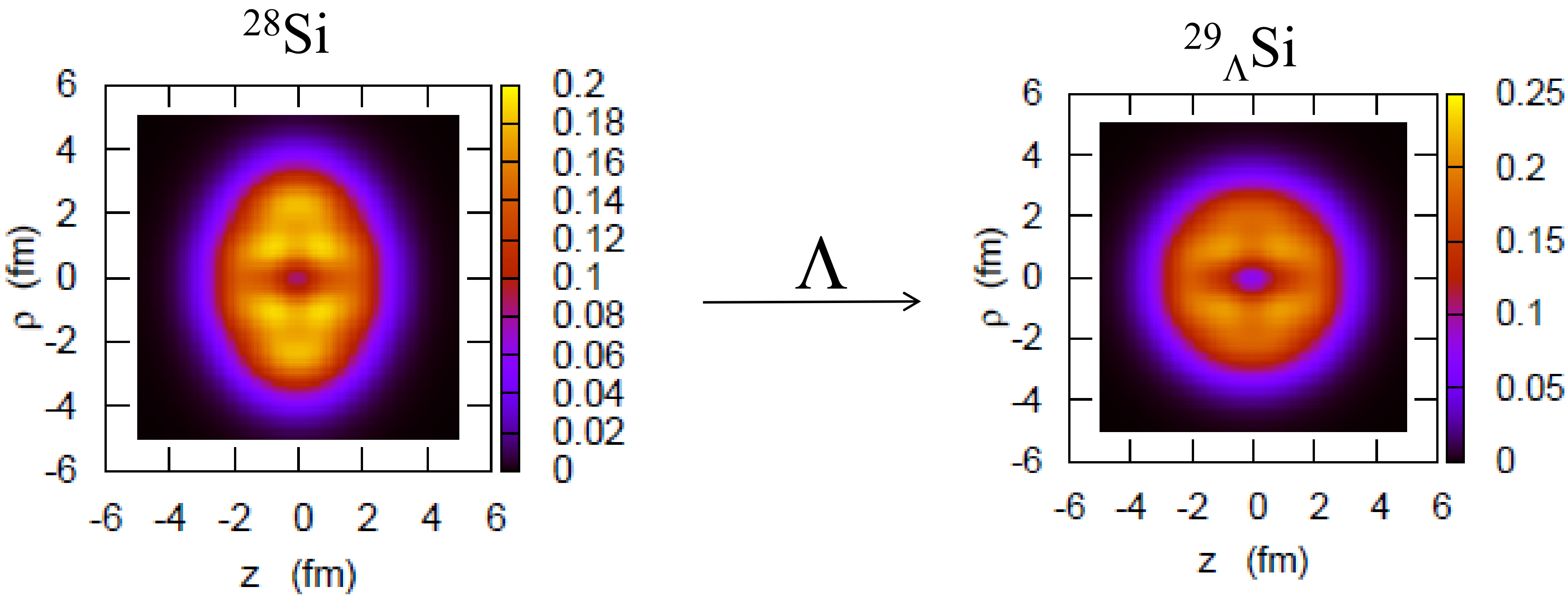

Potential energy surface

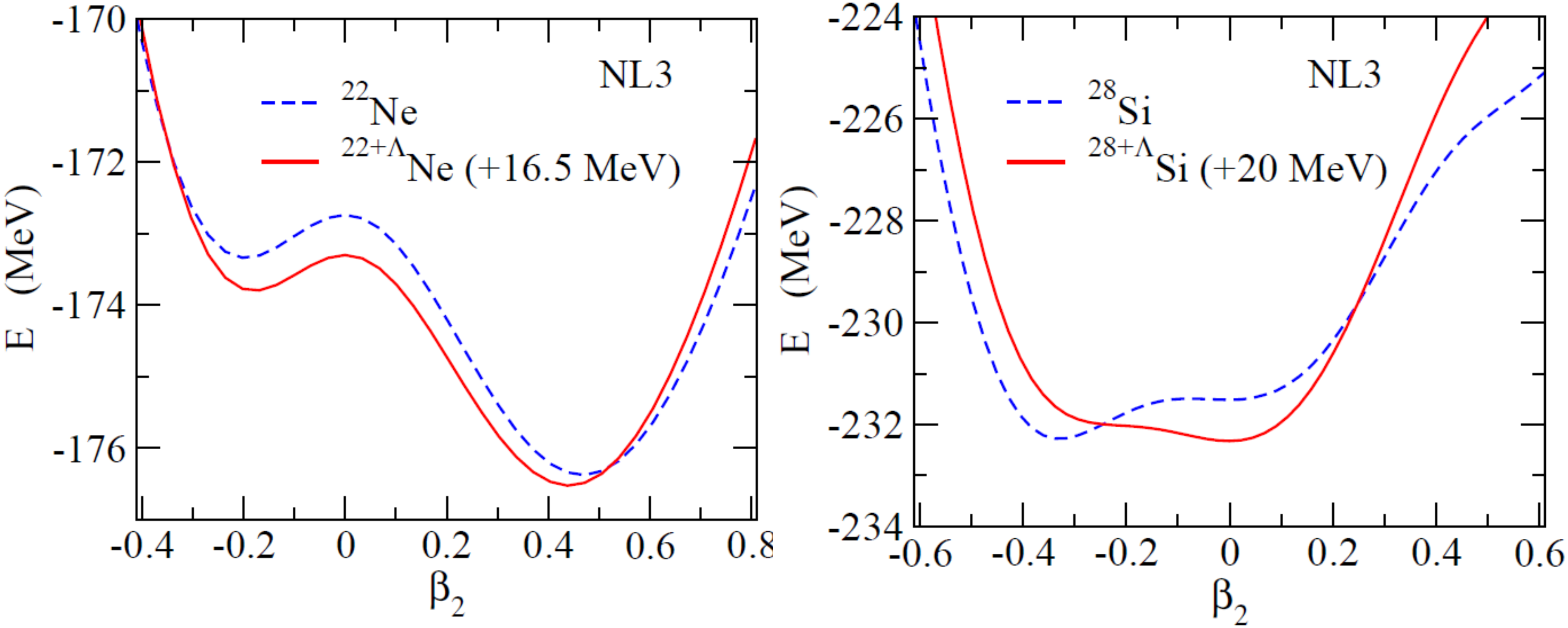

Myaing Thi Win and K.H., PRC78('08)054311

Another example: $^{13}{}_{\Lambda}C$

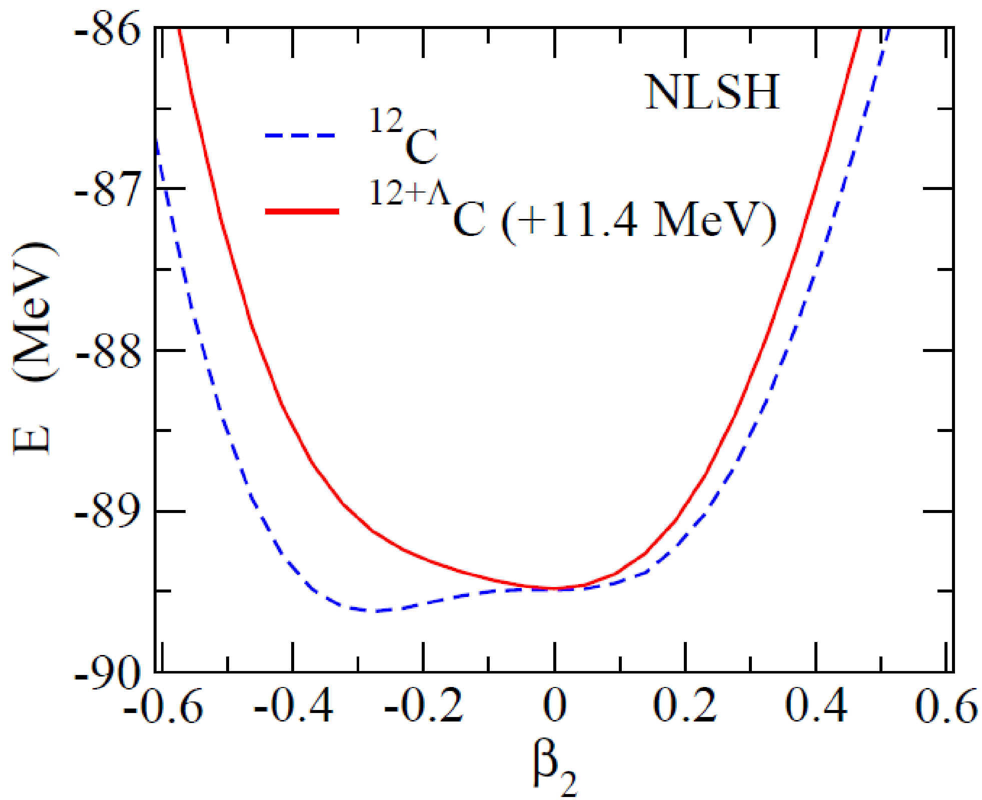

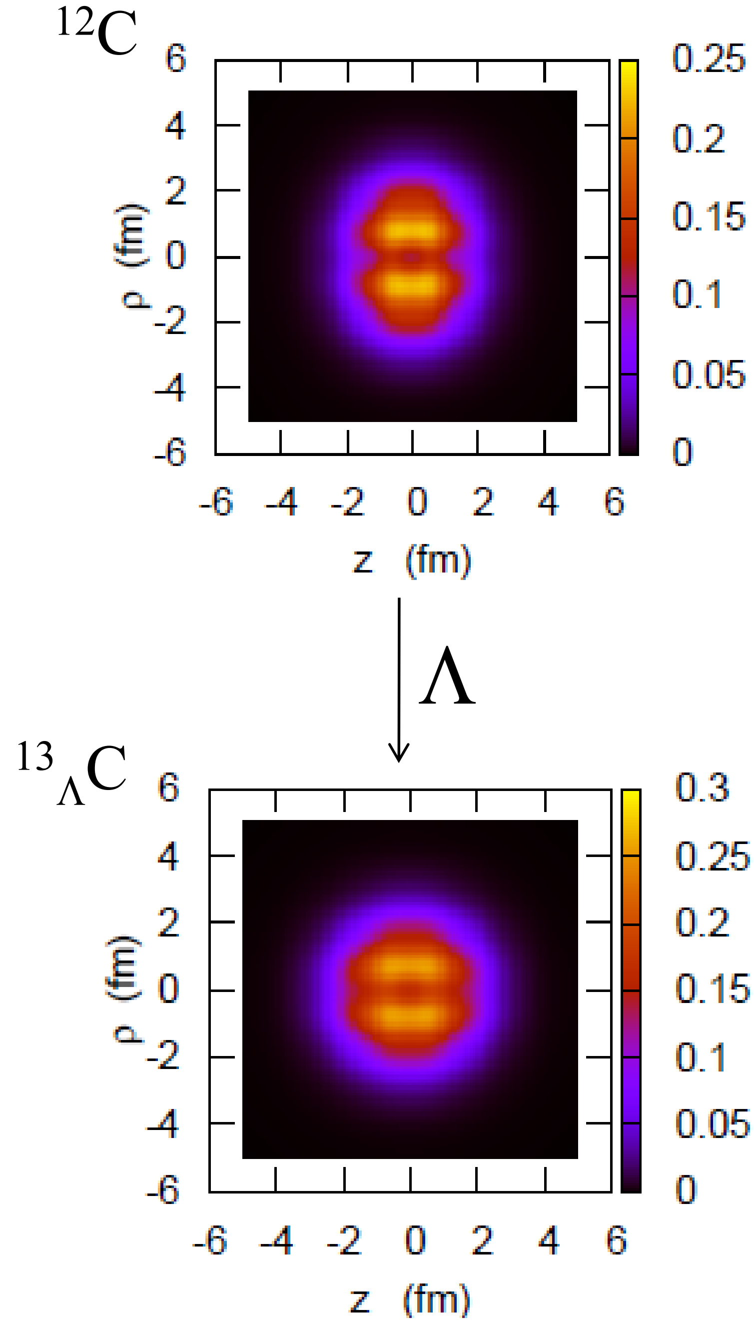

Myaing Thi Win and K.H., PRC78('08)054311

Angular Momentum Projection

Rotated wave function: $|\Psi_\Omega\rangle = \hat{\mathcal{R}}(\Omega)|\Psi\rangle$

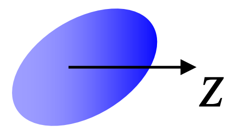

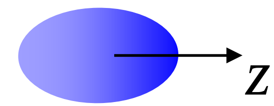

(deformed HF solution)

(note)

$$\langle\Psi_\Omega|H|\Psi_\Omega\rangle = \langle\Psi|\underbrace{\hat{\mathcal{R}}^{-1}H\hat{\mathcal{R}}}_{=\text{ H (for rot. symmetric Hamiltonian)}}|\Psi\rangle = \langle\Psi|H|\Psi\rangle$$

a better wf: a superposition of rotated wave functions

$$\boxed{|\Psi_{\text{proj}}\rangle = \int d\Omega\, f(\Omega)|\Psi_\Omega\rangle}$$

$f(\Omega) \longleftarrow$ variational principle $\langle\delta\Psi_{\text{proj}}|H - E|\Psi_{\text{proj}}\rangle = 0$

$$\int [\langle\Psi_\Omega|H|\Psi_{\Omega'}\rangle - E\,\langle\Psi_\Omega|\Psi_{\Omega'}\rangle]\, f(\Omega')d\Omega' = 0$$

$$\boxed{|\Psi_{\rm proj}\rangle = \int d\Omega\, f(\Omega)|\Psi_\Omega\rangle}$$

$f(\Omega) \longleftarrow$ variational principle

$$\boxed{\int \left[\langle\Psi_\Omega|H|\Psi_{\Omega'}\rangle - E\,\langle\Psi_\Omega|\Psi_{\Omega'}\rangle\right] f(\Omega')d\Omega' = 0}$$

(Hill-Wheeler equation)
cf. Generator Coordinate Method

Solution: Wigner's D-function $\boxed{f(\Omega) = D^{I*}_{MK}(\Omega)}$

(note)

$$\hat{\mathcal{R}}(\Omega)|\phi_{IK}\rangle = \sum_M |\phi_{IM}\rangle\underbrace{\langle\phi_{IM}|\hat{\mathcal{R}}(\Omega)|\phi_{IK}\rangle}_{D^I_{MK}(\Omega)}$$

$$D^I_{M0}(\phi,\theta,\chi) = \sqrt{\frac{4\pi}{2I+1}}Y^*_{IM}(\theta,\phi)$$

$$\int d\Omega D^{I*}_{MK}(\Omega)D^{I'}_{M'K'}(\Omega) = \frac{8\pi^2}{2I+1}\delta_{I,I'}\delta_{M,M'}\delta_{K,K'}$$

Projection Operator

Consider a HF state with the axial symmetry

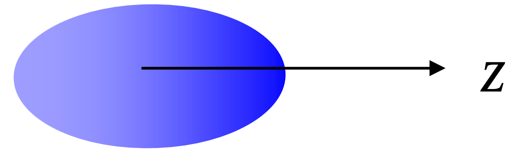

$$|\Psi\rangle = \sum_I C_I |\Psi_{IK}\rangle$$

rotated state:

$$|\Psi_\Omega\rangle = \hat{\mathcal{R}}(\Omega)|\Psi\rangle = \sum_{I,M} C_I \, D^I_{MK}(\Omega)|\Psi_{IM}\rangle$$

$$\boxed{\begin{aligned} |\Psi_{\rm proj}\rangle &= \int d\Omega \, D^{I*}_{MK}(\Omega)|\Psi_\Omega\rangle \\ &= \frac{8\pi^2}{2I+1} C_I \, |\Psi_{IM}\rangle \end{aligned}}$$

or

$$\hat{P}^I_{MK} = \frac{2I+1}{8\pi^2}\int D^{I*}_{MK}(\Omega)\hat{\mathcal{R}}(\Omega)\, d\Omega = |IM\rangle\langle IK|$$

Projected wave function:

$$|\Psi_{IM}\rangle = \hat{P}^I_{MK}|\Psi\rangle = \frac{2I+1}{8\pi^2}\int d\Omega\, D^{I*}_{MK}(\Omega)\hat{\mathcal{R}}(\Omega)\,|\Psi\rangle$$

Projected energy surface:

$$\boxed{E_I = \frac{\langle\Psi_{IM}|H|\Psi_{IM}\rangle}{\langle\Psi_{IM}|\Psi_{IM}\rangle} = \frac{\langle\Psi|(\hat{P}^I_{MK})^\dagger H\,\hat{P}^I_{MK}|\Psi\rangle}{\langle\Psi|(\hat{P}^I_{MK})^\dagger\,\hat{P}^I_{MK}|\Psi\rangle}}$$

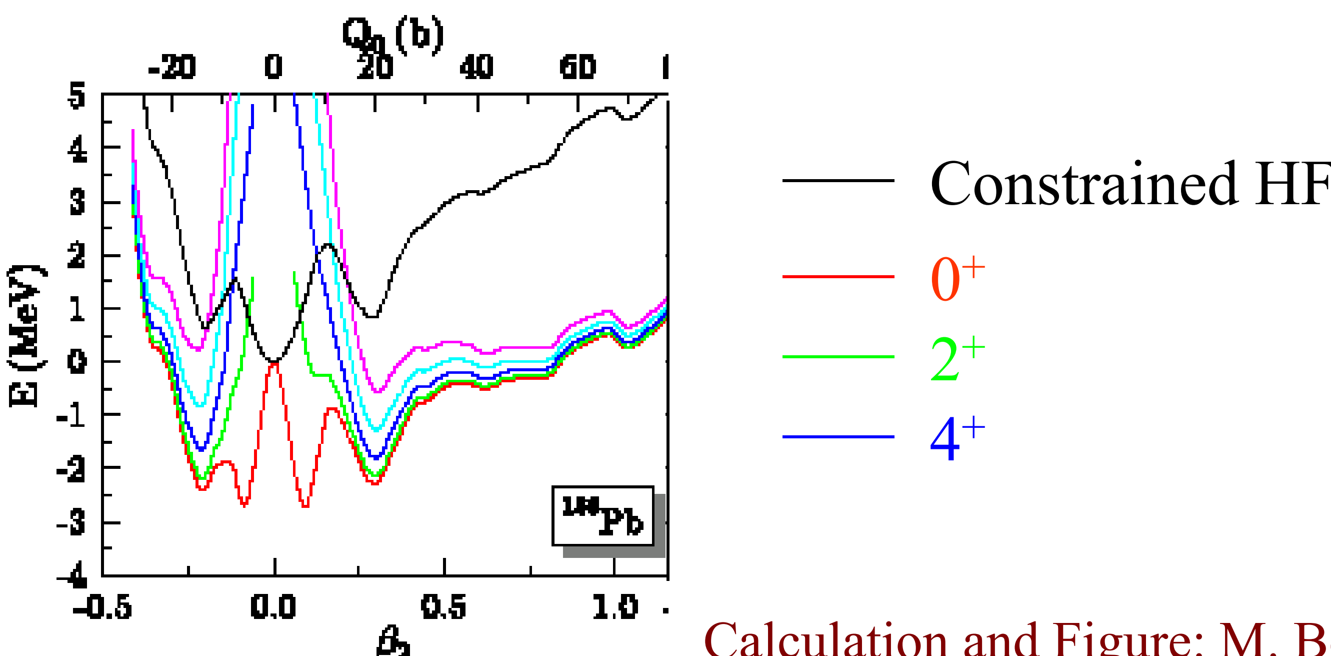

Calculation and Figure: M. Bender

VAP v.s. VBP

➢ Variation *Before* Projection (VBP)

$$\text{minimize } \langle\Psi|H|\Psi\rangle/\langle\Psi|\Psi\rangle \longrightarrow |\Psi_{IM}\rangle = \hat{P}^I_{MK}|\Psi\rangle$$

➢ Variation *After* Projection (VAP)

$$|\Psi_{IM}\rangle = \hat{P}^I_{MK}|\Psi\rangle \longrightarrow \text{minimize } \langle\Psi_{IM}|H|\Psi_{IM}\rangle/\langle\Psi_{IM}|\Psi_{IM}\rangle$$

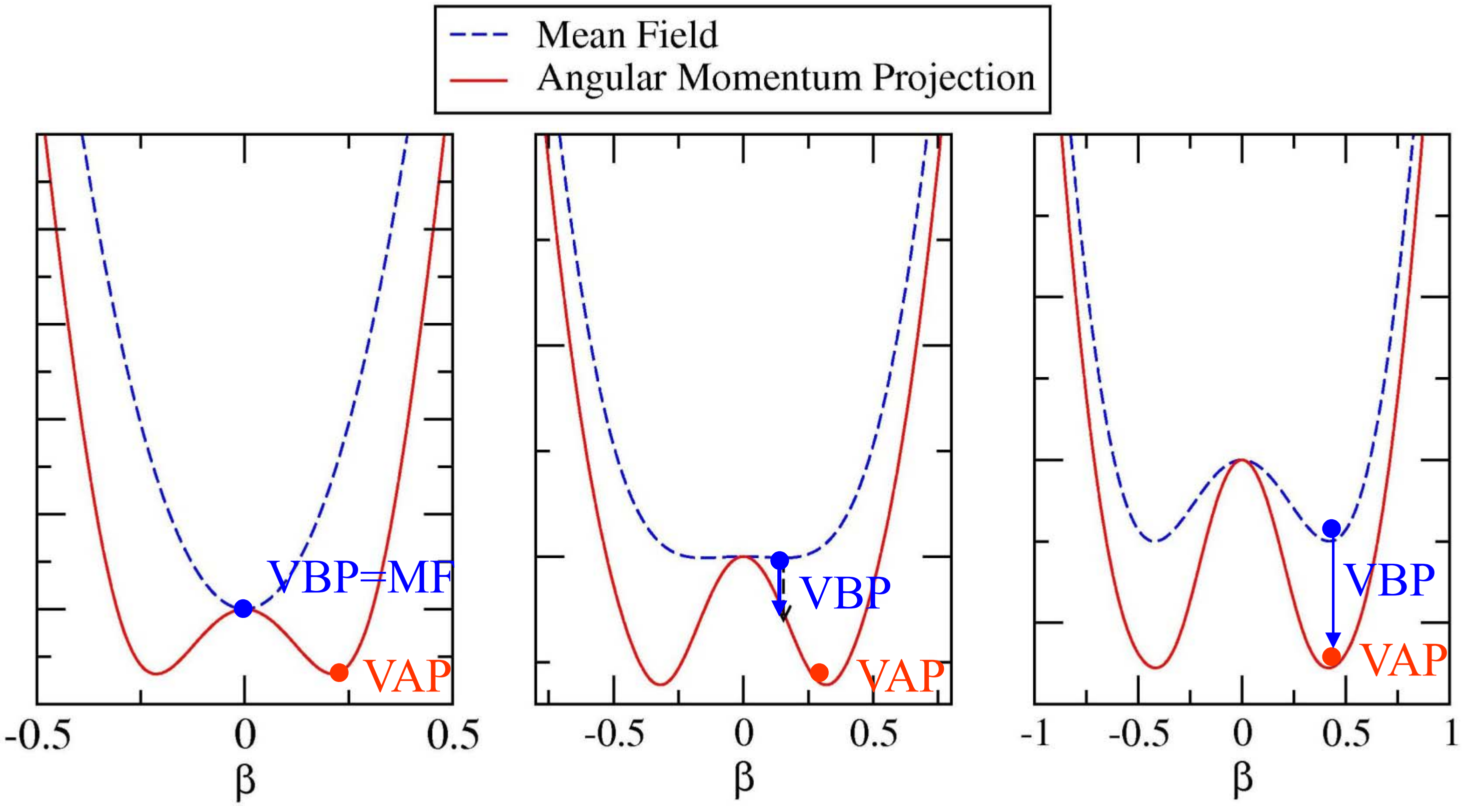

VBP:
simple, but does not work for small deformation. Also, a discontinuity problem

VAP:
robust, but very expensive

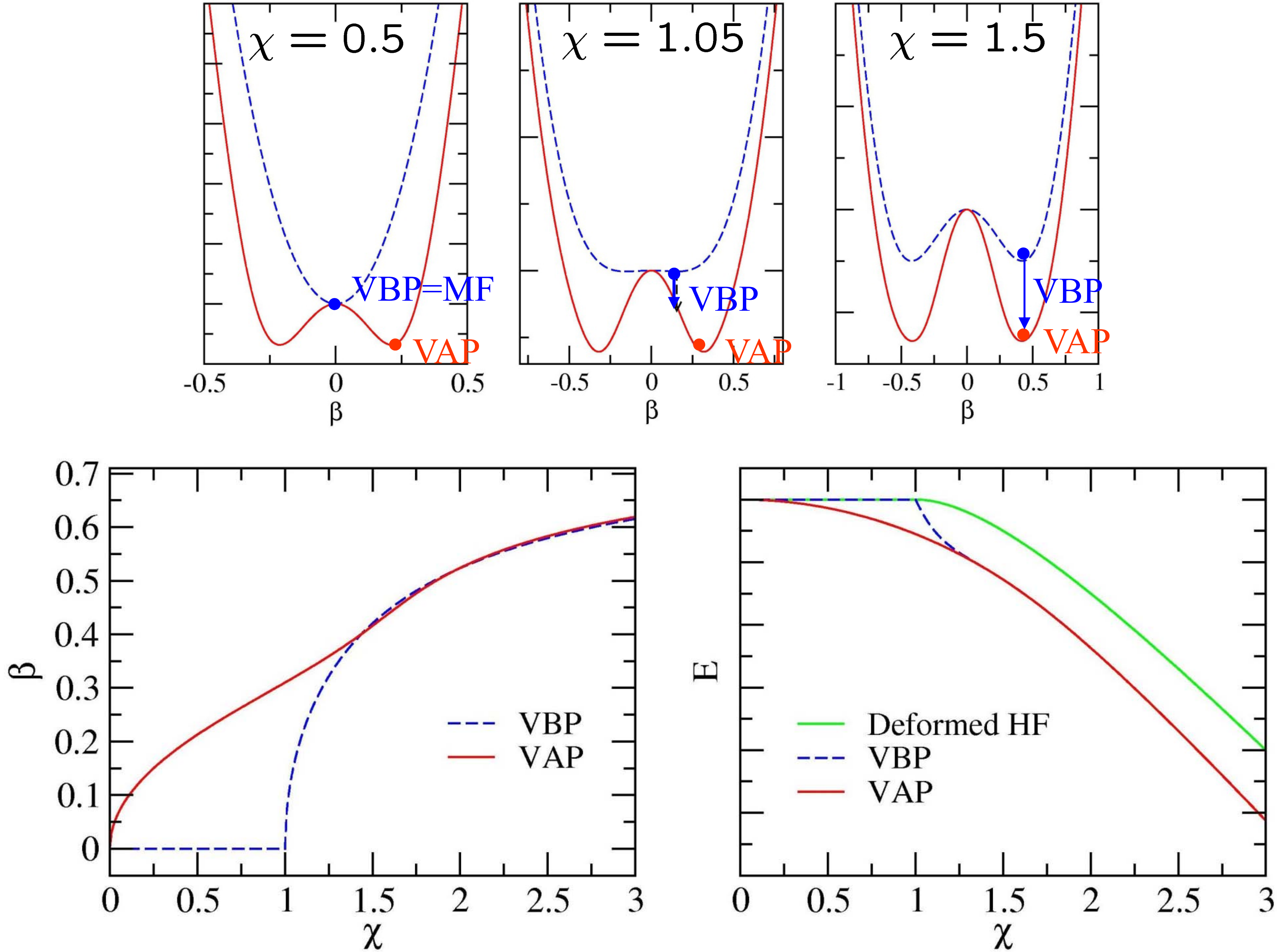

χ : the strength of two-body interaction (for a three-level Lipkin model)

Ref. K. Hagino, P.-G. Reinhard, G.F. Bertsch, PRC65('02)064320

Approximate Projection for large deformation

Projected wave function:

$$|\Psi_{IM}\rangle = \hat{P}^I_{MK}|\Psi\rangle = \frac{2I+1}{8\pi^2}\int d\Omega\, D^{I*}_{MK}(\Omega)\hat{\mathcal{R}}(\Omega)\,|\Psi\rangle$$

Projected energy surface:

$$E_I = \frac{\langle\Psi_{IM}|H|\Psi_{IM}\rangle}{\langle\Psi_{IM}|\Psi_{IM}\rangle} = \frac{\langle\Psi|(\hat{P}^I_{MK})^\dagger H\,\hat{P}^I_{MK}|\Psi\rangle}{\langle\Psi|(\hat{P}^I_{MK})^\dagger\,\hat{P}^I_{MK}|\Psi\rangle}$$

Axial Symmetry, even-even nucleus

$$\boxed{E_{0+} = \frac{\int_0^\pi \sin\theta\,\langle\Psi|H\hat{\mathcal{R}}(\theta)|\Psi\rangle\,d\theta}{\int_0^\pi \sin\theta\,\langle\Psi|\hat{\mathcal{R}}(\theta)|\Psi\rangle\,d\theta} \equiv \frac{\int_0^\pi \sin\theta\,H(\theta)\,d\theta}{\int_0^\pi \sin\theta\,N(\theta)\,d\theta}}$$

For large deformation:

$$\boxed{\begin{aligned} N(\theta) &\sim e^{-\alpha\theta^2} \\ H(\theta) &\sim N(\theta)\cdot(H_0 + H_2\,\theta^2) \end{aligned}}$$

Gaussian Overlap Approximation (GOA)

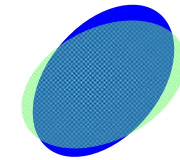

Large deformation

Small deformation

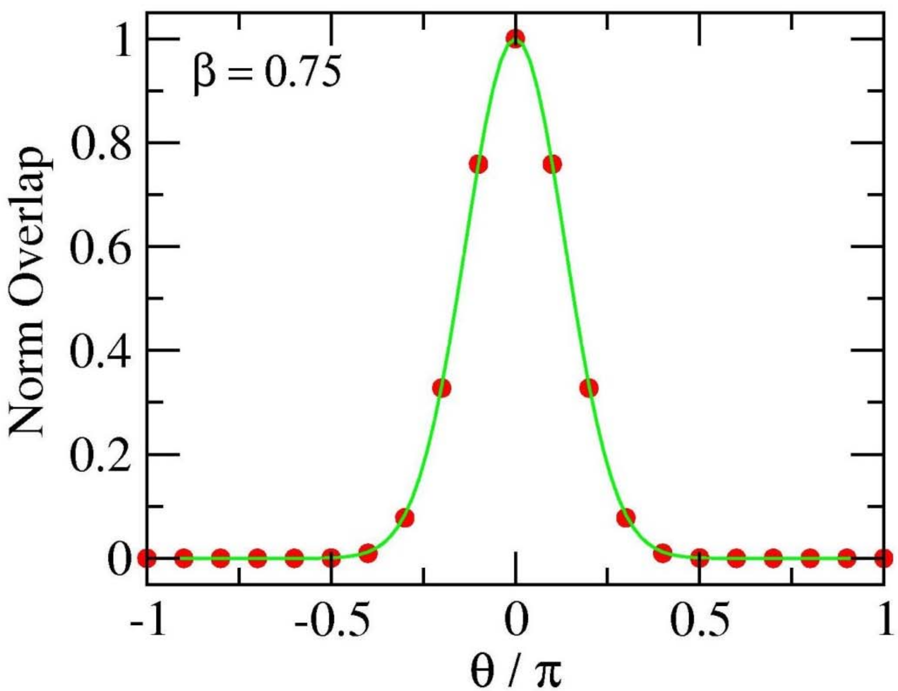

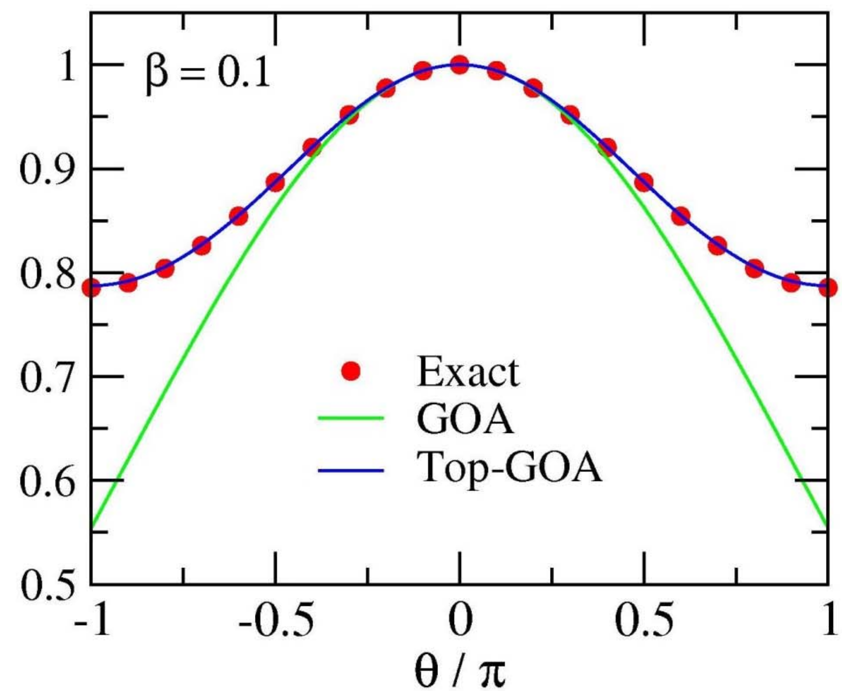

Three-level Lipkin model

K. Hagino, P.-G. Reinhard, G.F. Bertsch, PRC65('02)064320

<u>Topological extension of GOA (top-GOA)</u>

K. Hagino, P.-G. Reinhard, G.F. Bertsch, PRC65('02)064320

$N(\theta),\ \ H(\theta)$: periodicity of 2π

$$\boxed{\begin{aligned} N(\theta) &\sim \exp(-4\alpha\sin^2(\theta/2)) \\ H(\theta) &\sim N(\theta)\cdot(H_0 + 4H_2\sin^2(\theta/2)) \end{aligned}}$$

(Top-GOA)

(note) $\cos\theta = 1 - 2\sin^2(\theta/2) \sim \exp(-2\sin^2(\theta/2))$

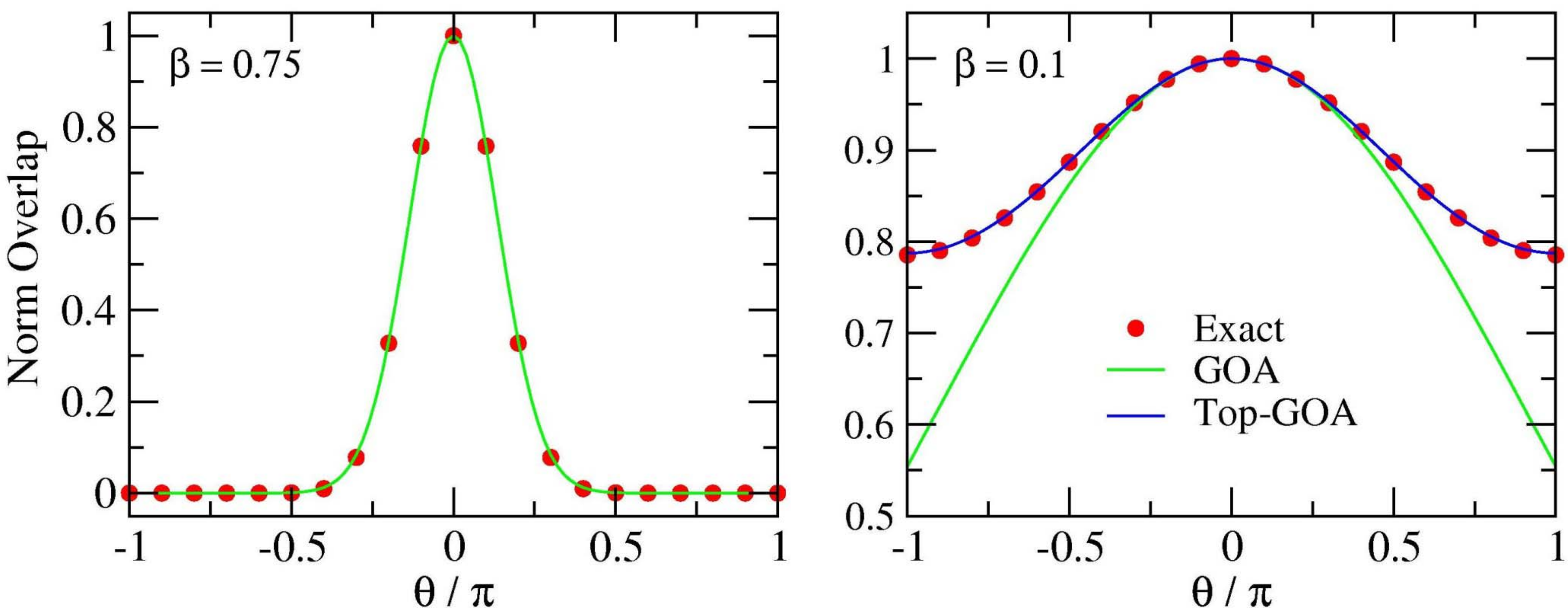

VAP calculations: feasible

Deformed Potential

Deformed density distribution ⇨ deformed single-particle potential

(note) for an axially symmetric spheroid

$$R(\theta) = R_0(1 + \beta_2 Y_{20}(\theta))$$

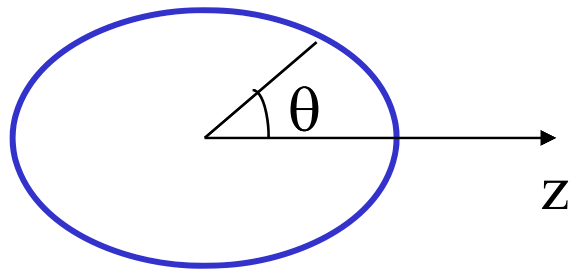

Woods-Saxon potential

$V(r) = -V_0/[1 + \exp((r - R_0)/a]$

⇨ Deformed Woods-Saxon potential

$$\begin{aligned} V(r,\theta) &= -V_0/[1 + \exp((r - R_0 - R_0\beta_2 Y_{20}(\theta))/a] \\ &\sim V_0(r) - \beta_2 R_0 \frac{dV_0}{dr} Y_{20}(\theta) \end{aligned}$$

$$\boxed{\Psi_K(\boldsymbol{r}) = \sum_{j,l} \frac{u_{jlK}(r)}{r} \mathcal{Y}_{jlK}(\hat{\boldsymbol{r}})}$$

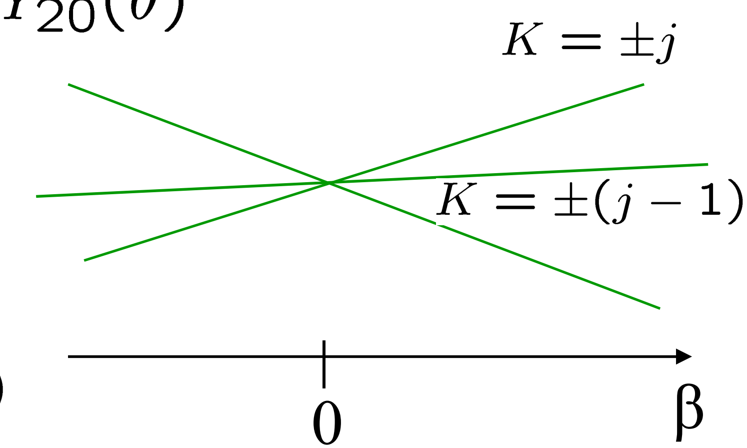

(note) $\langle Y_{lK} | Y_{20} | Y_{lK} \rangle \propto -(3K^2 - l(l+1))$

Geometrical interpretation

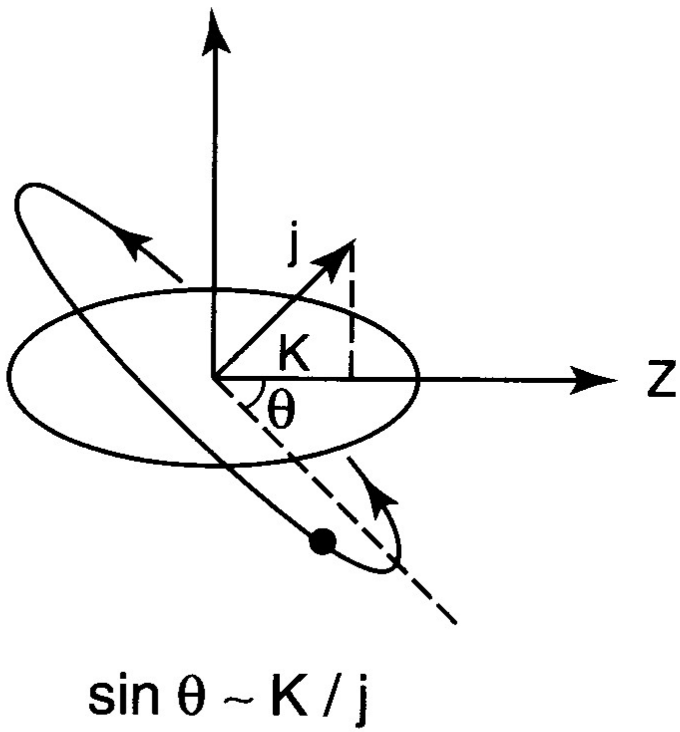

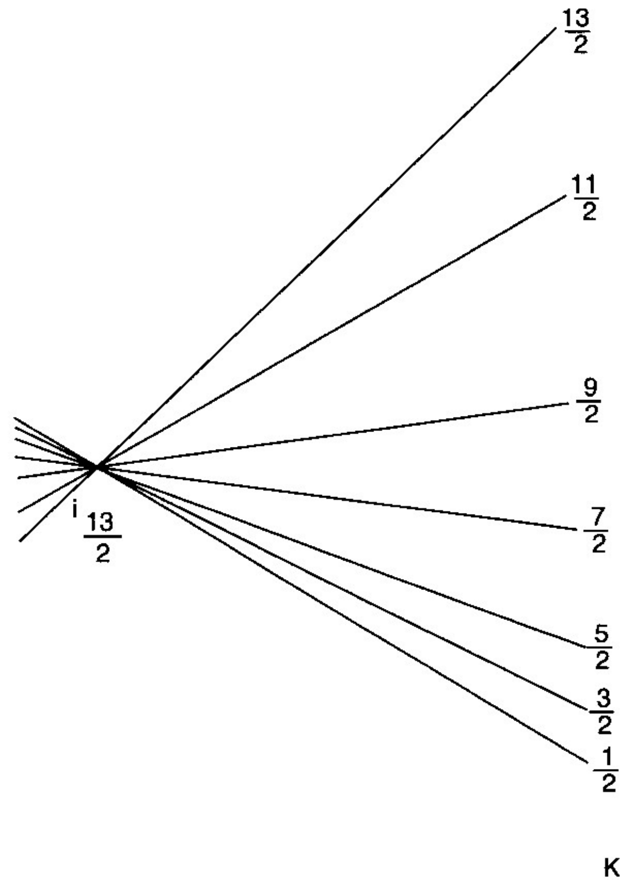

The lower K, the more attraction the orbit feels (for prolate shape).

For large deformation: mixing of j and l quantum numbers

$$\Psi_K(\boldsymbol{r}) = \sum_{j,l} \frac{u_{jlK}(r)}{r} \mathcal{Y}_{jlK}(\hat{\boldsymbol{r}})$$

$$V(r,\theta) \sim V_0(r) - \beta_2 R_0 \frac{dV_0}{dr} Y_{20}(\theta)$$

$$Y_{20}(\theta):\ \text{parity even},\ \delta m_z = 0$$

$\Rightarrow$ Good quantum numbers: parity, K

$$\begin{aligned}
|K^\pi\rangle = \left|\frac{1}{2}^+\right\rangle &= C^{(1/2)}_{s_{1/2}}|s_{1/2}\rangle + C^{(1/2)}_{d_{3/2}}|d_{3/2}\rangle + C^{(1/2)}_{d_{5/2}}|d_{5/2}\rangle + \cdots \\
\left|\frac{3}{2}^+\right\rangle &= C^{(3/2)}_{d_{3/2}}|d_{3/2}\rangle + C^{(3/2)}_{d_{5/2}}|d_{5/2}\rangle + \cdots \\
\left|\frac{1}{2}^-\right\rangle &= C^{(1/2)}_{p_{1/2}}|p_{1/2}\rangle + C^{(1/2)}_{f_{5/2}}|f_{5/2}\rangle + C^{(1/2)}_{f_{7/2}}|f_{7/2}\rangle + \cdots
\end{aligned}$$

変形したポテンシャル中の粒子の運動（簡単のためスピンなし）

$$\boxed{\left[-\frac{\hbar^2}{2m}\nabla^2 + V_0(r) + V_2(r)Y_{20}(\theta) - E\right]\Psi(\boldsymbol{r}) = 0}$$

結合チャンネル法

$$\Psi(\boldsymbol{r}) = \Psi_K(\boldsymbol{r}) = \sum_l \frac{u_l(r)}{r} Y_{lK}(\hat{\boldsymbol{r}})$$ と展開

$$\langle Y_{lK}|H - E|\Psi\rangle = 0$$

coupled-channels equations

$$\left[-\frac{\hbar^2}{2m}\frac{d^2}{dr^2} + V_0(r) + \frac{l(l+1)\hbar^2}{2mr^2} - E\right] u_l(r)$$

$$= -V_2(r)\sum_{l'}\langle Y_{lK}|Y_{20}|Y_{l'K}\rangle\, u_{l'}(r)$$

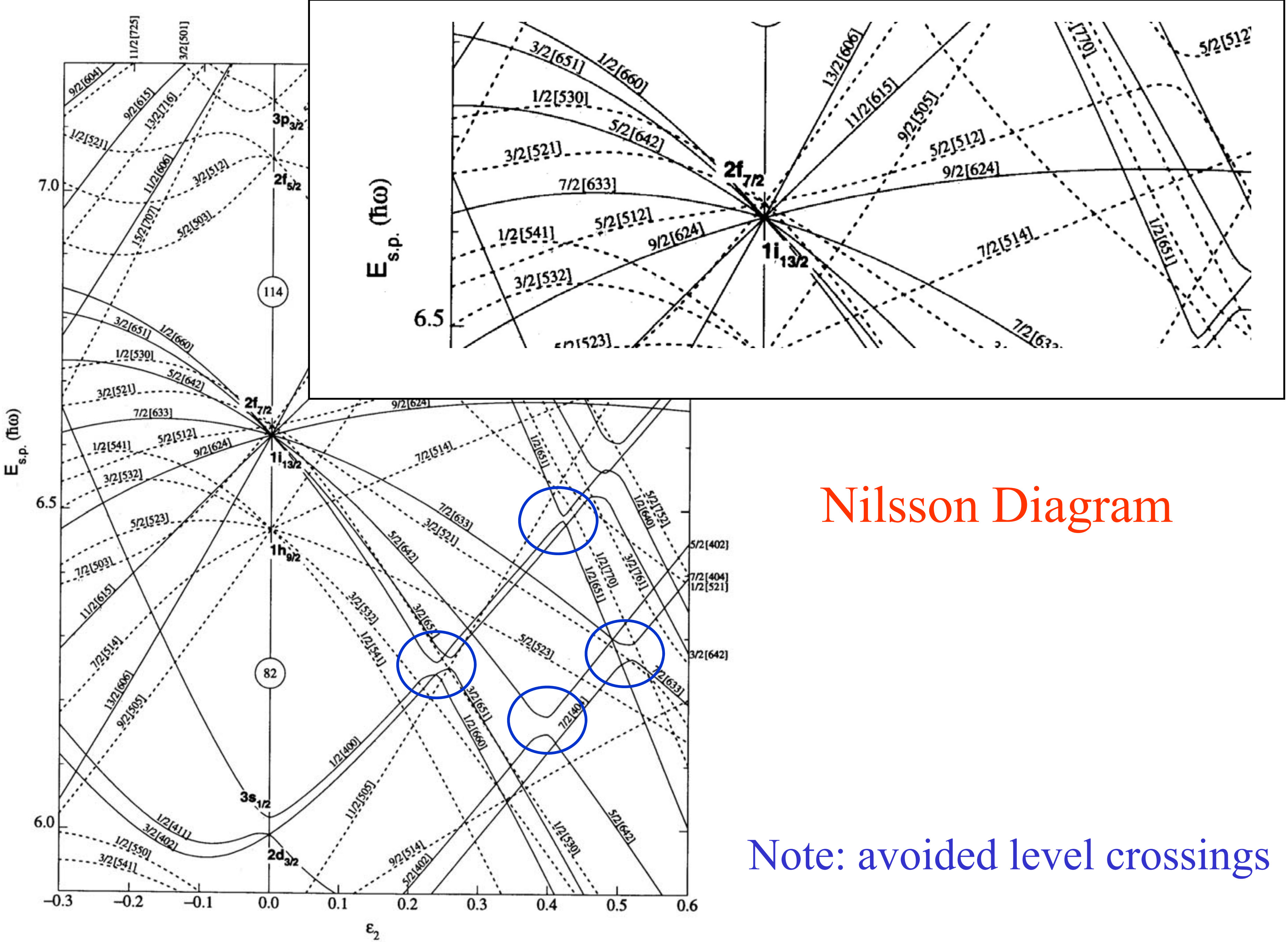

Figure 13. Nilsson diagram for protons, $Z \geq 82$ ($\varepsilon_4 = \varepsilon_2^2/6$).

Nilsson Diagram

Note: avoided level crossings

Avoided level crossing

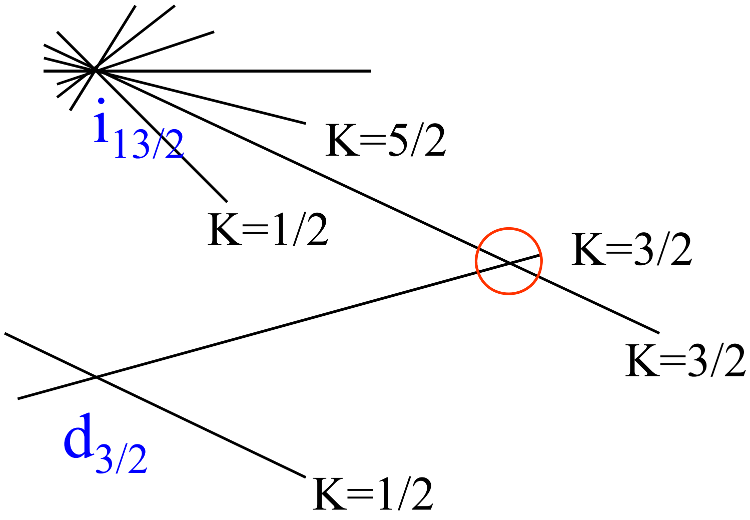

Example:

$$\begin{pmatrix} -\epsilon x & V \\ V & \epsilon x \end{pmatrix}$$

$$\rightarrow \lambda_{\pm}(x) = \pm\sqrt{\epsilon^2 x^2 + V^2}$$

diagonalization

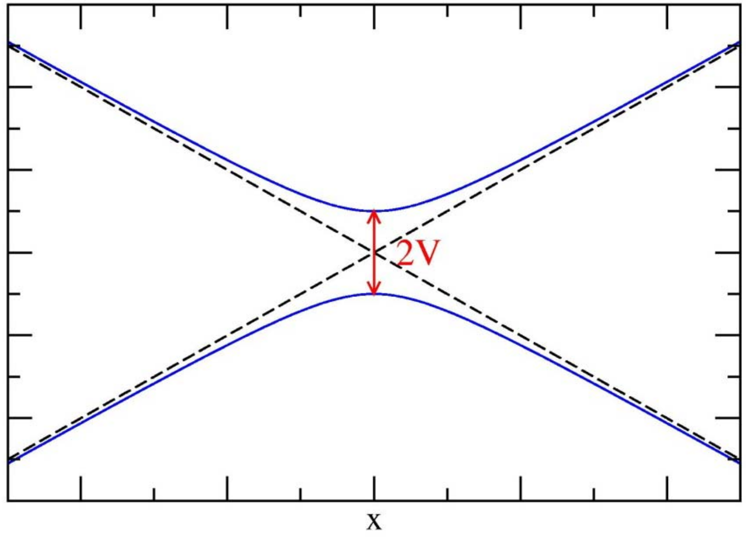

Interaction between $|\mathcal{Y}_{\frac{13}{2},6,\frac{3}{2}}\rangle$ and $|\mathcal{Y}_{\frac{3}{2},2,\frac{3}{2}}\rangle$

$$\begin{pmatrix} \langle\mathcal{Y}_{\frac{13}{2},6,\frac{3}{2}}|H|\mathcal{Y}_{\frac{13}{2},6,\frac{3}{2}}\rangle & \langle\mathcal{Y}_{\frac{13}{2},6,\frac{3}{2}}|H|\mathcal{Y}_{\frac{3}{2},2,\frac{3}{2}}\rangle \\ \langle\mathcal{Y}_{\frac{3}{2},2,\frac{3}{2}}|H|\mathcal{Y}_{\frac{13}{2},6,\frac{3}{2}}\rangle & \langle\mathcal{Y}_{\frac{3}{2},2,\frac{3}{2}}|H|\mathcal{Y}_{\frac{3}{2},2,\frac{3}{2}}\rangle \end{pmatrix}$$

Two levels with the same quantum numbers never cross (an infinitesimal interaction causes them to repel).

"avoided crossing" or "level repulsion"

結合チャンネル方程式の解き方

変形したポテンシャル中の粒子の運動（簡単のためスピンなし）

$$\left[-\frac{\hbar^2}{2m}\nabla^2 + V_0(r) + V_2(r)Y_{20}(\theta) - E\right]\Psi(\boldsymbol{r}) = 0$$

●基底展開法　または
●座標表示（結合チャンネル方程式）

結合チャンネル法

$$\Psi(\boldsymbol{r}) = \Psi_K(\boldsymbol{r}) = \sum_l \frac{u_l(r)}{r} Y_{lK}(\hat{\boldsymbol{r}})$$ と展開

$$\langle Y_{lK}|H - E|\Psi\rangle = 0$$

coupled-channels equations

$$\left[-\frac{\hbar^2}{2m}\frac{d^2}{dr^2} + V_0(r) + \frac{l(l+1)\hbar^2}{2mr^2} - E\right] u_l(r) = -V_2(r)\sum_{l'}\langle Y_{lK}|Y_{20}|Y_{l'K}\rangle\, u_{l'}(r)$$

$$\Psi_K(\boldsymbol{r}) = \sum_l \frac{u_l(r)}{r} Y_{lK}(\hat{\boldsymbol{r}})$$

$$\boxed{\left[-\frac{\hbar^2}{2m}\frac{d^2}{dr^2} + V_0(r) + \frac{l(l+1)\hbar^2}{2mr^2} - E\right] u_l(r) = -V_2(r)\sum_{l'}\langle Y_{lK}|Y_{20}|Y_{l'K}\rangle\, u_{l'}(r)}$$

境界条件（束縛状態）: $u_l \sim r^{l+1} \qquad (r \sim 0)$

$$\rightarrow h_l^{(+)}(i\kappa r) \sim e^{-\kappa r} \qquad (r \to \infty)$$

解き方

2階の N 次連立微分方程式（N はチャンネルの数）

$\longrightarrow$ N 個の線形独立な（原点で）正則解（+ N 個の非正則解）

1. N 個の線形独立な原点正則解を用意
2. 無限遠の境界条件を満たすように線形結合をとる

$$\Psi_K(\boldsymbol{r}) = \sum_l \frac{u_l(r)}{r} Y_{lK}(\hat{\boldsymbol{r}})$$

$$\boxed{\left[-\frac{\hbar^2}{2m}\frac{d^2}{dr^2} + V_0(r) + \frac{l(l+1)\hbar^2}{2mr^2} - E\right] u_l(r) = -V_2(r) \sum_{l'} \langle Y_{lK}|Y_{20}|Y_{l'K}\rangle\, u_{l'}(r)}$$

境界条件（束縛状態）: $u_l \sim r^{l+1} \qquad (r \sim 0)$

$$\to h_l^{(+)}(i\kappa r) \sim e^{-\kappa r} \qquad (r \to \infty)$$

解き方

1．N 個の線形独立な原点正則解を用意: $\vec{\phi}^{(1)}, \cdots, \vec{\phi}^{(N)}$

2．無限遠の境界条件を満たすように線形結合をとる:

$$\vec{u}(r) = \sum_i C_i \vec{\phi}^{(i)}$$

例えば

$\phi_l^{(i)}(r) \to r^{l+1}\delta_{l,i} \qquad r \to 0$ となる N 個の線形独立解

$\phi_l^{(i)}(r) \to A_{li}e^{-\kappa r} + B_{li}e^{+\kappa r} \qquad r \to \infty$ のように振舞うとすると

$u_l(r) \to \sum_i C_i A_{li} e^{-\kappa r} + \sum_i C_i B_{li} e^{\kappa r}$ ➡ $\boxed{\sum_i C_i B_{li} = 0}$ が束縛条件

波動関数のノード（球形の場合）

$V_0 = 58$ MeV,
$R = 4.62$ fm
$a = 0.65$ fm

$l = 0$

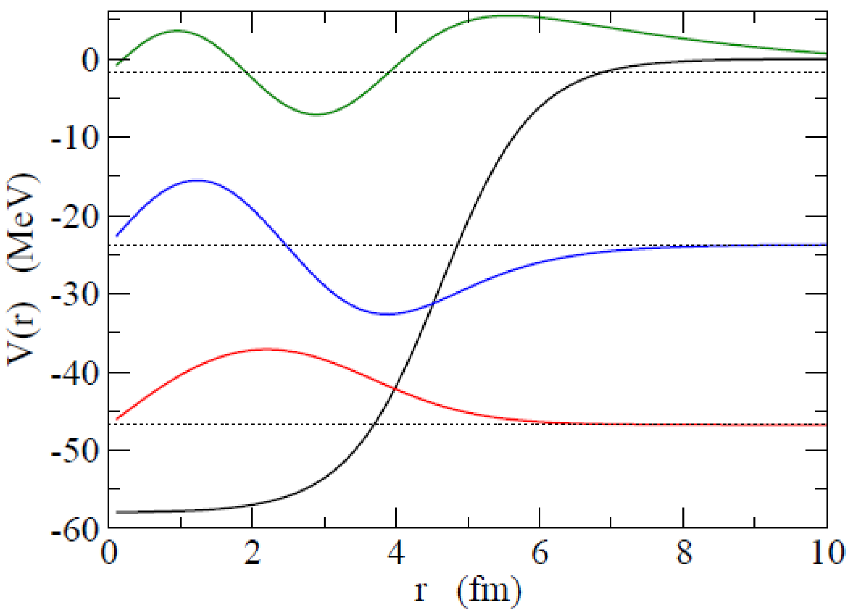

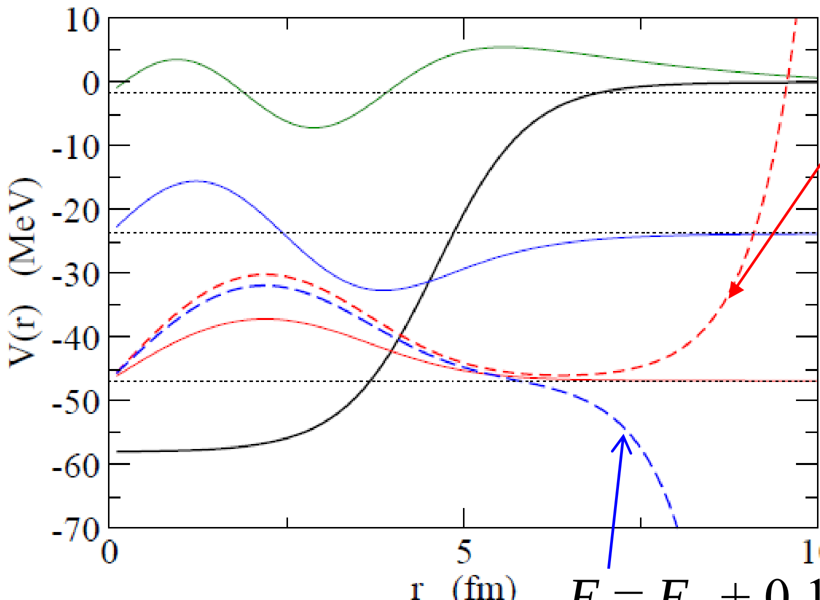

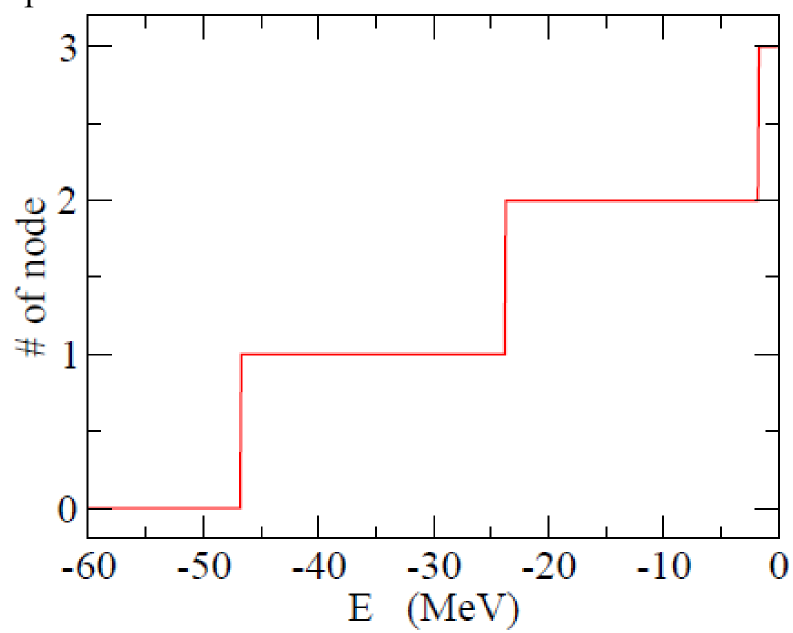

一般化された波動関数のノード（変形核の場合）

B.R. Johnson, J. Chem. Phys. 69('78)4678

1．N 個の線形独立な原点正則解を用意： $\vec{\phi}^{(1)},\cdots,\vec{\phi}^{(N)}$

2．無限遠の境界条件を満たすように線形結合をとる：

$$\vec{u}(r)=\sum_i C_i\vec{\phi}^{(i)}$$

用意した N 個の線形独立解から行列 $\psi_{li}(r)\equiv\phi_l^{(i)}(r)$
を構成

$\Rightarrow$ $f(r)\equiv det(\psi(r))$ がゼロを切るところを一般化されたノードと定義する

(note) $f(R_{\rm box})=0$ が満たされれば、$\vec{u}(r=R_{\rm box})=0$
となる解を作ることができる。
（一般化された box boundary condition）

K.H. and N. Van Giai, NPA735('04)55

計算例: $\beta = 0.2,\ K^{\pi} = 0^{+}$

$$\Psi(\boldsymbol{r}) = \frac{u_0(r)}{r} Y_{00}(\hat{\boldsymbol{r}}) + \frac{u_2(r)}{r} Y_{20}(\hat{\boldsymbol{r}})$$

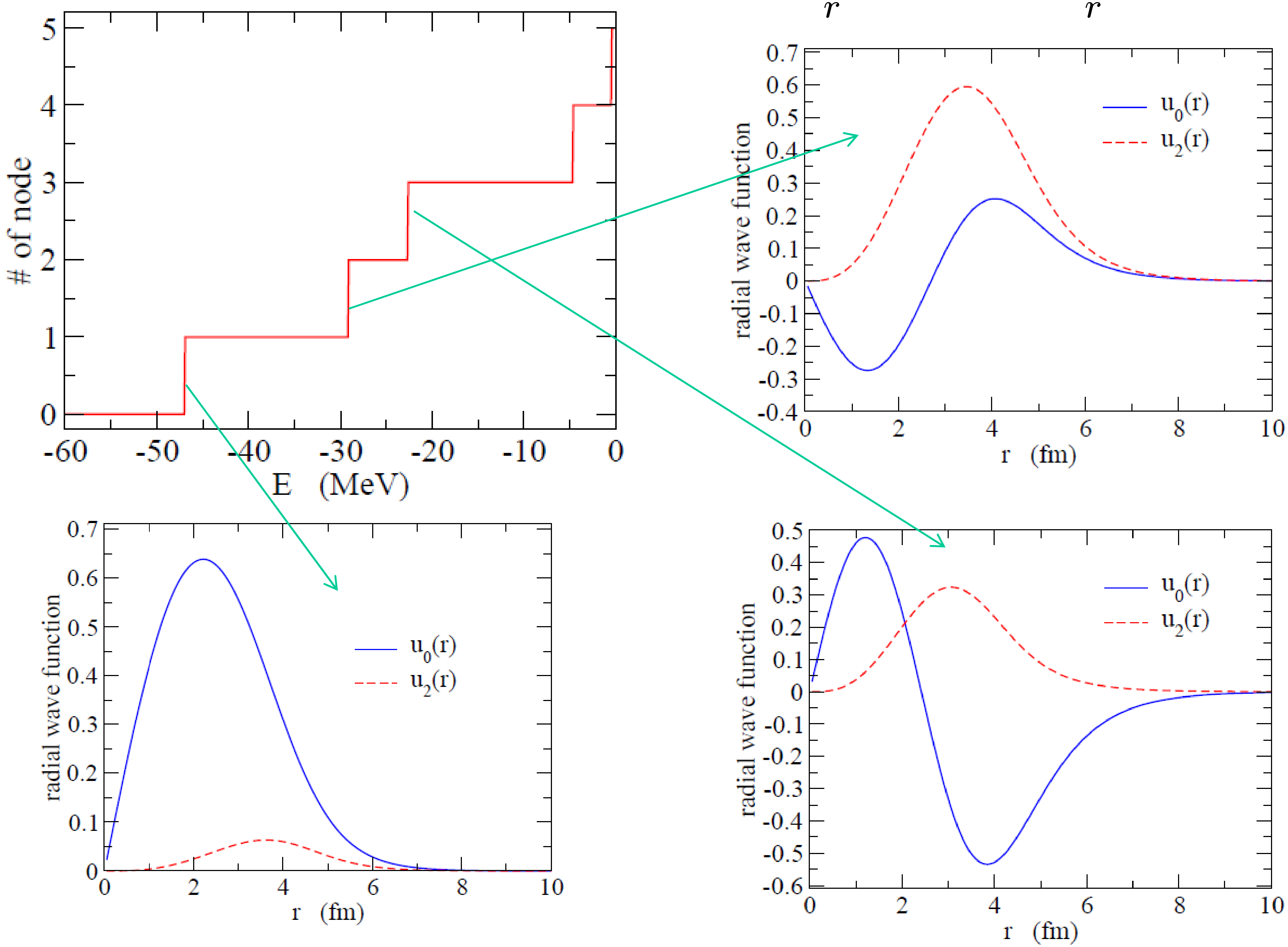

変形核の（一粒子）共鳴状態

Resonances: important role in nuclear structure and reaction

- Pairing correlation in the ground state
  - ➢Large contribution from resonances near the Fermi surface (cf. resonance BCS: Sandulecscu, Van Giai, Liotta, PRC61('00)061301)
  - ➢HFB: many quasi-particle states appear as resonances
- RPA
  - ➢1p1h excitations to a resonance state

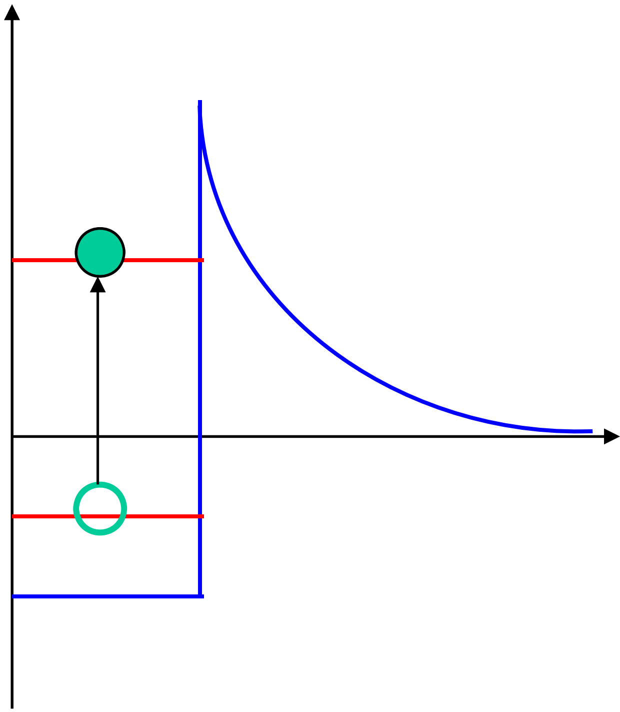

Introduction: Resonances

Resonances: important role in nuclear structure and reaction

- Pairing correlation in the ground state
  - ➢Large contribution from resonances near the Fermi surface (cf. resonance BCS: Sandulecscu, Van Giai, Liotta, PRC61('00)061301)
  - ➢HFB: many quasi-particle states appear as resonances
- RPA
  - ➢1p1h excitations to a resonance state
- Radiative capture reaction

$$(n,\gamma)$$

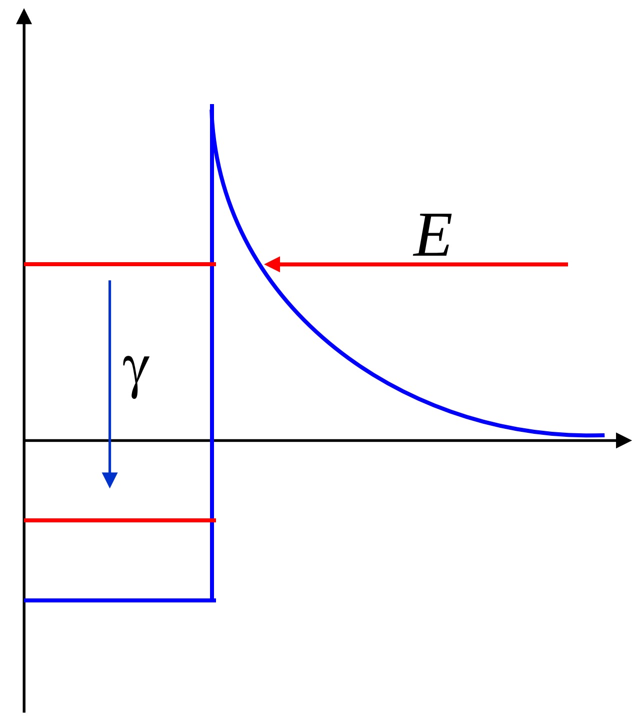

Theoretical methods for resonance

1. Complex E methods

- Gamow state (outgoing boundary condition)

$$u_l(r) \sim \exp[i(kr - l\pi/2)]$$

- Complex scaling method
- Gamow shell model (Berggren basis)

2. Real E method

- Stabilization method (A.U. Hazi and H.S. Taylor, PRA1('70)1109)
- Phase shift analysis

$$\delta(E) = \delta_0(E) + \tan^{-1}\frac{\Gamma}{2(E_R - E)}$$

3. Extrapolation from bound state to resonance

- ACCC method

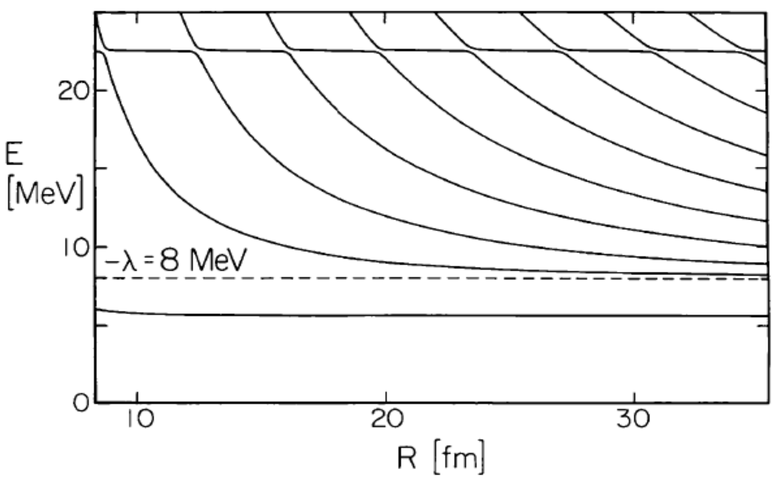

J. Dobaczewski et al., NPA422('84)103

1. Complex *E* methods

- Clear separation between resonance and non-resonant continuum
- Discretization: larger *E* step (cf. Gamow shell model)
- Relatively easy to apply to many-body systems (cf. Hokkaido group)
- Narrow resonance (cf. proton emitter)
- Observable: complex number (in the pole approximation)
- regularization

2. Real *E* method

- Resonance embedded in non-resonant continuum
- Discretization: smaller *E* step
- Many-body systems?
- Narrow resonance: difficult to evaluate Γ
- Observable: real number

3. Extrapolation from bound state to resonance

- Intuitive, and easy to use
- Wave function?
- Accuracy of extrapolation?

1. Complex *E* methods

- Clear separation between resonance and non-resonant continuum
- Discretization: smaller *E* step (cf. Gamow shell model)
- Relatively easy to apply to many-body systems (cf. Hokkaido group)
- Narrow resonance (cf. proton emitter)
- Observable: complex number (in the pole approximation)
- regularization

2. Real *E* method

- Resonance embedded in non-resonant continuum
- Discretization: larger *E* step
- Many-body systems?
- Narrow resonance: difficult to evaluate Γ
- Observable: real number

may not be
big defects for
mean-field calc.

application to
deformed
m.f. potential

3. Extrapolation from bound state to resonance

- Intuitive, and easy to use
- Wave function?
- Accuracy of extrapolation?

Resonance for a spherical potential

$$\left[-\frac{\hbar^2}{2m}\frac{d^2}{dr^2}+V(r)+\frac{l(l+1)\hbar^2}{2mr^2}-E\right]u_l(r)=0$$

$$u_l(r) \sim r^{l+1} \qquad (r\sim 0)$$
$$\to \sin(kr-l\pi/2+\delta) \qquad (r\to\infty)$$

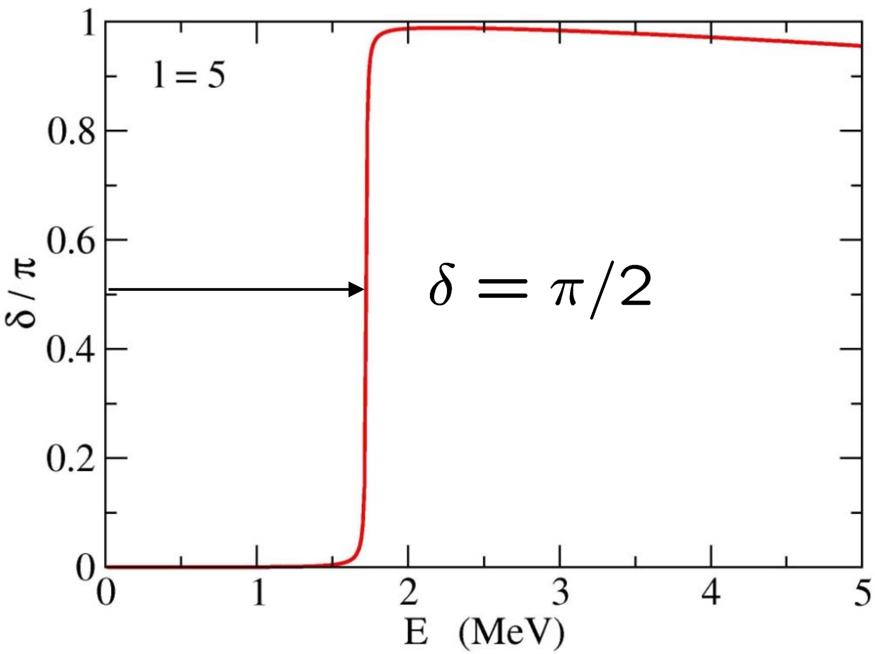

Breit-Wigner formula:

$$\delta(E)=\tan^{-1}\frac{\Gamma}{2(E_R-E)}+\delta_0(E)$$

$$\Longrightarrow \quad \Gamma=\frac{2}{\delta'(E)}$$

cf. 全散乱断面積: $\sigma=\frac{4\pi}{k^2}\sum_l(2l+1)\sin^2\delta_l$

(note) for a broad resonance

$$\delta(E) = \tan^{-1}\frac{\Gamma}{2(E_R - E)} + \delta_0(E)$$

background phase shift

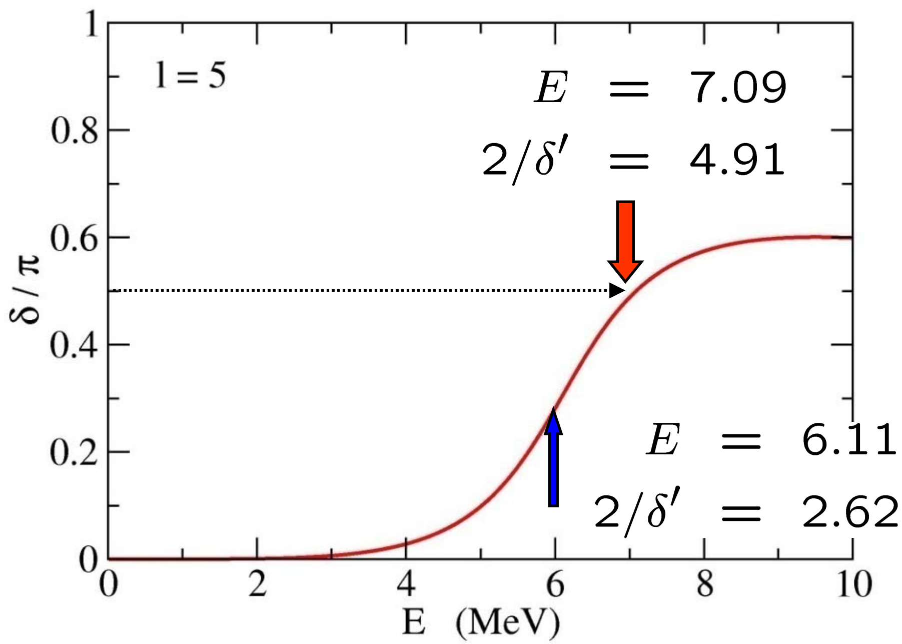

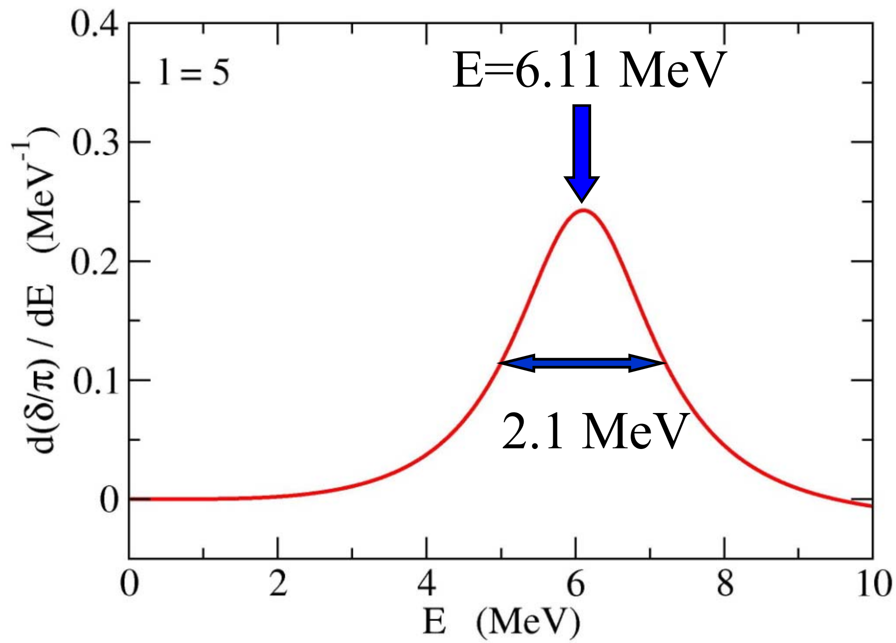

Gamow state: $E = 6.01$ MeV

$\Gamma = 2.22$ MeV

Potential model calculations

(i) WKB method

$$\Gamma_0 = \mathcal{N}\frac{\hbar^2}{4\mu}\exp\left(-2\int_{r_1}^{r_2}|k(r)|dr\right)$$

(ii) Direct method

$$\left[-\frac{\hbar^2}{2\mu}\frac{d^2}{dr^2}+V_{\rm cent}(r)+V(r)-(E-\frac{i}{2}\Gamma_0)\right]u(r)=0$$

$$\begin{aligned} u(r) &\sim r^{l+1} && (r\to 0)\\ &\to \mathcal{N}(G_l(kr)+iF_l(kr)) && (r\to\infty)\end{aligned}$$

$$\Gamma_0 = \text{(outgoing flux) / (normalization):}$$

$$= \frac{\hbar^2 k}{\mu}\mathcal{N}^2 \Big/ \int_0^{r_2}|u(r)|^2 dr$$

(iii) Green's function method (very narrow resonance)

$$\left[-\frac{\hbar^2}{2\mu}\frac{d^2}{dr^2} + V_{\text{cent}}(r) + V(r) - (E - \frac{i}{2}\Gamma_0)\right] u(r) = 0$$

First set $\Gamma_0 = 0$ and find a standing wave:

$$\begin{aligned} \phi(r) &\sim r^{l+1} && (r \to 0) \\ &\to \widetilde{\mathcal{N}} G_l(kr) && (r \to \infty) \end{aligned}$$

Green's function method (Gell-Mann-Goldberger)

$$\begin{aligned} &[\hat{T} + V - E]\Psi = 0 \\ &\hookrightarrow \left[\hat{T} + \frac{Z_D e^2}{r} - E\right]\Psi = \left(\frac{Z_D e^2}{r} - V\right)\Psi \\ &\hookrightarrow \Psi \sim \frac{1}{\hat{T} + \frac{Z_D e^2}{r} - E - i\eta}\left(\frac{Z_D e^2}{r} - V\right)\Phi \end{aligned}$$

$$\Psi \sim \frac{1}{\hat{T} + \frac{Z_D e^2}{r} - E - i\eta} \left(\frac{Z_D e^2}{r} - V \right) \Phi$$

(note)

$$\left\langle \boldsymbol{r} \left| \left(\hat{T} + \frac{Z_D e^2}{r} - E - i\eta \right)^{-1} \right| \boldsymbol{r}' \right\rangle$$

$$= \frac{2\mu}{k\hbar^2} \frac{O_l(kr_>)}{r_>} \mathcal{Y}_{jl}(\hat{\boldsymbol{r}}_>) \cdot \mathcal{Y}^*_{jl}(\hat{\boldsymbol{r}}_<) \frac{F_l(kr_<)}{r_<}$$

For $r \to \infty, \; u(r) \to \mathcal{N}(G_l(kr) + iF_l(kr))$
with

$$\boxed{\mathcal{N} = -\frac{2\mu}{\hbar^2 k} \int_0^\infty F_l(kr)(V(r) - Z_D e^2/r)\phi(r)}$$

Resonances in multi-channel systems

Mean-field equation: $[T + V - E]\,\psi = 0$

deformed potential: $V(\boldsymbol{r}) = V_0(r) + \underbrace{V_2(r)Y_{20}(\hat{\boldsymbol{r}}) + \cdots}_{\text{mixing of ang. mom.}}$

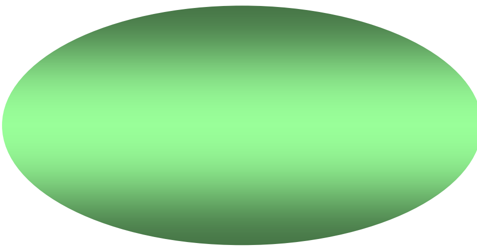

single particle wave function: $\boxed{\psi(\boldsymbol{r}) = \sum_l \frac{u_l(r)}{r} Y_{lK}(\hat{\boldsymbol{r}})}$

$\langle Y_{lK}|H - E|\psi\rangle = 0$

coupled-channels equations

$$\boxed{\begin{aligned}&\left[-\frac{\hbar^2}{2m}\frac{d^2}{dr^2} + V_0(r) + \frac{l(l+1)\hbar^2}{2mr^2} - E\right] u_l(r)\\ &\qquad = -V_2(r)\sum_{l'}\langle Y_{lK}|Y_{20}|Y_{l'K}\rangle\, u_{l'}(r) + \cdots\end{aligned}}$$

coupled-channels equations

$$\left[-\frac{\hbar^2}{2m}\frac{d^2}{dr^2}+V_0(r)+\frac{l(l+1)\hbar^2}{2mr^2}-E\right]u_l(r)$$
$$=-V_2(r)\sum_{l'}\langle Y_{lK}|Y_{20}|Y_{l'K}\rangle\,u_{l'}(r)+\cdots$$

spherical case

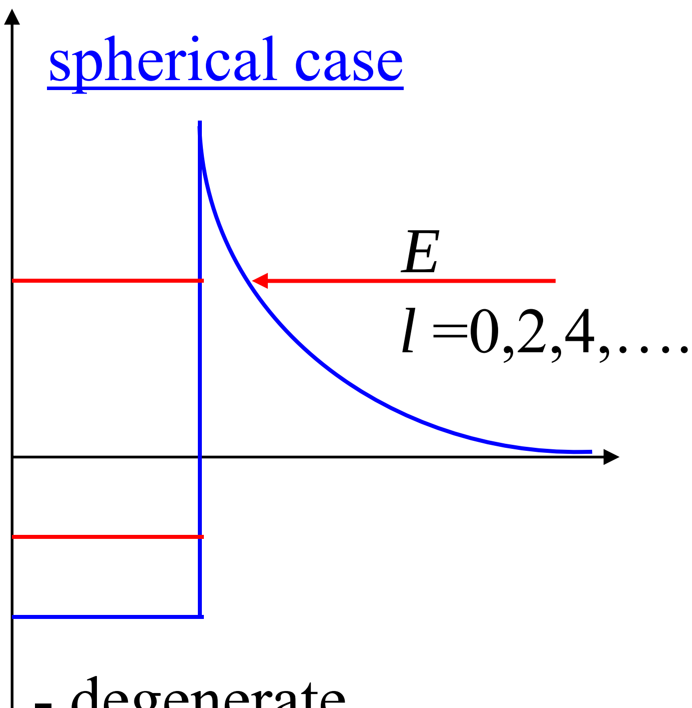

- degenerate
- form a complete set
  (linear indep. solution)

deformed case

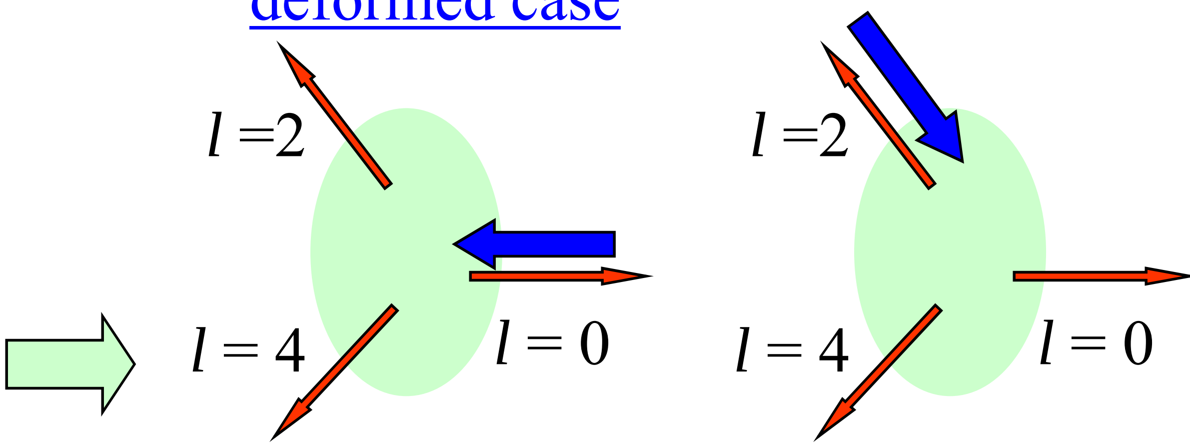

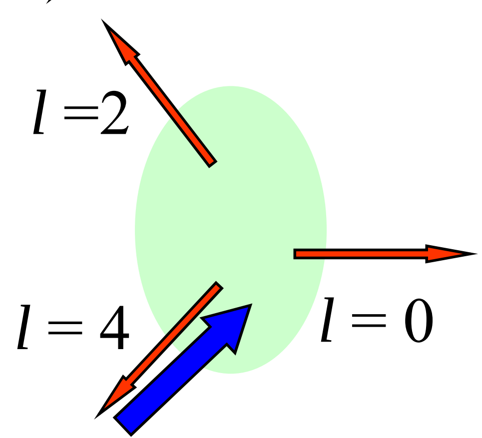

the same # of lin. indep. solutions

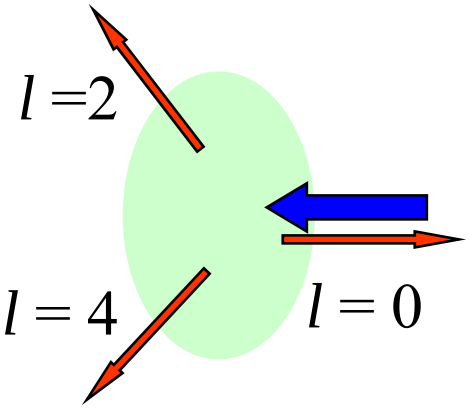

$l_0 = 0$

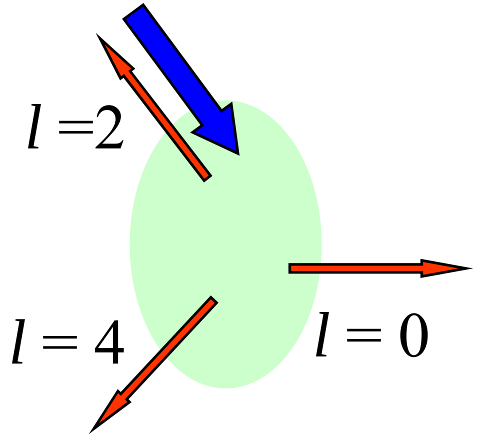

$l_0 = 2$

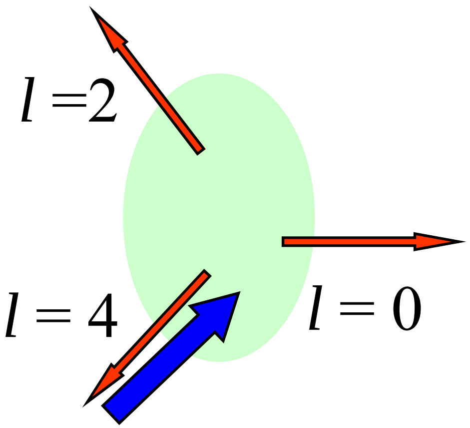

$l_0 = 4$

$$\boxed{\psi_{l_0}(\boldsymbol{r}) = \sum_l \frac{u_{ll_0}(r)}{r} Y_{lK}(\hat{\boldsymbol{r}})}$$

$$u_{ll_0}(r) \;\to\; e^{-i(kr - l\pi/2)}\delta_{l,l_0} - S_{ll_0} e^{i(kr - l\pi/2)}$$

S-matrix

How to characterize a multi-channel resonance?

$$\boxed{u_{ll_0}(r) \to e^{-i(kr-l\pi/2)}\delta_{l,l_0} - S_{ll_0}\,e^{i(kr-l\pi/2)}}$$

(note) spherical case: $S_{ll_0} = S_l\,\delta_{l,l_0} = e^{2i\delta_l}\,\delta_{l,l_0}$

✧ How about looking at the diagonal components???

$$S_{ll} = \eta_l \cdot e^{2i\delta_{ll}}$$

cf. S-matrix from an optical potential

Model:

$$V(r,\theta) = V_{\rm WS}(r) - \beta_2 R_0 \frac{dV_{\rm WS}}{dr} Y_{20}(\theta)$$

$$\begin{aligned} V_0 &= 48\ \mathrm{MeV} \\ R_0 &= 4.5\ \mathrm{fm} \\ a &= 0.63\ \mathrm{fm} \\ \beta_2 &= 0.1 \\ K &= 0 \end{aligned}$$

<u>Gamow states:</u>

1. $E_{res} = 3.78$ MeV
   $\Gamma = 0.53$ MeV
   (*g*-wave dominance)

2. $E_{res} = 1.59$ MeV
   $\Gamma = 1.57$ MeV
   (*d*-wave dominance)

s, *d*, *g* –wave mixing ($K^\pi = 0^+$)

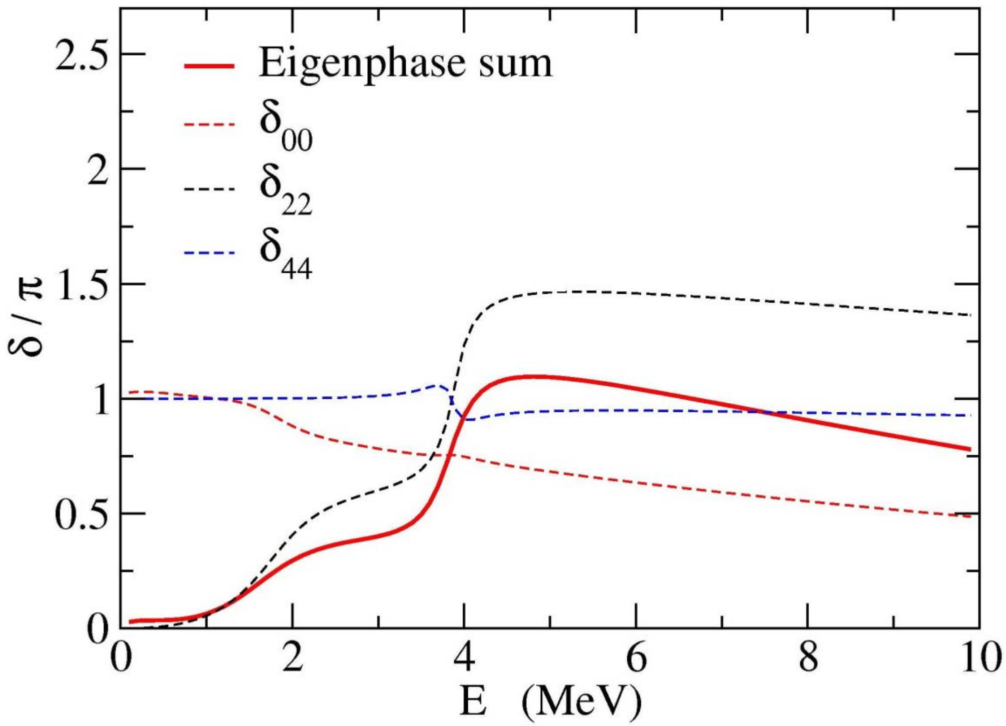

cf. wf component for a resonance: K. Yoshida and K.H., PRC72('05)064311

Eigen-channel approach

ref. D. Loomba et al., JCP75 ('81) 4546

$$\begin{cases} \psi_{l_0}(\boldsymbol{r}) = \sum_l \frac{u_{ll_0}(r)}{r} Y_{lK}(\hat{\boldsymbol{r}}) \\ u_{ll_0}(r) \to e^{-i(kr-l\pi/2)}\delta_{l,l_0} - S_{ll_0}\, e^{i(kr-l\pi/2)} \end{cases}$$

<u>mix the basis states so that the resonance can be visualized clearly</u>

1. diagonalize the S-matrix:

$$\boxed{(U^\dagger S U)_{aa'} = e^{2i\delta_a}\delta_{a,a'}}$$

2. define the eigen-channel with *U*:

$$\tilde{\psi}_a(\boldsymbol{r}) \equiv \sum_{l_0} \psi_{l_0}(\boldsymbol{r}) U_{l_0 a}$$

(note) as $r \to \infty$

$$\boxed{\tilde{\Psi}_a(\boldsymbol{r}) \to \frac{1}{r}\sum_l \left\{ e^{-i(kr-l\pi/2)} - e^{2i\delta_a} e^{i(kr-l\pi/2)} \right\} U_{la} Y_{lK}(\hat{\boldsymbol{r}})}$$

(note) Low energy Heavy-Ion reactions

$$\psi(\boldsymbol{r}) = \sum_{l} \frac{u_I(r)}{r} Y_{J0}(\hat{\boldsymbol{r}}) |\phi_I\rangle$$

- physical channel: spin of the rotor (I)
- eigen-channel: orientation angle of the rotor

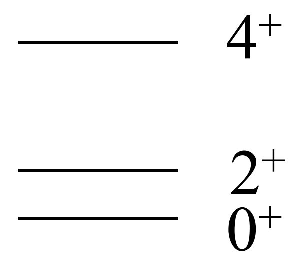

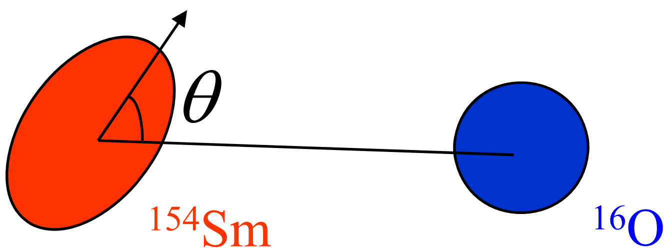

$$\boxed{\sigma_{\rm fus}(E) = \int_0^1 d(\cos\theta)\sigma_{\rm fus}(E;\theta)}$$

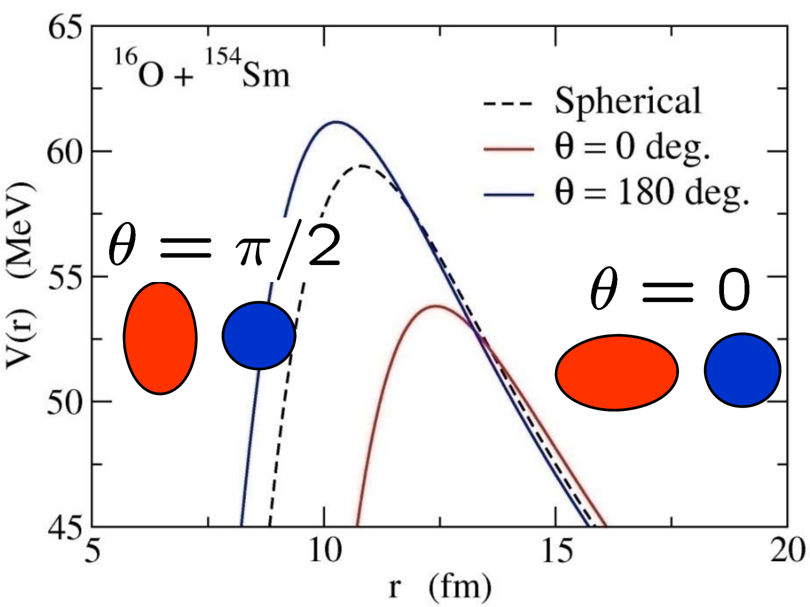

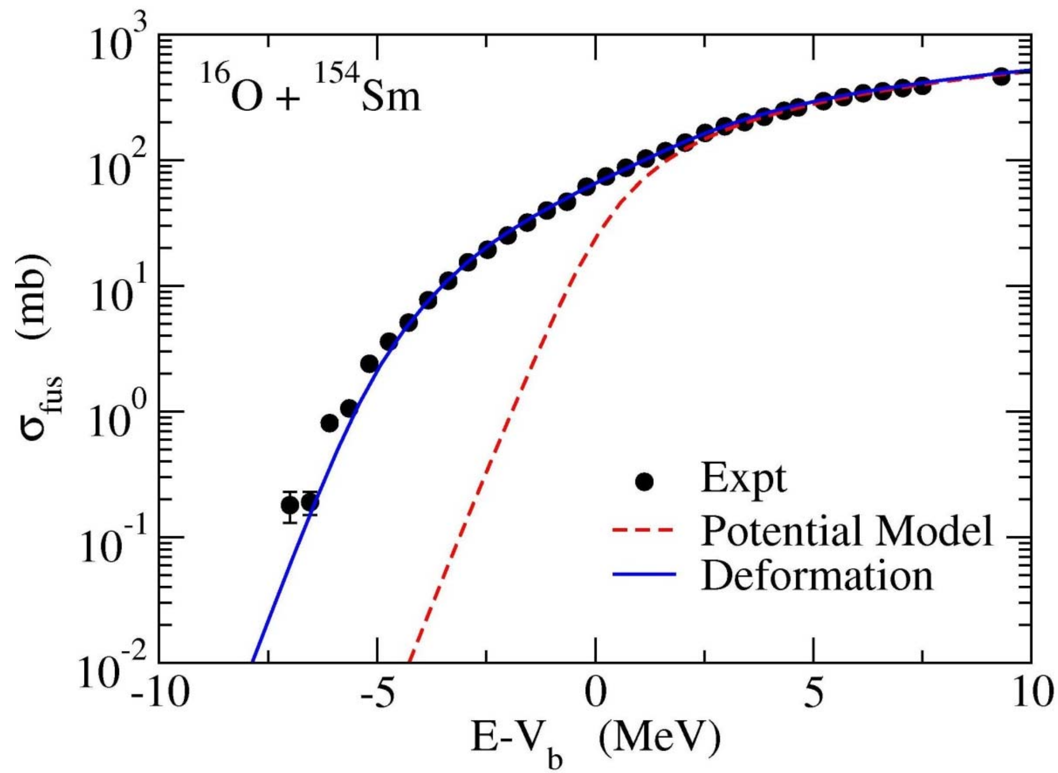

Eigen-phase sum

H.A. Weidenmuller, Phys. Lett. 24B('67)441
A.U. Hazi, PRA19('79)920
K.H. and N. Van Giai, NPA735 ('04) 55

$$(U^\dagger S U)_{aa'} = e^{2i\delta_a}\delta_{a,a'} \longrightarrow \boxed{\Delta \equiv \sum_a \delta_a}$$

Breit-Wigner formula

$$S_{\alpha\beta} = e^{2i\phi_\alpha}\,\delta_{\alpha,\beta} - i\frac{\sqrt{\Gamma_\alpha\Gamma_\beta}}{E-E_R+i\Gamma/2}\,e^{i(\phi_\alpha+\phi_\beta)}$$

$$\Longrightarrow \boxed{\Delta(E) = \tan^{-1}\frac{\Gamma}{2(E_R-E)} + \Delta_0(E)}$$

Eigenphase sum: satisfies the single channel formula

s, d, g –wave mixing ($K^{\pi} = 0^{+}$)

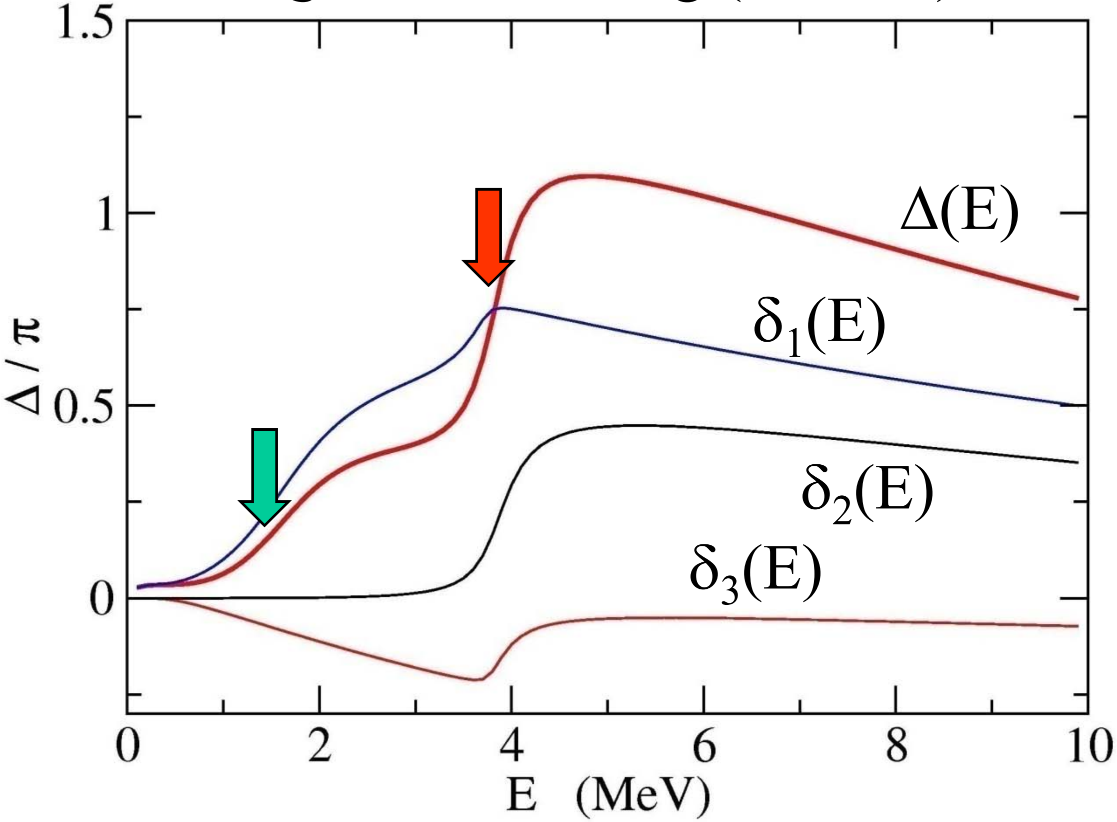

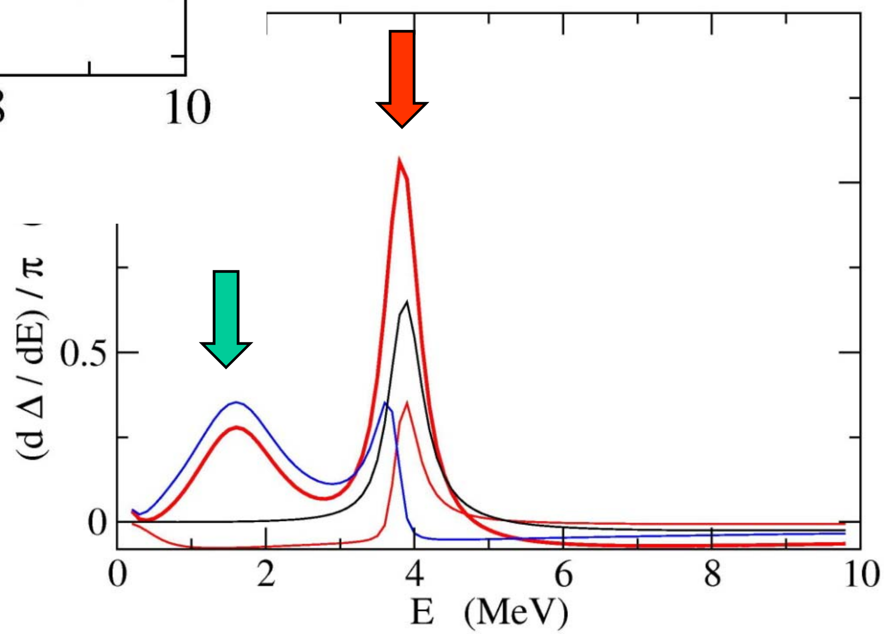

<u>Gamow states:</u>

1. $E_{res} = 3.78$ MeV
   $\Gamma = 0.53$ MeV
2. $E_{res} = 1.59$ MeV
   $\Gamma = 1.57$ MeV

Multi-channel resonance with box discretization

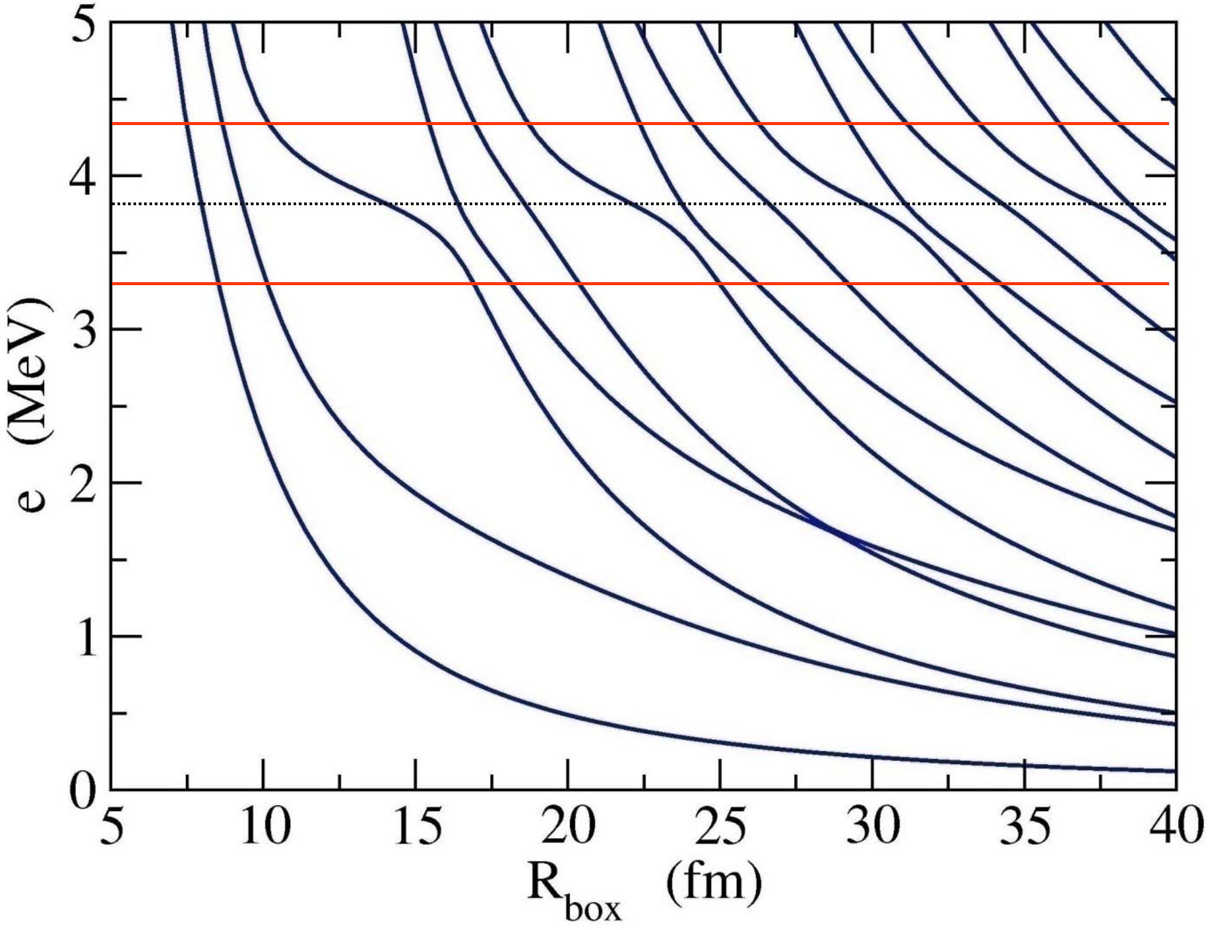

Gamow states:

1. $E_{res} = 3.78$ MeV
   $\Gamma = 0.53$ MeV
2. $E_{res} = 1.59$ MeV
   $\Gamma = 1.57$ MeV

（参考）Particle-Rotor Model (strong coupling limit)

変形した芯核と一粒子運動の結合

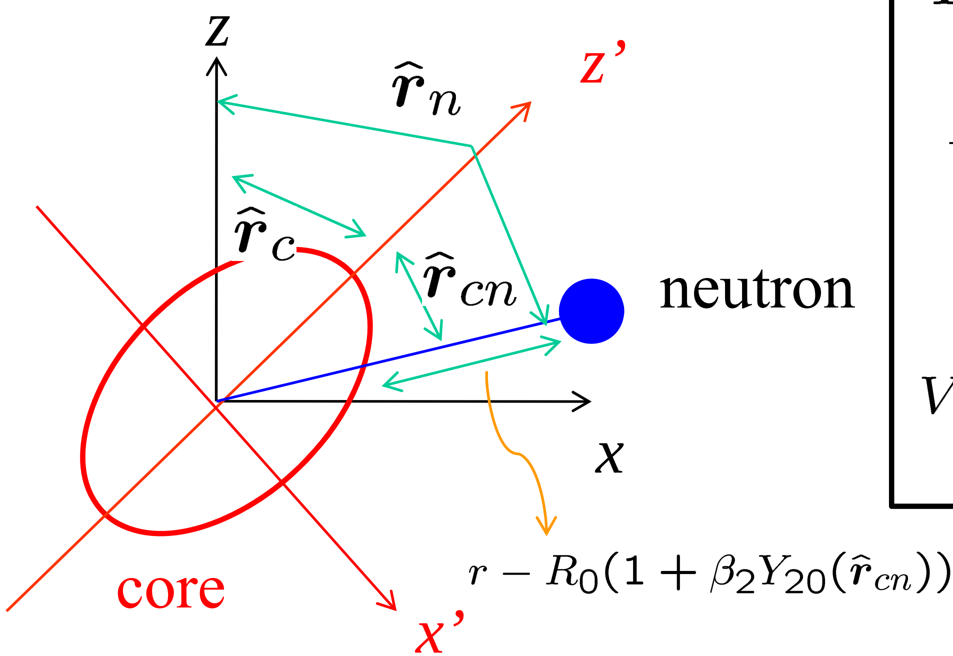

$$H = H_{\rm rot} + H_n + H_{\rm coup}$$

$$H_{\rm rot} = \sum_k \frac{(I_c)_k^2}{2\mathcal{J}_k}$$

$$H_n = \frac{\boldsymbol{p}_n^2}{2m} + V_0(r)$$

$$V_{\rm coup} = V_2(r)\sum_\mu Y_{2\mu}(\hat{\boldsymbol{r}}_c)Y_{2\mu}^*(\hat{\boldsymbol{r}}_n)$$

$$R_0\beta_2 Y_{20}(\hat{\boldsymbol{r}}_{cn}) = R_0\beta_2\sqrt{\frac{4\pi}{5}}\sum_\mu Y_{2\mu}(\hat{\boldsymbol{r}}_c)Y_{2\mu}^*(\hat{\boldsymbol{r}}_n)$$

固有関数:

$$\Psi_{IM}(\boldsymbol{r}_n, \boldsymbol{r}_c) = \sum_{l,j,I_c} \frac{\phi^I_{ljI_c}(r_n)}{r_n}\,|(ljI_c)IM\rangle$$

$$H = H_{\text{rot}} + H_n + V_{\text{coup}}$$

$$H_n = \frac{\boldsymbol{p}_n^2}{2m} + V_0(r)$$

$$V_{\text{coup}} = V_2(r)\sum_\mu Y_{2\mu}(\hat{\boldsymbol{r}}_c)Y^*_{2\mu}(\hat{\boldsymbol{r}}_n)$$

$$= \tilde{V}_2(r)Y_{20}(\hat{\boldsymbol{r}}_{cn})$$

$$\Psi_{IM}(\boldsymbol{r}_n,\boldsymbol{r}_c) = \sum_{l,j,I_c}\frac{\phi^I_{ljI_c}(r_n)}{r_n}|(ljI_c)IM\rangle$$

(ref.)
H. Esbensen and C.N. Davids,
PRC63('00)014315

V_{coup} にくらべて H_{rot} が無視できる場合（strong coupling limit)

$H_{\text{n}}+V_{\text{coup}}$ の固有状態を物体固定系で求め、H_{rot} を摂動的に扱う

$$\left[\frac{\boldsymbol{p}_n^2}{2m} + V_0(r) + \tilde{V}_2(r)Y_{20}(\hat{\boldsymbol{r}}_{cn}) - \epsilon_K\right]\varphi_K(r_n,\hat{\boldsymbol{r}}_{cn}) = 0$$

$$\Psi_{IMK}(\boldsymbol{r}_n,\boldsymbol{r}_c) = \sqrt{\frac{2I+1}{16\pi^2}}\left[D^I_{MK}(\hat{\boldsymbol{r}}_c)\varphi_K(\boldsymbol{r}_{cn}) + \{-K\}\right]$$

(note)

$$\varphi_K(\boldsymbol{r}_{cn}) = \sum_{l,j}\frac{\phi_{ljK}(r_n)}{r_n}\mathcal{Y}_{jlK}(\hat{\boldsymbol{r}}_{cn}) \Rightarrow \begin{cases} \phi^I_{ljI_c}(r) = A^{IK}_{jI_c}\phi_{ljK}(r) \\ A^{IK}_{jI_c} = \sqrt{\frac{2(2I_c+1)}{2I+1}}\langle jKI_c0|IK\rangle \end{cases}$$

変形した陽子過剰核の陽子放出崩壊

Proton Radioactivity

Nuclei beyond the proton drip-line

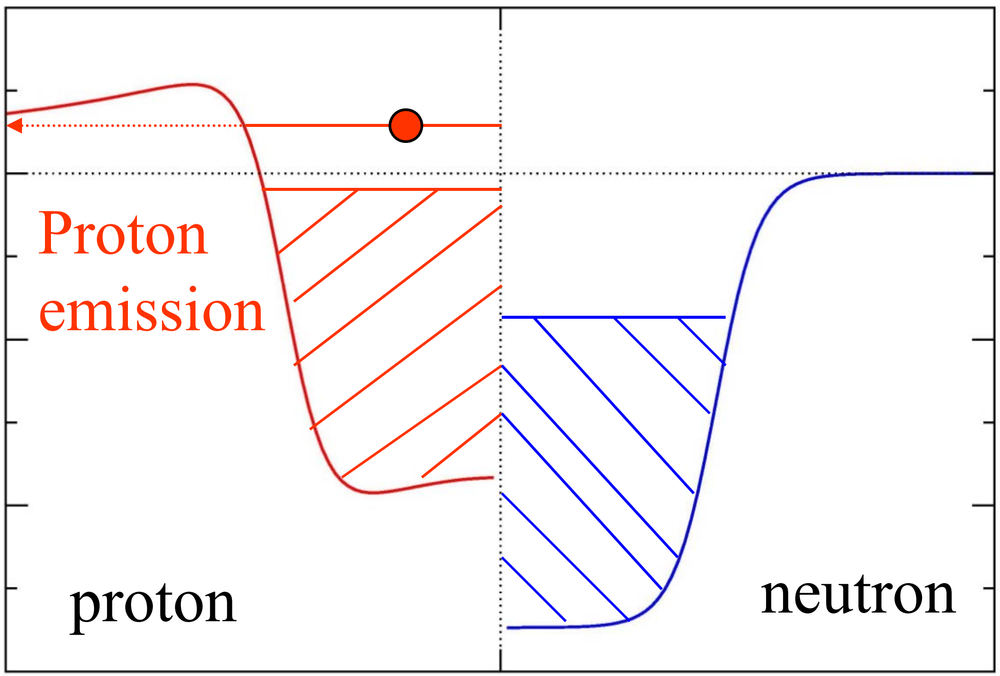

Proton: has to penetrate the Coulomb barrier

→ Very narrow (long lived) resonance

$V_b \sim 10$ MeV (l=0)
$E_p \sim 1$ MeV
R_{turn}: 80~100 fm
Γ : 10^{-18}~10^{-22} MeV
$T_{1/2}$: 100 μs~1 sec

Many g.s. and isomeric proton emittors: have been found recently

ORNL, ANL

Experimental observables: E_p and $T_{1/2}$

Differences from α decays

1. Smaller reduced mass μ

→ Much stronger *l* dependence (centrifugal potential)

→ Spectroscopic information for proton s.p. states can be extracted

2. Much simpler spectroscopic factor

$$^{A+1}_{Z+1}X \rightarrow ^{A}_{Z}X + p$$

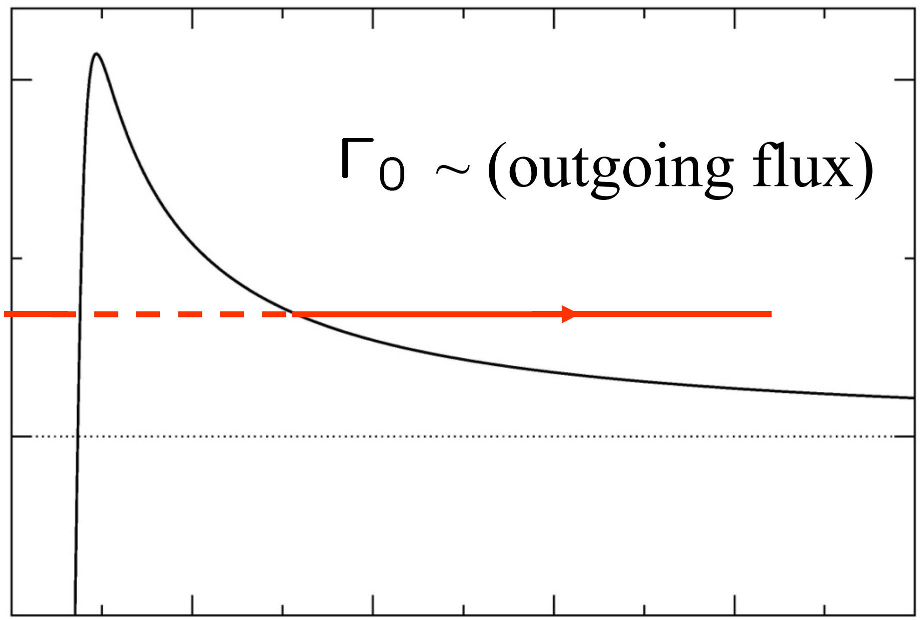

$$\Gamma = \Gamma_0 \cdot S$$
$$S = |\langle (A+1)|(A)+1\rangle|^2$$

Simple estimation:

$$|(A+1)\rangle = \alpha^\dagger|(A)\rangle$$
$$\alpha^\dagger = ua^\dagger - va$$
$$|(A)+1\rangle = a^\dagger|(A)\rangle$$

→ $\boxed{S = u^2}$

Spectroscopic factor

Decay half-life:

$$T_{1/2} = \frac{\hbar}{\Gamma}\log 2 = \frac{\hbar}{S\Gamma_0}\log 2$$

Experimental spectroscopic factor:

$$S_{\mathrm{exp}} \equiv \frac{T_{1/2}^{\mathrm{th}}}{T_{1/2}^{\mathrm{exp}}} = \left(\frac{\hbar}{\Gamma_0}\log 2\right)\Big/\, T_{1/2}^{\mathrm{exp}}$$

$\longleftrightarrow$ Theoretical spectroscopic factor

$$S_{\mathrm{th}} = u^2 \quad \text{or} \quad S_{\text{shell model}}$$

Prediction of potential model

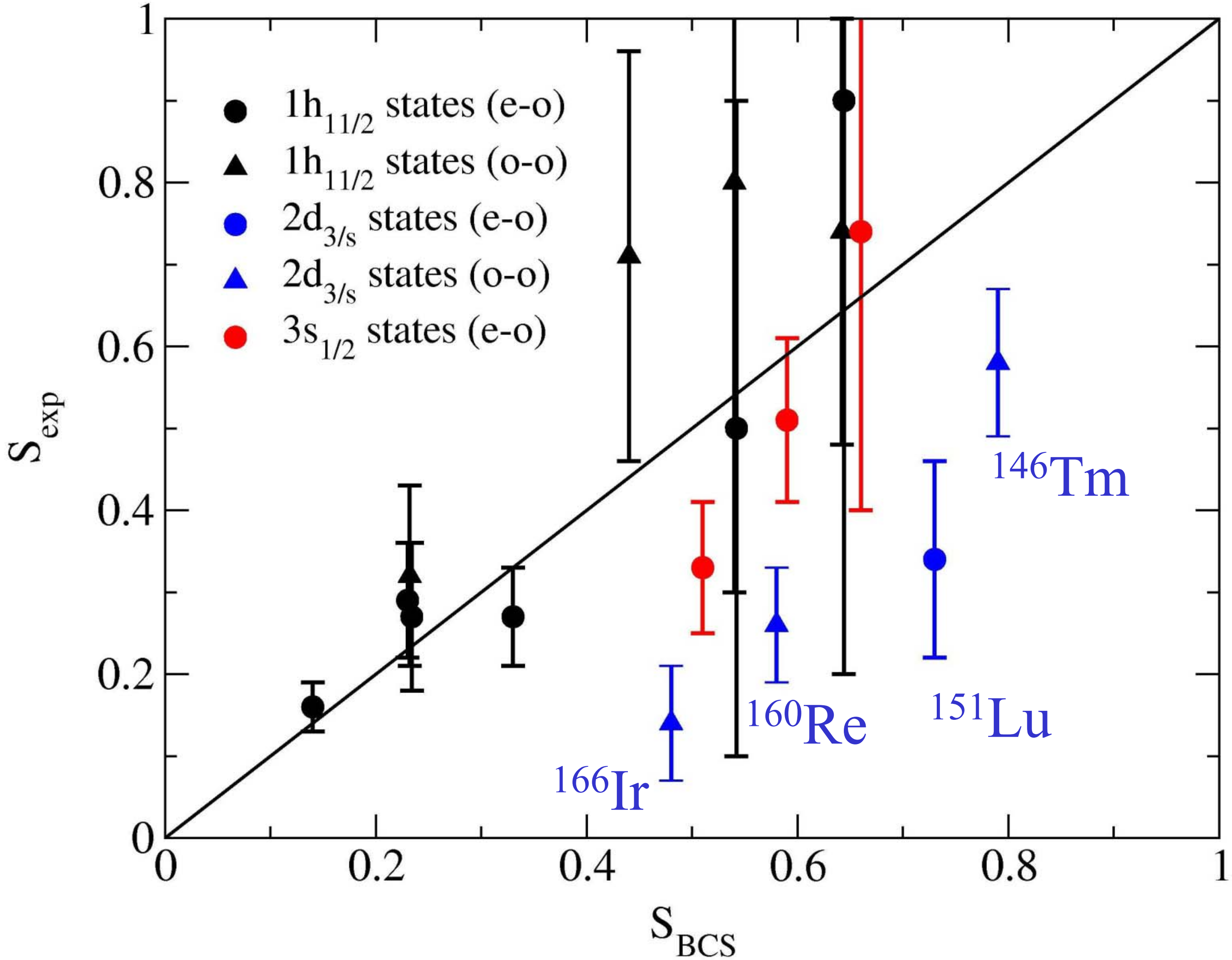

Calculations: S. Aberg et al., PRC56('97)1762
(spherical optical pot. description)

Role of channel couplings

Deformation effects? $\longrightarrow$ alter both $u^2_{\rm BCS}$ and Γ_0

^{151}Lu: β_2 ~ - 0.15 (Moller and Nix)

Ferreira and Maglione: coupled-channels calculation (PRC61('00))

^{160,161}Re: Nearly spherical

$^{161}_{75}\mathrm{Re} \to \mathrm{p} + {}^{160}_{74}\mathrm{W}$ (β_2= 0.089 for $^{160}_{74}$W)

$^{160}_{75}\mathrm{Re} \to \mathrm{p} + {}^{159}_{74}\mathrm{W}$ (β_2= 0.080 for $^{159}_{74}$W)

$\boxed{\text{Vibrational effects?}}$

$$|jm\rangle = \sum_{l_p,j_p} \sum_{n,I} \left[|j_p l_p\rangle \bigotimes |nI\rangle \right]^{(jm)}$$

K.H., PRC64('01)041304(R)

C.N. Davids and H. Esbensen, PRC64('01)034317

Nuclear Structure Effect – a quantal treatment

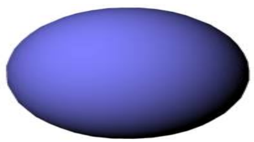

deformation

≡ Rotational excitation

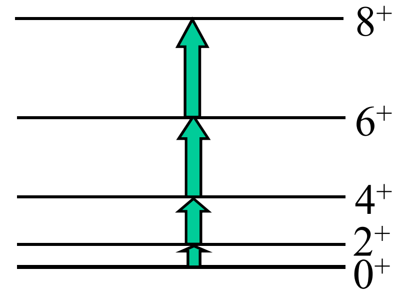

In general

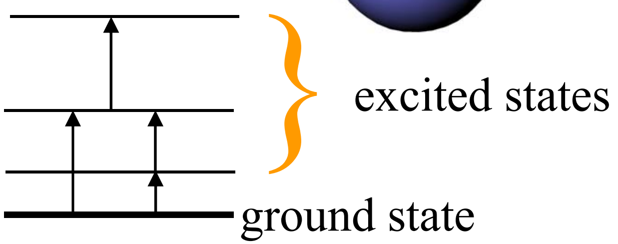

≡ Coupling between the relative motion and intrinsic degrees of freedom

Rotational, vibrational states **(Low-lying collective excitations)**

Coupled channels model

Vibrational coupling

$$\hat{O} = \frac{\beta}{\sqrt{4\pi}}(a + a^\dagger)$$

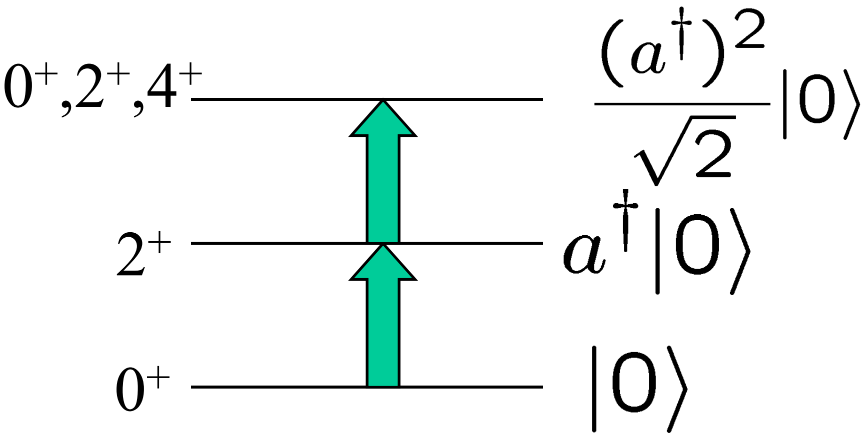

$$\begin{pmatrix} 0 & F & 0 \\ F & \epsilon & \sqrt{2}F \\ 0 & \sqrt{2}F & 2\epsilon \end{pmatrix}$$

Rotational coupling

$$\hat{O} = \beta Y_{20}(\theta)$$

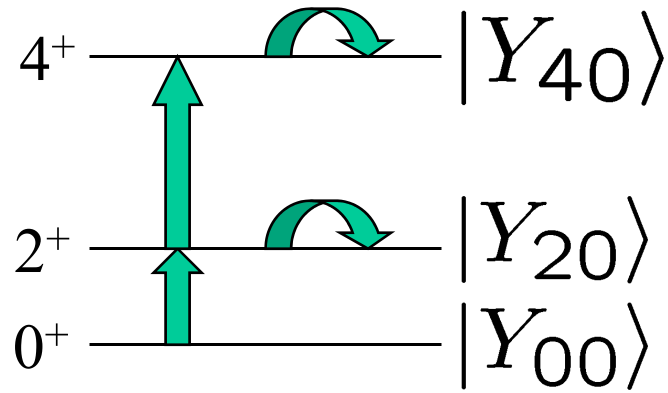

$$\begin{pmatrix} 0 & F & 0 \\ F & \epsilon + \frac{2\sqrt{5}}{7}F & \frac{6}{7}F \\ 0 & \frac{6}{7}F & \frac{10\epsilon}{3} + \frac{20\sqrt{5}}{77}F \end{pmatrix}$$

$$F = \frac{\beta}{\sqrt{4\pi}}$$

Role of particle-vibration coupling

$$|jm\rangle = \sum_{l_p,j_p}\sum_{n,I}\left[|j_pl_p\rangle \bigotimes |nI\rangle\right]^{(jm)}$$

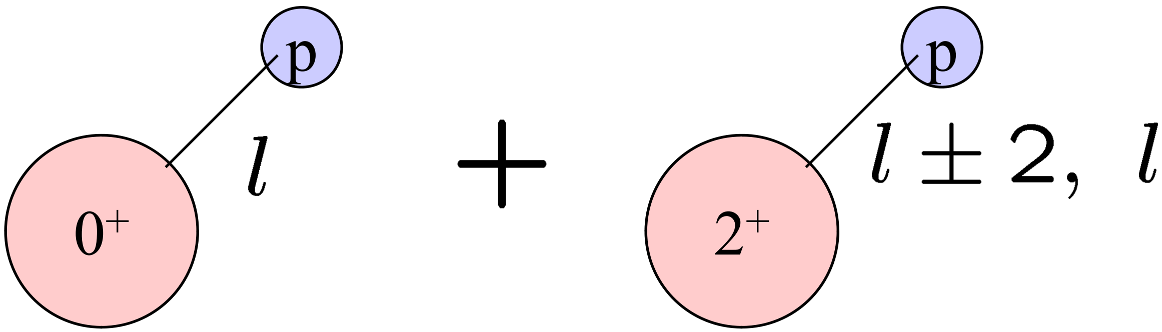

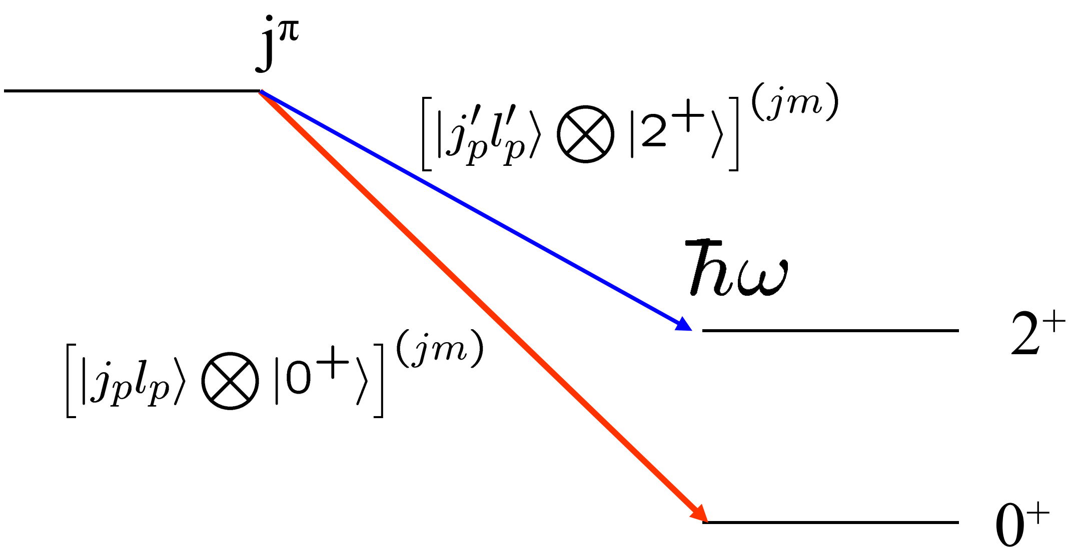

Role of particle-vibration coupling

$$|jm\rangle = \sum_{l_p,j_p}\sum_{n,I}\left[|j_pl_p\rangle \bigotimes |nI\rangle\right]^{(jm)}$$

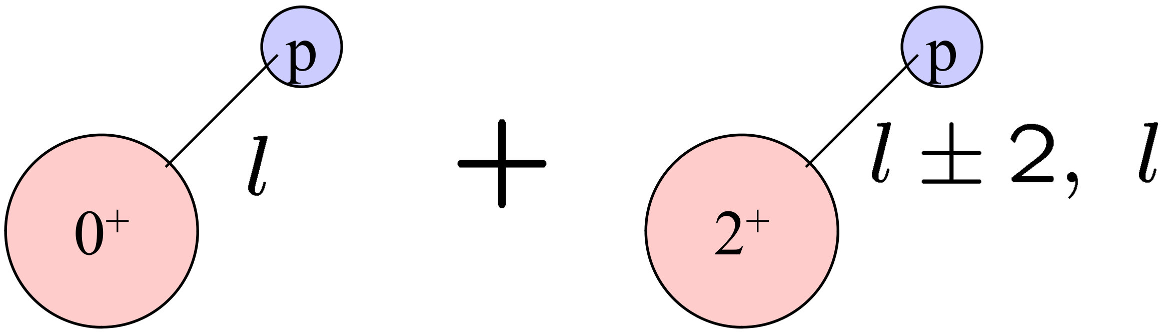

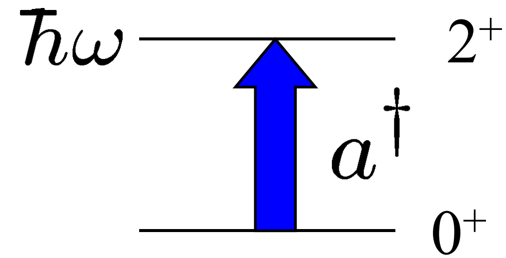

$$\boxed{H = -\frac{\hbar^2}{2\mu}\nabla^2 + V_0(r) + V_{\text{coup}}(\boldsymbol{r},\alpha) + \hbar\omega\sum_\mu a^\dagger_{\lambda\mu}a_{\lambda\mu}}$$

$$\alpha_{\lambda\mu} = \frac{\beta_\lambda}{\sqrt{2\lambda+1}}(a^\dagger_{\lambda\mu} + (-)^\mu a_{\lambda\mu})$$

$$\boxed{V^{(N)}_{\text{coup}}(r,\alpha) = -\frac{V_0}{1+\exp[(r-R-R\alpha\cdot Y_\lambda(\hat{\boldsymbol{r}}))/a]}}$$

+ Coulomb and spin-orbit couplings

Coupled-channels Method

$$H = -\frac{\hbar^2}{2\mu}\nabla^2 + V_0(r) + H_0(\xi) + V_{\rm coup}(\boldsymbol{r},\xi)$$

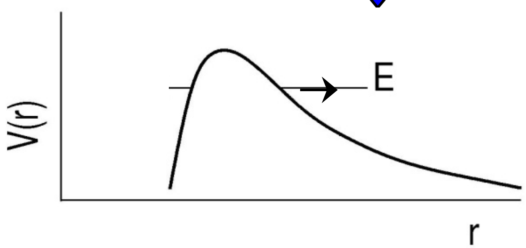

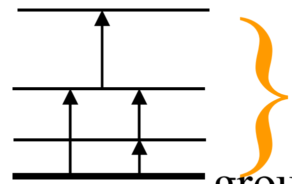

$$H_0(\xi)\phi_{nIm_I}(\xi) = \epsilon_{nI}\,\phi_{nIm_I}(\xi)$$

$$\Psi(\boldsymbol{r},\xi) = \sum_{n,l,I}\frac{u_{nlI}(r)}{r}[Y_l(\hat{\boldsymbol{r}})\phi_{nI}(\xi)]^{(JM)}$$

$$\langle [Y_l\phi_{nI}]^{(JM)}|H-E|\Psi\rangle = 0$$

$$\boxed{\begin{aligned}&\left[-\frac{\hbar^2}{2\mu}\frac{d^2}{dr^2} + \frac{l(l+1)\hbar^2}{2\mu r^2} + V_0(r) - E + \epsilon_{nI}\right]u_{nlI}(r)\\ &\quad + \sum_{n'l'I'}\langle [Y_l\phi_{nI}]^{(JM)}|V_{\rm coup}(r)|[Y_{l'}\phi_{n'I'}]^{(JM)}\rangle u_{n'l'I'}(r) = 0\end{aligned}}$$

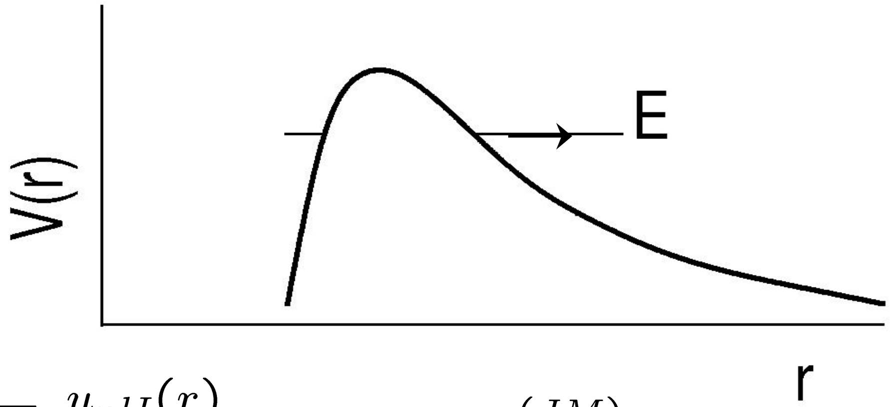

$$\Psi(\boldsymbol{r},\xi) = \sum_{n,l,I} \frac{u_{nlI}(r)}{r}[Y_l(\hat{\boldsymbol{r}})\phi_{nI}(\xi)]^{(JM)}$$

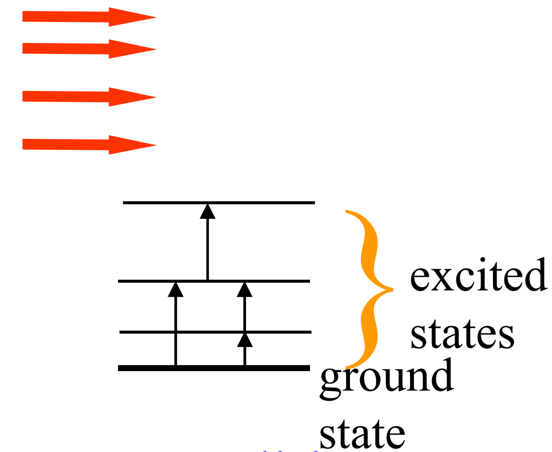

Two alternative ways for the multi-channel resonance condition:

(i) $u_{ljnI}(r) \to \mathcal{N}_{ljnI}\, G_l(k_{nI}r)$ for all the channels

$\longleftrightarrow$ Eigen-phase $\delta_a = \pi/2$

K.H. and N. Van Giai, NPA735('04)55

Real E; Width $\longrightarrow$ E dependence of δ_a

(ii) $u_{ljnI}(r) \to \mathcal{N}_{ljnI}\, e^{ik_{nI}r_I r}$ for all the channels

$\longleftrightarrow E = E_R - i\Gamma/2$

(i) $u_{ljnI}(r) \to \mathcal{N}_{ljnI} G_l(k_{nI} r)$ for all the channels

(ii) $u_{ljnI}(r) \to \mathcal{N}_{ljnI} e^{ik_{nI} r}$ for all the channels

(i) and (ii) are equivalent (for a very narrow resonance)

We use

- the definition (i) for E_R
- the definition (ii) for Γ with the Green's function technique

S.G. Kadmensky et al., Sov. J. Nucl. Phys. 14('72)193
C.N. Davids and H. Esbensen, PRC61('00)054302

$$^{160,161}_{75}\mathrm{Re} \rightarrow p + ^{160,159}_{74}\mathrm{W}$$

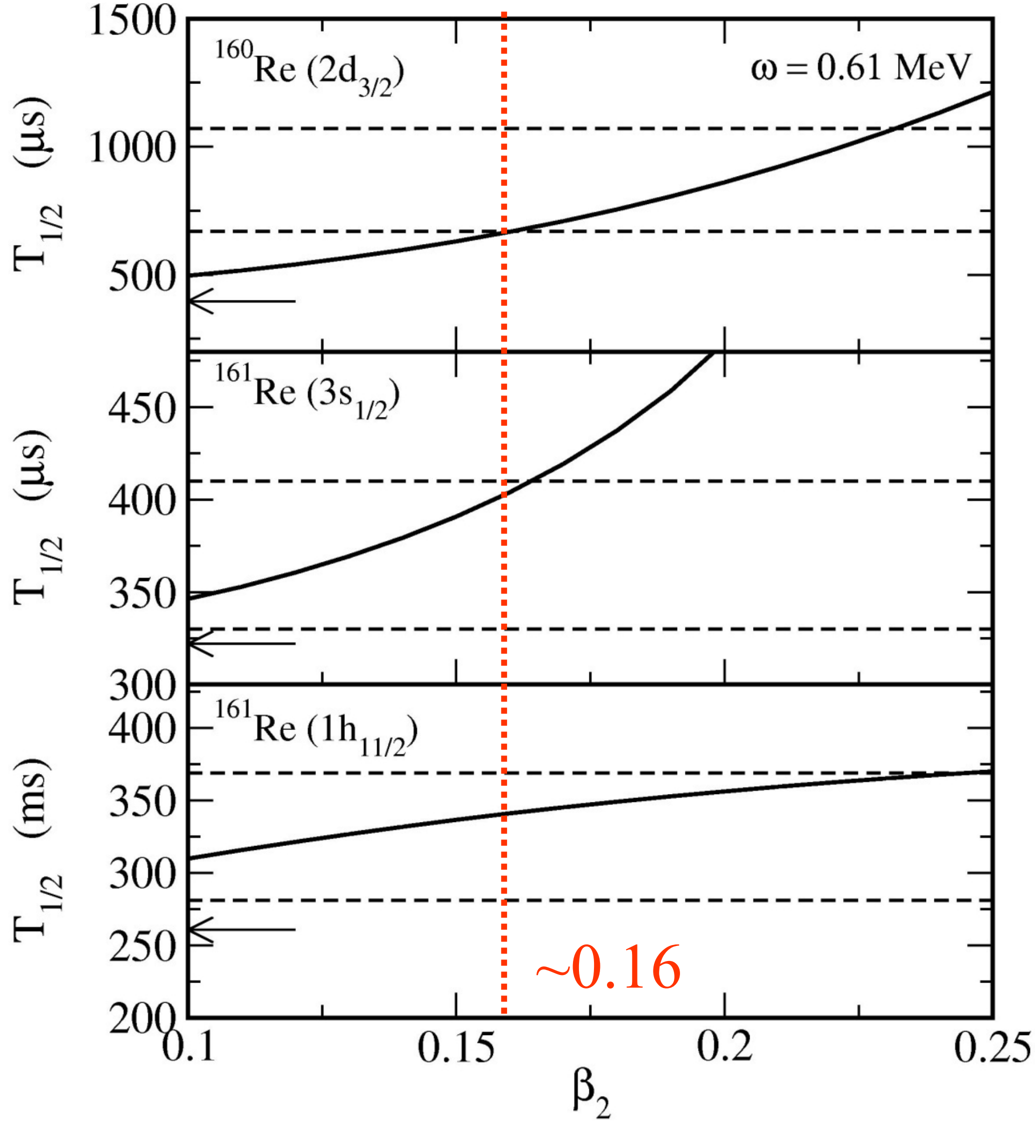

K.H., PRC64('01)041304

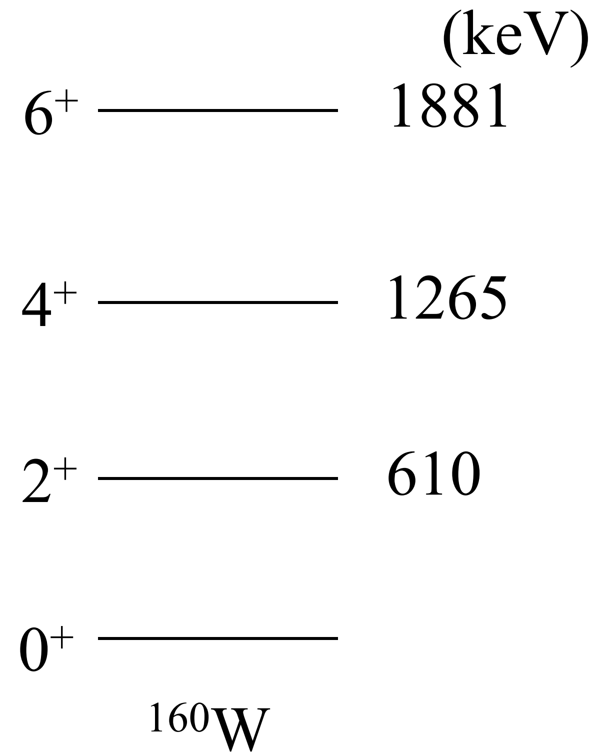

A. Keenen et al., PRC63('01)064309

s-wave proton emitters:

$$|1/2^+\rangle = |s_{1/2} \otimes 0^+\rangle + |d_{3/2} \otimes 2^+\rangle + |d_{5/2} \otimes 2^+\rangle \cdots$$

d-wave proton emitters:

$$|3/2^+\rangle = |d_{3/2} \otimes 0^+\rangle + |s_{1/2} \otimes 2^+\rangle + |d_{3/2} \otimes 2^+\rangle \cdots$$

h-wave proton emitters:

$$|11/2^-\rangle = |h_{11/2} \otimes 0^+\rangle + |f_{7/2} \otimes 2^+\rangle + |h_{11/2} \otimes 2^+\rangle \cdots$$

$$E_p^{\mathrm{eff}} \sim E_p - V_{\mathrm{cent}}(r) - V_0(r)$$

Coupling: effectively weaker than d-wave

Fine Structure (Branching Ratio)

Spherical emitter: ^{145}Tm (Oak Ridge group)

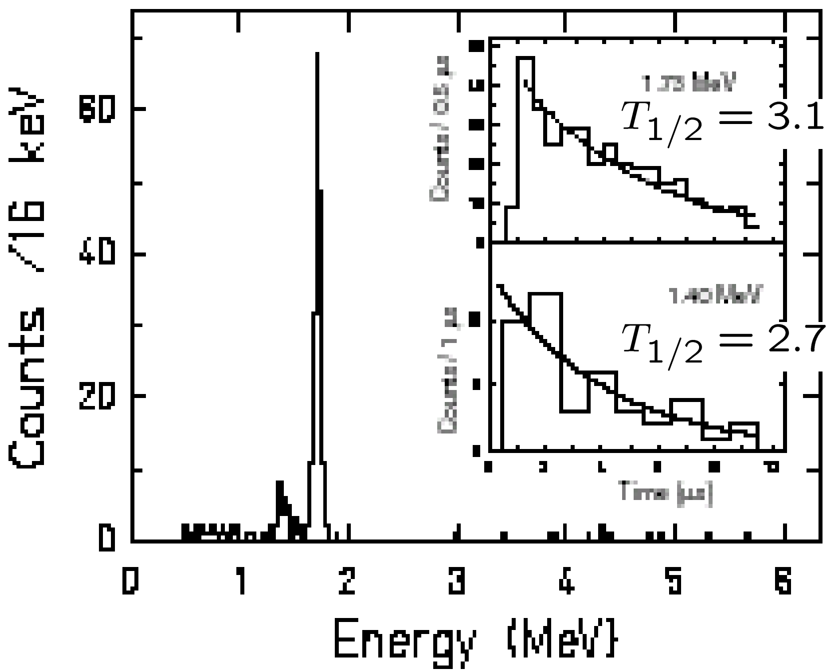

$$^{145}\mathrm{Tm}(h_{11/2})$$
$$\rightarrow {}^{144}\,\mathrm{Er}(0^+) \sim 90.4\%$$
$$\rightarrow {}^{144}\,\mathrm{Er}(2^+) \sim 9.6\%$$

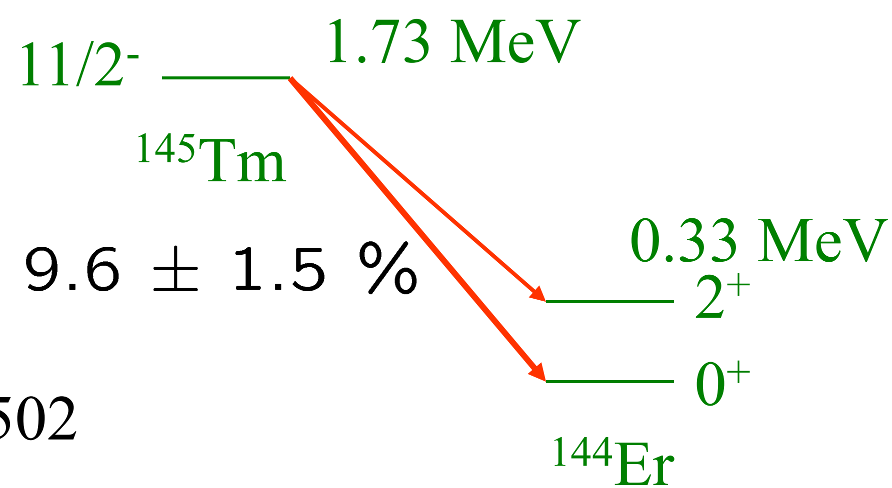

$$\mathrm{BR} = 9.6 \pm 1.5\ \%$$

M. Karny et al., PRL90('03)012502

Particle-vibration coupling

K.P. Rykaczewski, K.H., et al.

$$
\begin{aligned}
|11/2^-\rangle = {} & |h_{11/2}\rangle \otimes |0^+\rangle + |f_{7/2}\rangle \otimes |2^+\rangle \\
& + |h_{9/2}\rangle \otimes |2^+\rangle + |h_{11/2}\rangle \otimes |2^+\rangle \\
& + |j_{13/2}\rangle \otimes |2^+\rangle + |j_{15/2}\rangle \otimes |2^+\rangle
\end{aligned}
$$

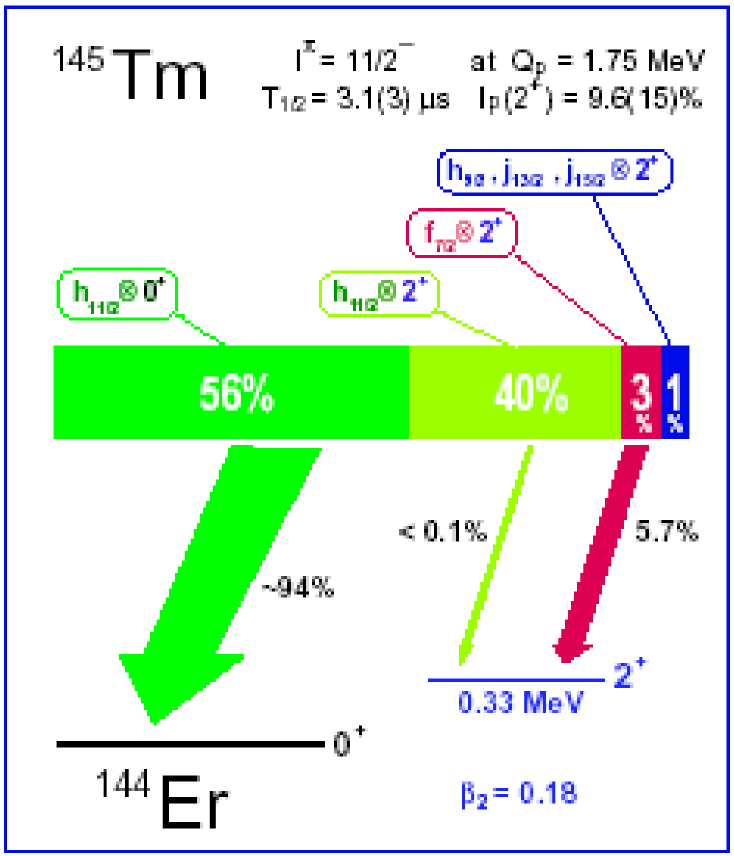

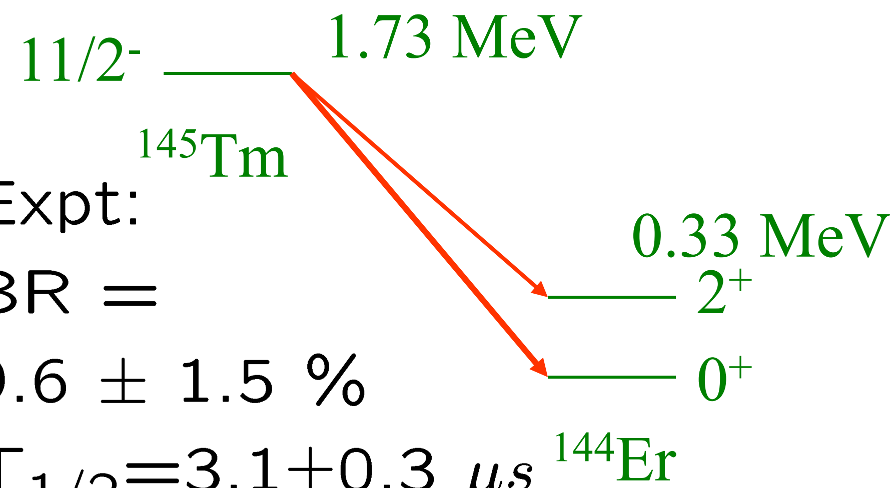

Expt:

BR $=$

9.6 ± 1.5 %

$T_{1/2}$=3.1 ± 0.3 μs

Calc.

$T_{1/2}$=3.0 ± 0.4 μs

I_p=5.7 ± 0.3 %

Odd-odd proton emitters

Fine structure in $^{146}Tm \longrightarrow p + {}^{145}Er$

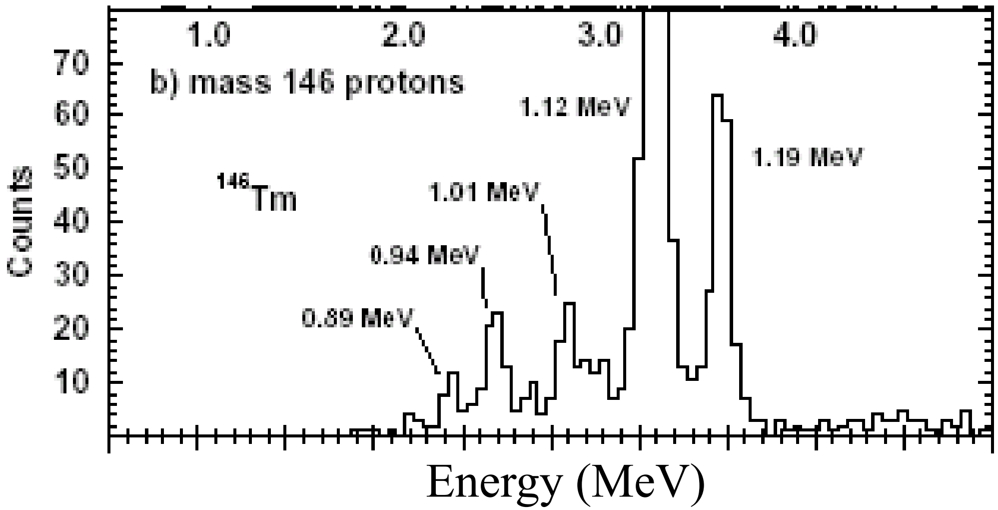

T.N. Ginter et al., PRC68('03)034330

Energy (keV)	$T_{1/2}$ (ms)	counts	Rel. Intensity
880(10)	190(80)	170(30)	1.8(3)
1119(5)	198(5)	9450(250)	100
938(10)	60(20)	290(30)	22(2)
1016(10)	70(15)	370(40)	28(3)
1189(5)	75(5)	1350(80)	100

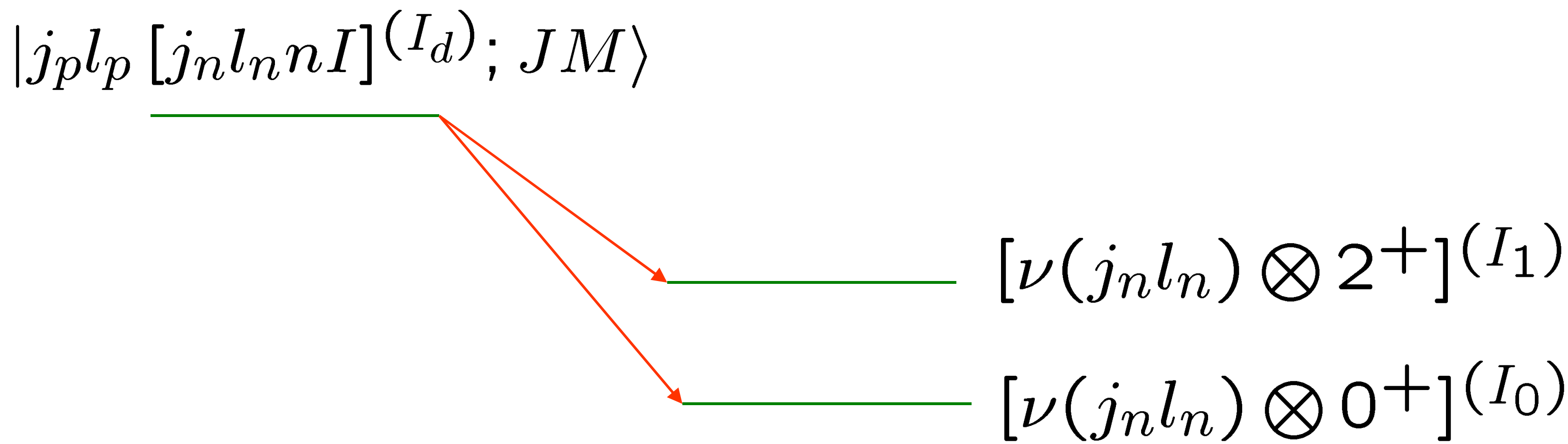

	$T_{1/2}$(ms)	BR(%)
$10^+ \longrightarrow 11/2^-, 13/2^-$	485	0.83
$10^+ \longrightarrow 11/2^-, 9/2^-$	524	0.041
$8^+ \longrightarrow 11/2^-, 9/2^-$	48	0.011

- spectroscopic information for proton s.p. levels
- collective excitation in the daughter nuclues
- spectroscopic information for *neutron* s.p. levels in the daughter

$10^+ \longrightarrow 11/2^-, 13/2^-$

$$\left[(h_{11/2})_\pi \otimes [(h_{11/2})_\nu \otimes 0^+]^{(11/2^-)}\right]^{(10^+)}$$

$$\left[(h_{11/2})_\pi \otimes [(h_{11/2})_\nu \otimes 2^+]^{(13/2^-)}\right]^{(10^+)}$$

$$\left[(f_{7/2})_\pi \otimes [(h_{11/2})_\nu \otimes 2^+]^{(13/2^-)}\right]^{(10^+)}$$

$10^+ \longrightarrow 11/2^-, 9/2^-$

$$\left[(h_{11/2})_\pi \otimes [(h_{11/2})_\nu \otimes 0^+]^{(11/2^-)}\right]^{(10^+)}$$

$$\left[(h_{11/2})_\pi \otimes [(h_{11/2})_\nu \otimes 2^+]^{(9/2^-)}\right]^{(10^+)}$$

$8^+ \longrightarrow 11/2^-, 9/2^-$

$$\left[(h_{11/2})_\pi \otimes [(h_{11/2})_\nu \otimes 0^+]^{(11/2^-)}\right]^{(8^+)}$$

$$\left[(h_{11/2})_\pi \otimes [(h_{11/2})_\nu \otimes 2^+]^{(9/2^-)}\right]^{(8^+)}$$

$$\left[(f_{7/2})_\pi \otimes [(h_{11/2})_\nu \otimes 0^+]^{(11/2^-)}\right]^{(8^+)}$$

55%	$(h_{11/2})_\pi \otimes (h_{11/2})_\nu \otimes 0^+$
42%	$(h_{11/2})_\pi \otimes (h_{11/2})_\nu \otimes 2^+$
2.5%	$(f_{7/2})_\pi \otimes (h_{11/2})_\nu \otimes 2^+$
0.5%	others

10^+ state:

	$T_{1/2}$(ms)	BR(%)
Calc.	748	1.24
Expt.	198(5)	1.7(3)

Cf. GT transition

$\pi h_{11/2} \longrightarrow \nu h_{11/2}$

$T_{1/2} \sim 200$ ms

53%	$(h_{11/2})_\pi \otimes (s_{1/2})_\nu \otimes 0^+$
41%	$(h_{11/2})_\pi \otimes (s_{1/2})_\nu \otimes 2^+$
4%	$(f_{7/2})_\pi \otimes (s_{1/2})_\nu \otimes 2^+$
2%	$(s_{1/2})_\pi \otimes (h_{11/2})_\nu \otimes 0^+$

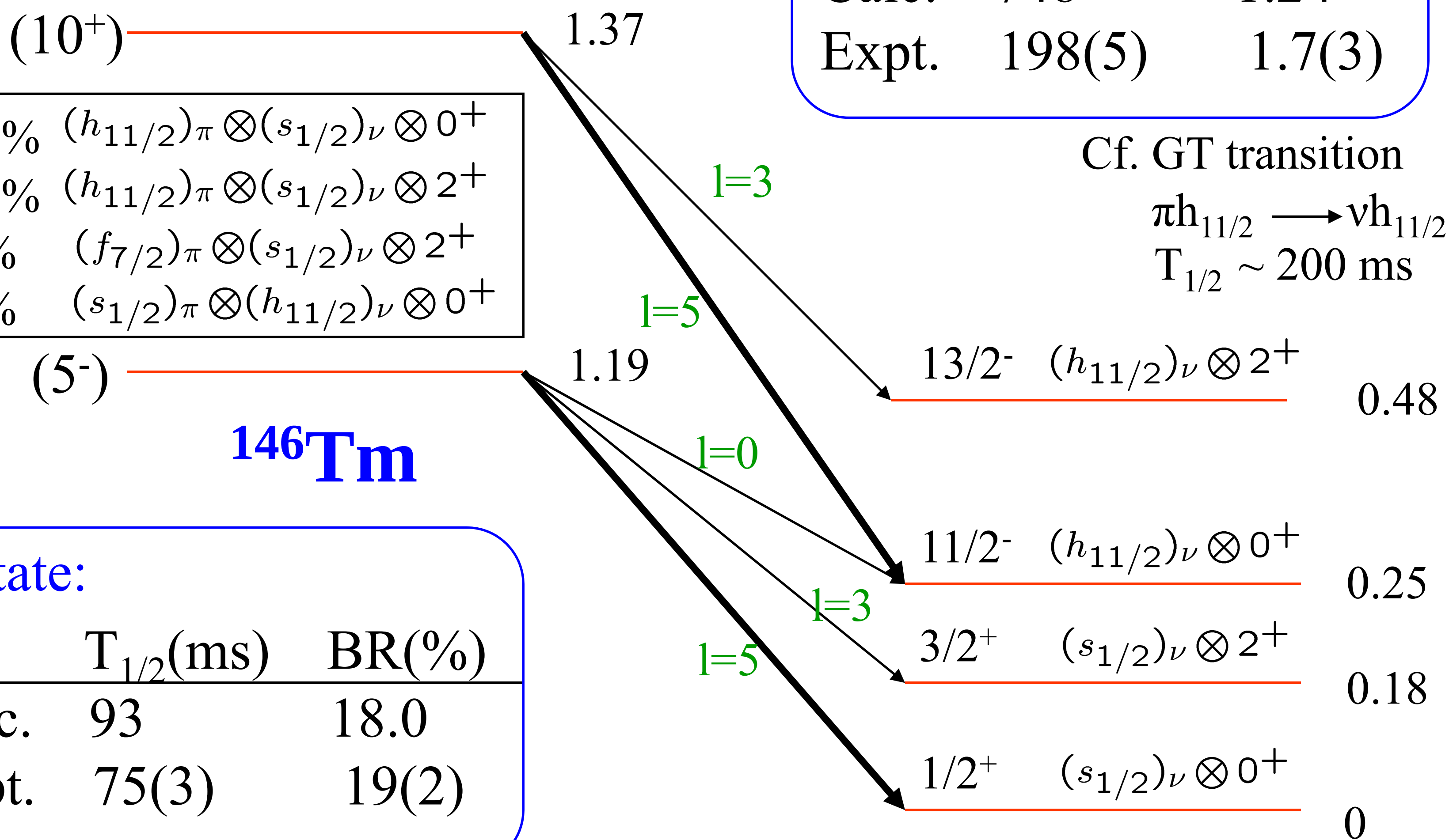

5^- state:

	$T_{1/2}$(ms)	BR(%)
Calc.	93	18.0
Expt.	75(3)	19(2)

M.N. Tantawy et al., PRC73('06)024316

Summary

Probing nuclear structure with proton radioactivities

⟷ Coupled-channels framework

Information on:

- **Proton orbitals** beyond the proton-drip line
- **Collective excitation** in the daughter nucleus
- **Neutron orbitals** in proton-rich nuclei

Fine structure in emission from an odd-odd nucleus

変形した原子核のα崩壊

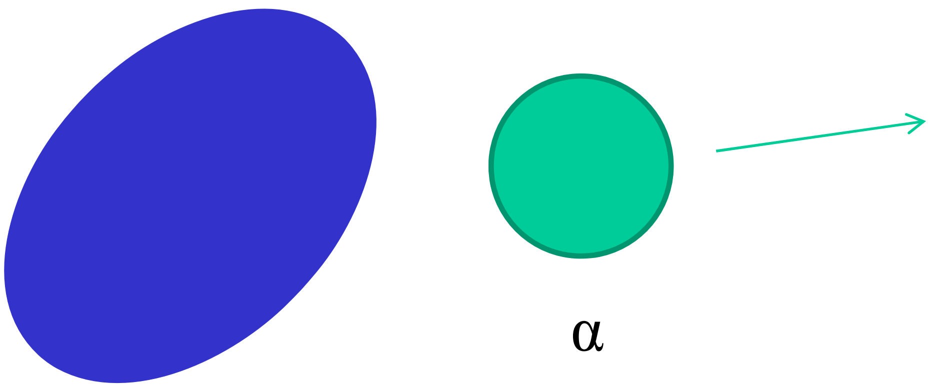

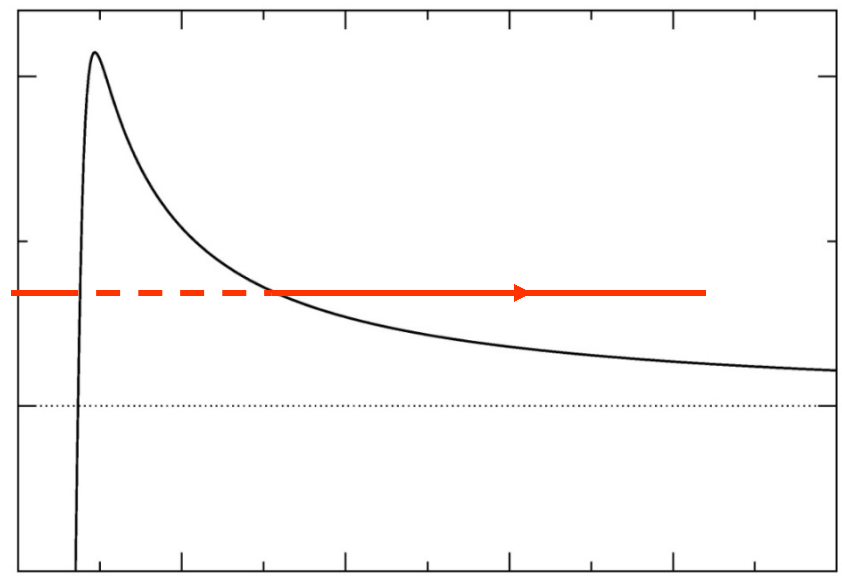

◆α粒子の角度分布

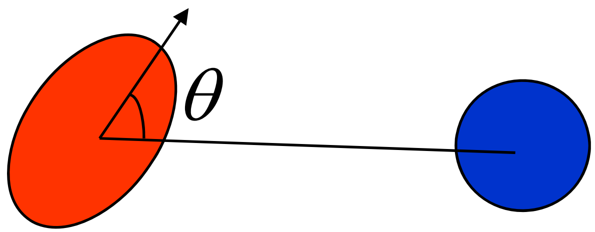

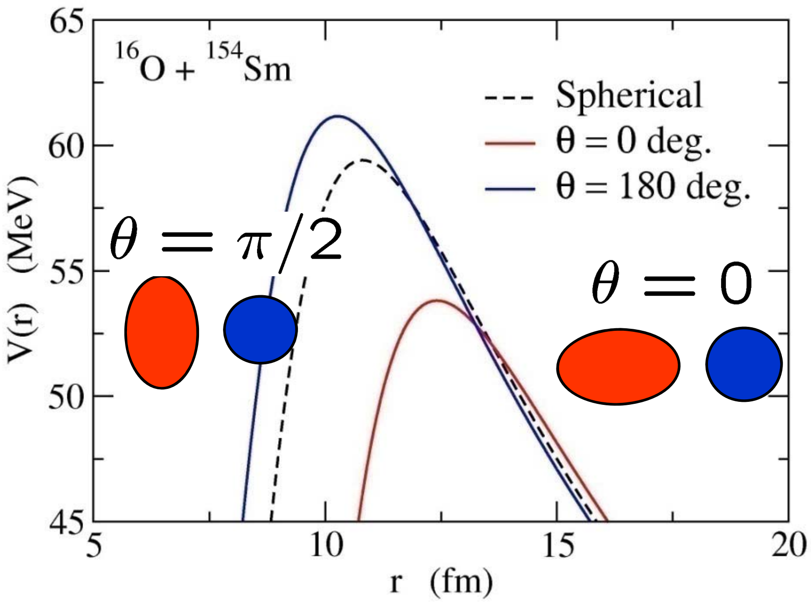

prolate 核の場合、θ = 0 の時ポテンシャルが最低

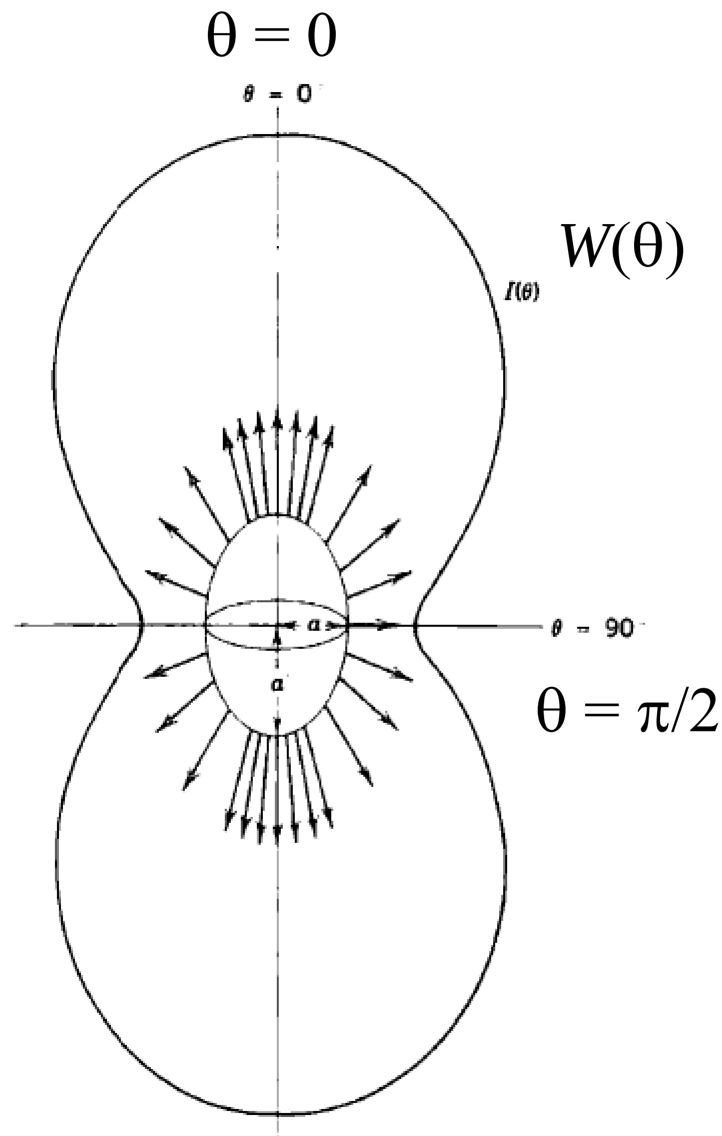

予想される角度分布

◆α粒子の角度分布

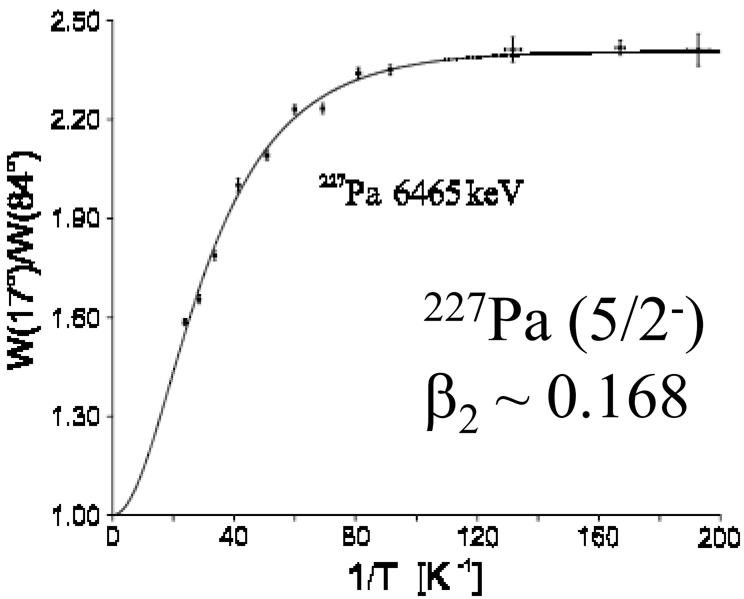

^{227}Pa (5/2$^-$)

$\beta_2 \sim 0.168$

P. Schuurmans et al.,
PRL82('99)4787

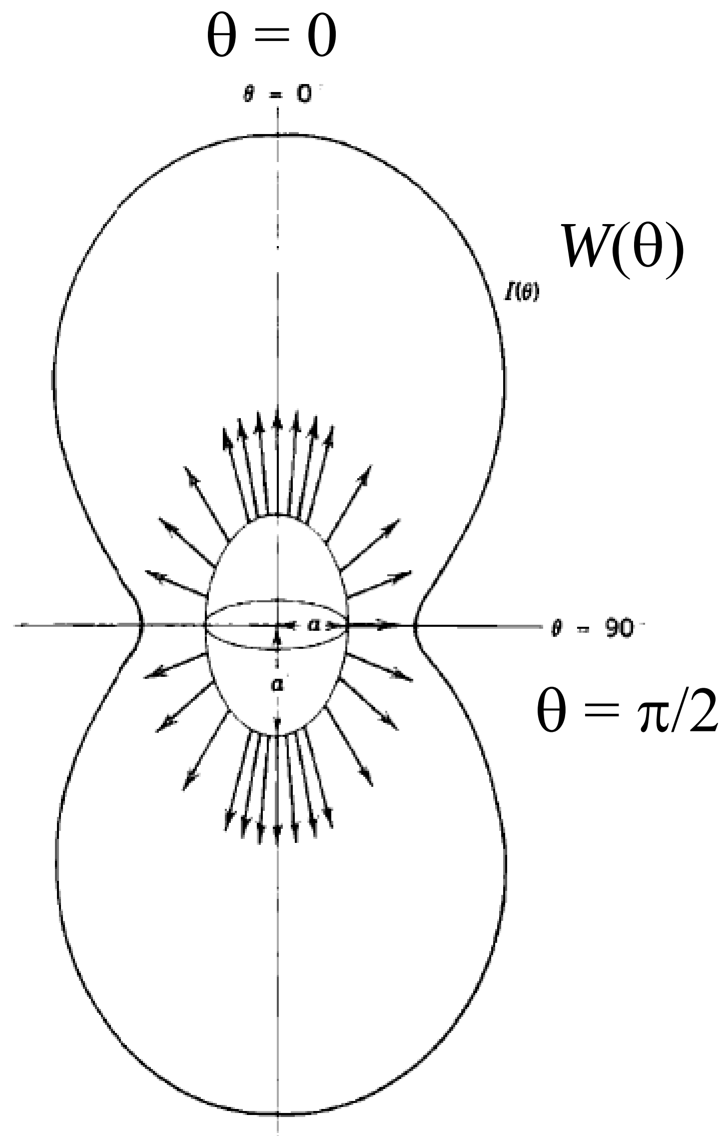

磁場で基底状態スピンを align させて
α崩壊を測定

⟹ W(17 deg) ~ 2.4 x W(84 deg)

予想される角度分布

◆α線の微細構造と超重核の核構造

0^+

^{242}Cm

$\beta_2 = 0.224$

α

(Q_{gg} = 6.216 MeV)

6^+ 0.0046%

4^+ 0.035%

2^+ 25.0 %

0^+ 74.0%

^{238}Pu intensity

$\beta_2 = 0.215$

- ●角運動量（遠心力バリア）の影響
- ●E_α の影響

α崩壊を用いた重核・超重核の 2_1^+ 状態のエネルギーの系統性の研究（日本原子力機構・浅井雅人氏）

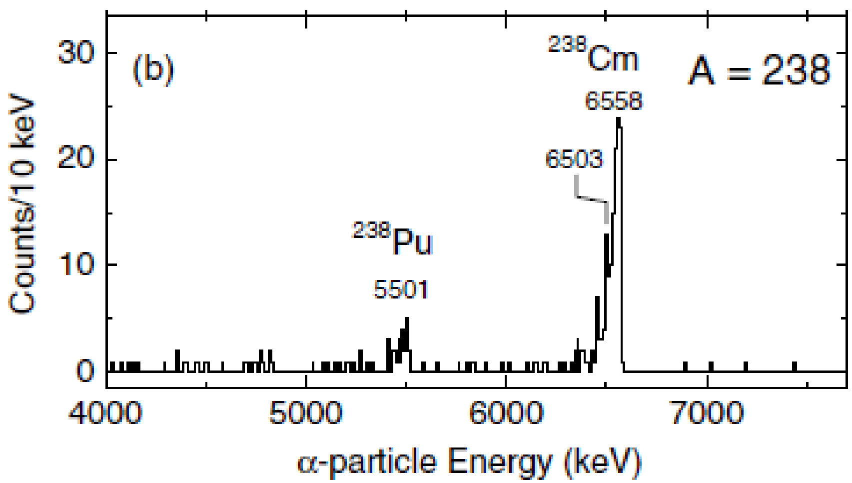

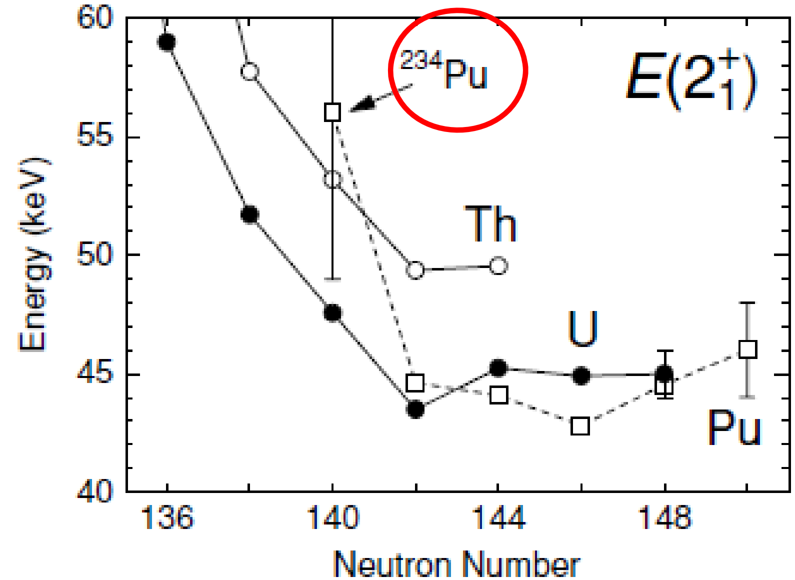

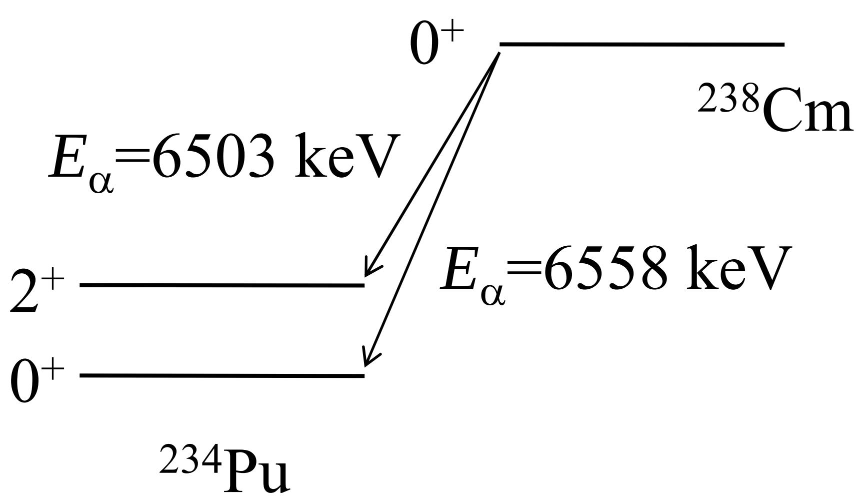

$\beta_2 = 0.216$

M. Asai et al., PRC73('06)067301

α崩壊を用いた重核・超重核における一粒子状態のスピン・パリティの決定（日本原子力機構・浅井雅人氏）

α−γ spectroscopy

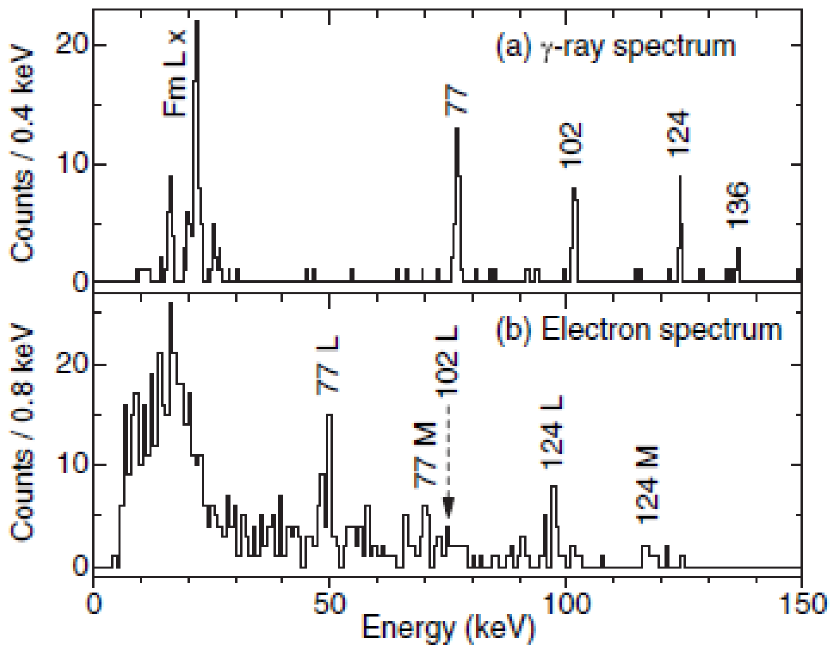

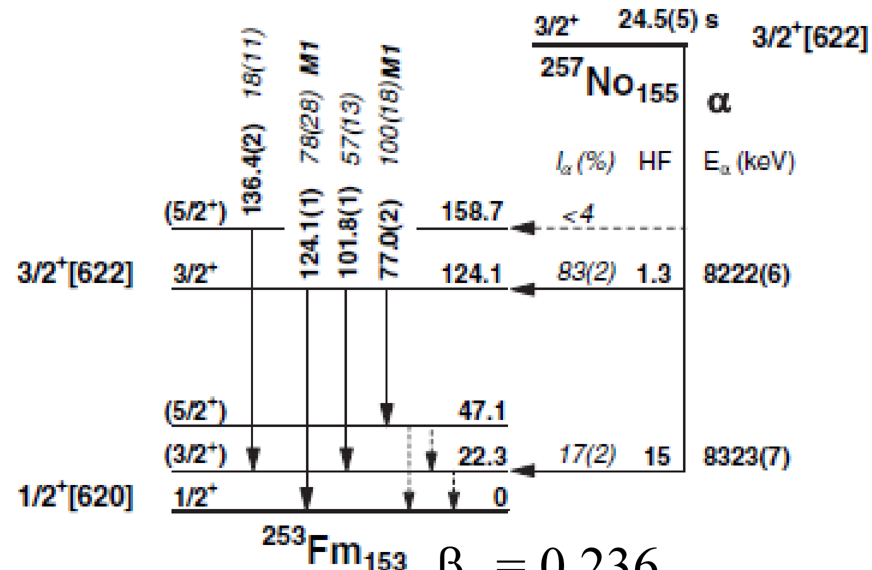

$\beta_2 = 0.236$

α線とγ線・内部転換電子の同時計測

^{257}No の基底状態を 3/2$^+$ と同定（以前のα線のみを使った解析だと 7/2$^+$）

超重核領域における殻構造の解明

M. Asai et al., PRL95(‘05)102502

変形した原子核の反応（核融合反応）

核反応論基礎：基本的概念と量子力学の復習

原子核の形や相互作用、励起状態の性質：衝突実験
cf. ラザフォードの実験（α 散乱）

Notation

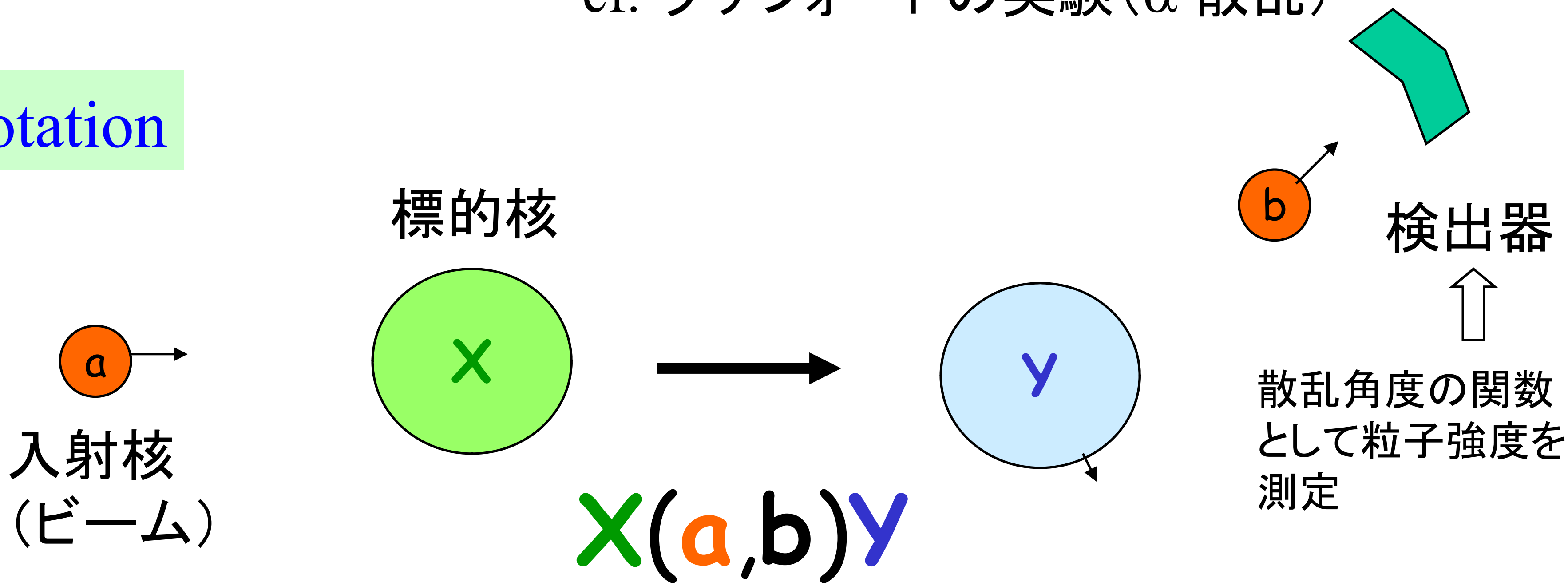

反応チャンネルの例

^{208}Pb(^{16}O,^{16}O)^{208}Pb : ^{16}O+^{208}Pb 弾性散乱

^{208}Pb(^{16}O,^{16}O)^{208}Pb* : ^{16}O+^{208}Pb 非弾性散乱

^{208}Pb(^{17}O,^{16}O)^{209}Pb : 1中性子移行反応

この他に複合核合成反応も

散乱断面積

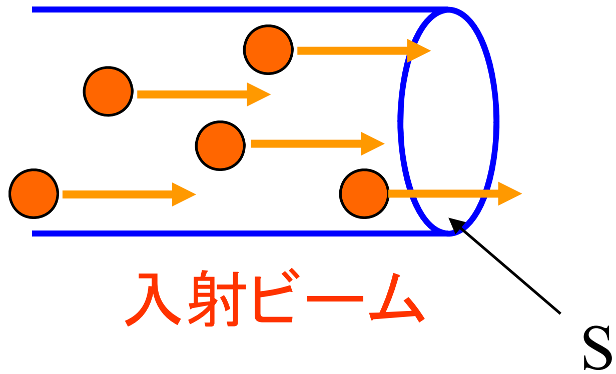

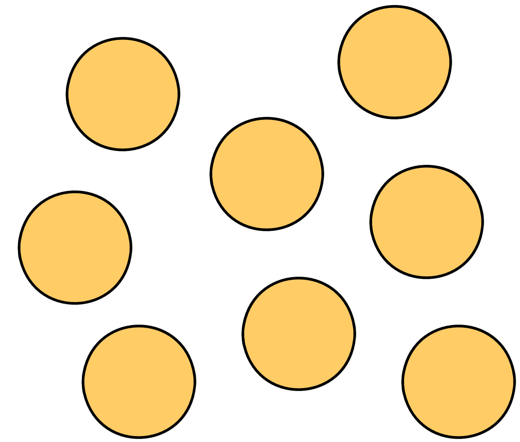

単位時間当たりに標的粒子1個に対する反応の起きる数	=	σ・単位時間当たり単位面積を通過する入射粒子の数

σ/S = ビーム中の入射粒子1個が標的1個と衝突した時に散乱の起こる確率

単位: 1 barn = 10^{-24} cm^2 = 100 fm^2　(1 mb = 10^{-3} b = 0.1 fm^2)

微分散乱断面積:

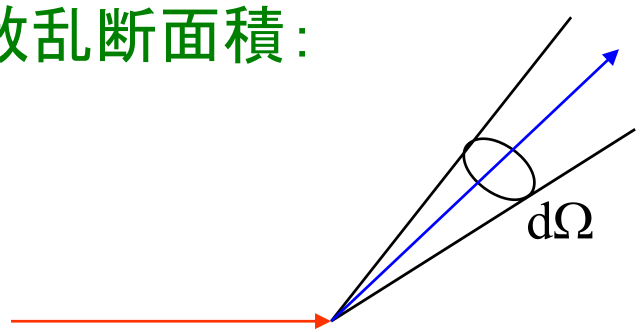

$$\frac{d\sigma}{d\Omega}$$

散乱振幅

自由粒子の運動: $-\frac{\hbar^2}{2m}\nabla^2\psi = E\psi = \frac{\boldsymbol{k}^2\hbar^2}{2m}\psi$

$$\psi(\boldsymbol{r}) = e^{i\boldsymbol{k}\cdot\boldsymbol{r}} = \sum_{l=0}^{\infty}(2l+1)\,i^l j_l(kr)P_l(\cos\theta)$$

$$\to \frac{i}{2kr}\sum_{l=0}^{\infty}(2l+1)i^l\left[e^{-i(kr-l\pi/2)} - e^{i(kr-l\pi/2)}\right]P_l(\cos\theta)$$

ポテンシャルがある場合: $\left[-\frac{\hbar^2}{2m}\nabla^2 + V(\boldsymbol{r}) - E\right]\psi = 0$

波動関数の漸近形

$$\boxed{\begin{aligned}\psi(\boldsymbol{r}) &\to \frac{i}{2kr}\sum_{l=0}^{\infty}(2l+1)i^l\left[e^{-i(kr-l\pi/2)} - \underline{\underline{S_l}}\,e^{i(kr-l\pi/2)}\right]P_l(\cos\theta)\\ &= e^{i\boldsymbol{k}\cdot\boldsymbol{r}} + \underbrace{\left[\sum_l(2l+1)\frac{S_l-1}{2ik}P_l(\cos\theta)\right]}_{f(\theta)}\frac{e^{ikr}}{r}\end{aligned}}$$

（散乱振幅）

$$\psi(\boldsymbol{r}) \;\rightarrow\; e^{i\boldsymbol{k}\cdot\boldsymbol{r}} + \left[\sum_l (2l+1)\,\frac{S_l - 1}{2ik} P_l(\cos\theta)\right]\frac{e^{ikr}}{r}$$

$$= \; e^{i\boldsymbol{k}\cdot\boldsymbol{r}} + f(\theta)\frac{e^{ikr}}{r}$$

＝（入射波）＋（散乱波）

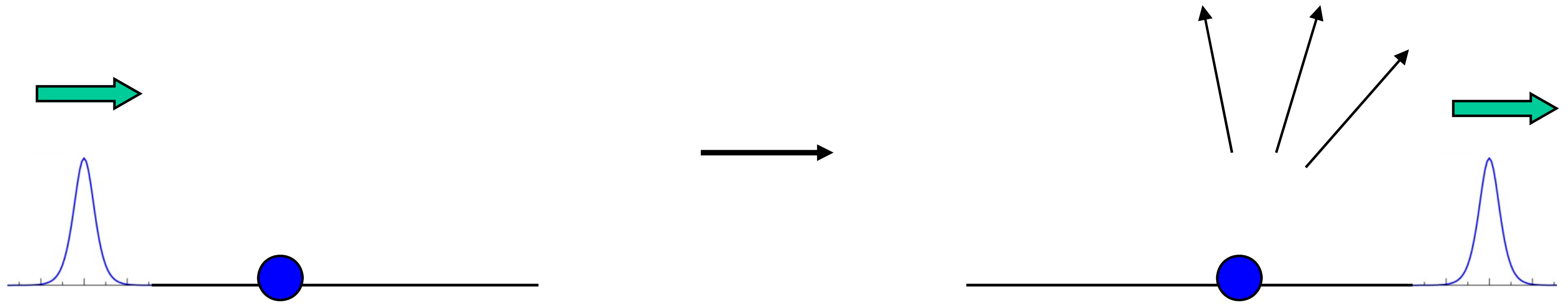

弾性散乱のみが起こる場合: $|S_l| = 1$ （フラックスの保存）

$$S_l = e^{2i\delta_l}$$

δ_l :位相のずれ（phase shift）

微分散乱断面積

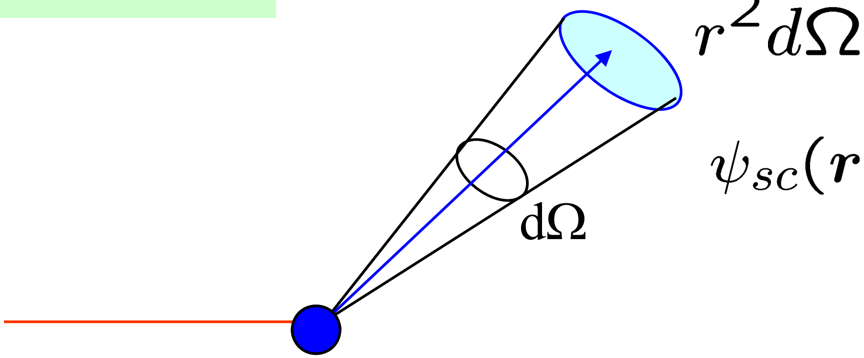

$$\psi_{sc}(\boldsymbol{r}) \sim f(\theta)\frac{e^{ikr}}{r}$$

単位時間に立体角 dΩ に散乱される粒子の数:

$$N_{\mathsf{scatt}} = \boldsymbol{j}_{sc} \cdot \boldsymbol{e}_r \, r^2 d\Omega$$

$$\boldsymbol{j}_{sc} = \frac{\hbar}{2im}\left[\psi_{sc}^* \boldsymbol{\nabla}\psi_{sc} - c.c.\right] \sim \frac{k\hbar}{m}\frac{|f(\theta)|^2}{r^2}\boldsymbol{e}_r$$

（散乱波に対するフラックス）

$$\boxed{\frac{d\sigma}{d\Omega} = |f(\theta)|^2}$$

$$f(\theta) = \sum_l (2l+1)\frac{S_l - 1}{2ik}P_l(\cos\theta)$$

光学ポテンシャルと吸収断面積

反応プロセス

- 弾性散乱
- 非弾性散乱
- 粒子移行
- 複合粒子形成（核融合）

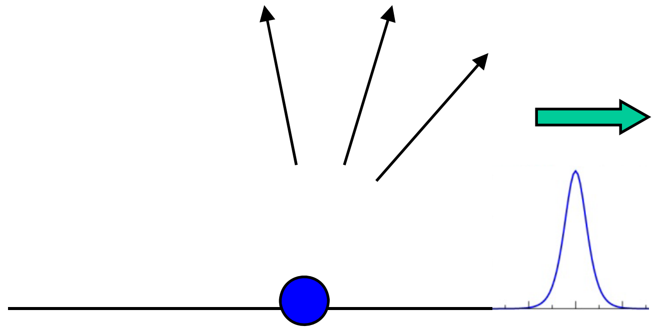

弾性フラックスの減少（吸収）

光学ポテンシャル

$$\boxed{V_{\rm opt}(\boldsymbol{r}) = V(\boldsymbol{r}) - iW(\boldsymbol{r}) \qquad (W > 0)}$$

$$\Longrightarrow \quad \boldsymbol{\nabla}\cdot\boldsymbol{j} = \cdots = -\frac{2}{\hbar}W|\psi|^2$$

(note) ガウスの定理

$$\int_S \boldsymbol{j}\cdot\boldsymbol{n}\,dS = \int_V \boldsymbol{\nabla}\cdot\boldsymbol{j}\,dV$$

$$\psi(\boldsymbol{r}) \to \frac{i}{2k}\sum_l (2l+1)\, i^l \frac{1}{r}\left[\underbrace{e^{-i(kr-l\pi/2)}}_{\psi_{\text{in}}} - \underbrace{S_l e^{i(kr-l\pi/2)}}_{\psi_{\text{out}}}\right] P_l(\cos\theta)$$

全内向フラックス:

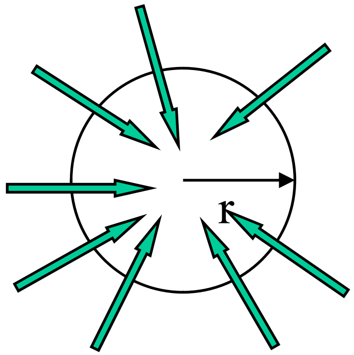

$$j_{\text{in}}^{\text{net}} = \frac{k\hbar}{m}\cdot\frac{\pi}{k^2}\sum_l (2l+1)$$

全外向フラックス:

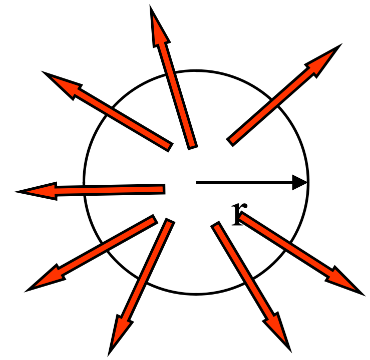

$$j_{\text{out}}^{\text{net}} = \frac{k\hbar}{m}\cdot\frac{\pi}{k^2}\sum_l (2l+1)|S_l|^2$$

減少したフラックス: $j_{\text{in}}^{\text{net}} - j_{\text{out}}^{\text{net}} = \frac{k\hbar}{m}\cdot\frac{\pi}{k^2}\sum_l (2l+1)(1-|S_l|^2)$

吸収断面積

$$\boxed{\sigma_{\text{abs}} = \frac{\pi}{k^2}\sum_l (2l+1)(1-|S_l|^2)}$$

重イオン反応の概観

重イオン：^{4}He より重い原子核

重イオン間ポテンシャル

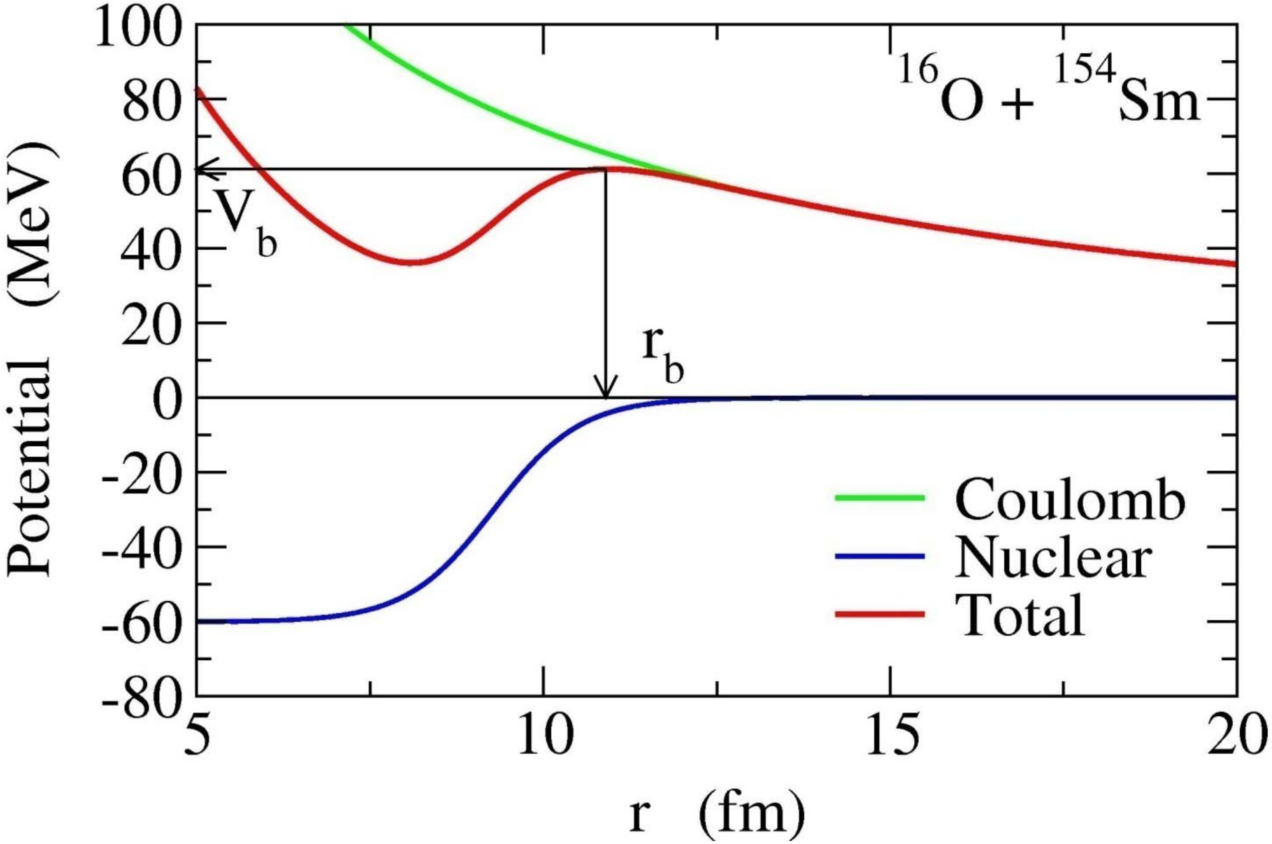

2つの力：

1. クーロン力
   長距離斥力
2. 核力
   短距離引力

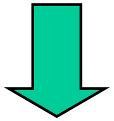

両者の打ち消しあいによりポテンシャル障壁が形成（クーロン障壁）

核融合反応と量子トンネル効果

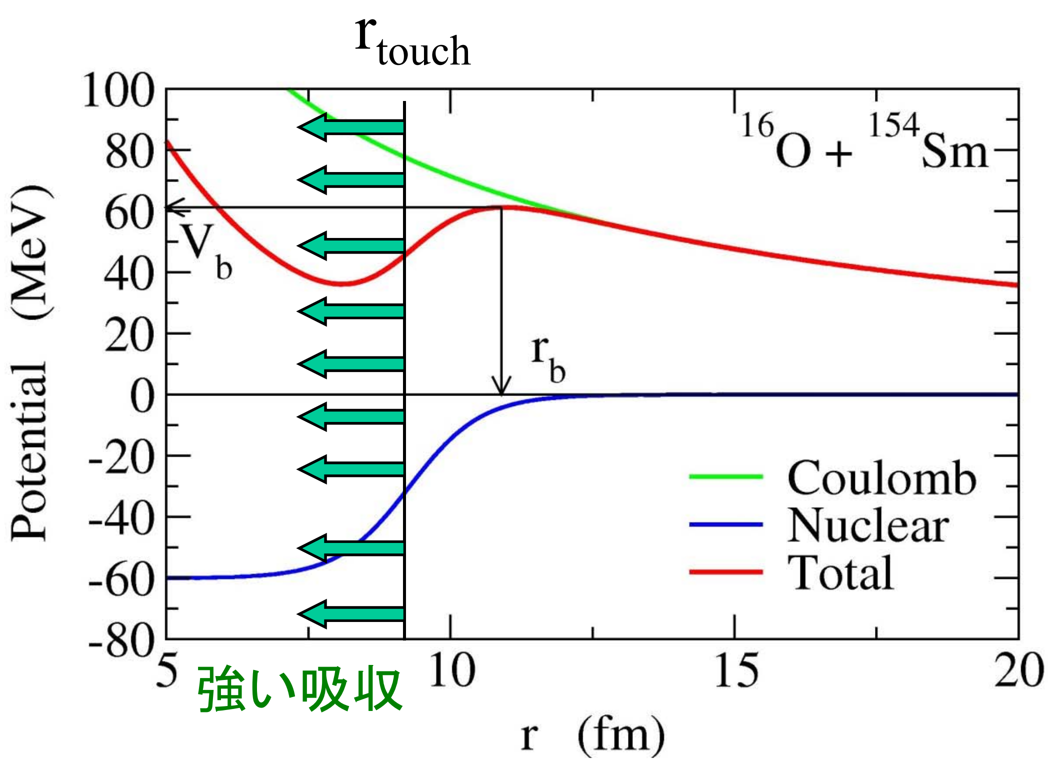

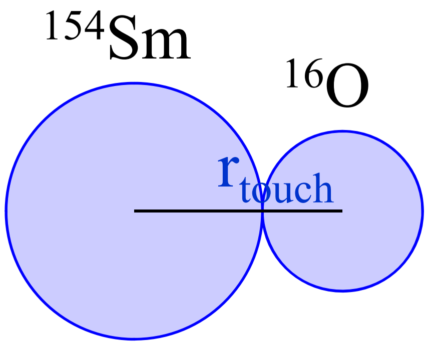

一度接触すると自動的に複合核を形成（強吸収の仮定）

核融合の確率
＝r_{touch} に到達する確率

障壁の透過確率

$$\sigma_{\text{fus}}(E) = \frac{\pi}{k^2}\sum_l (2l+1)P_l(E)$$

低エネルギーでは核融合反応はトンネル効果で起きる！

量子トンネル現象

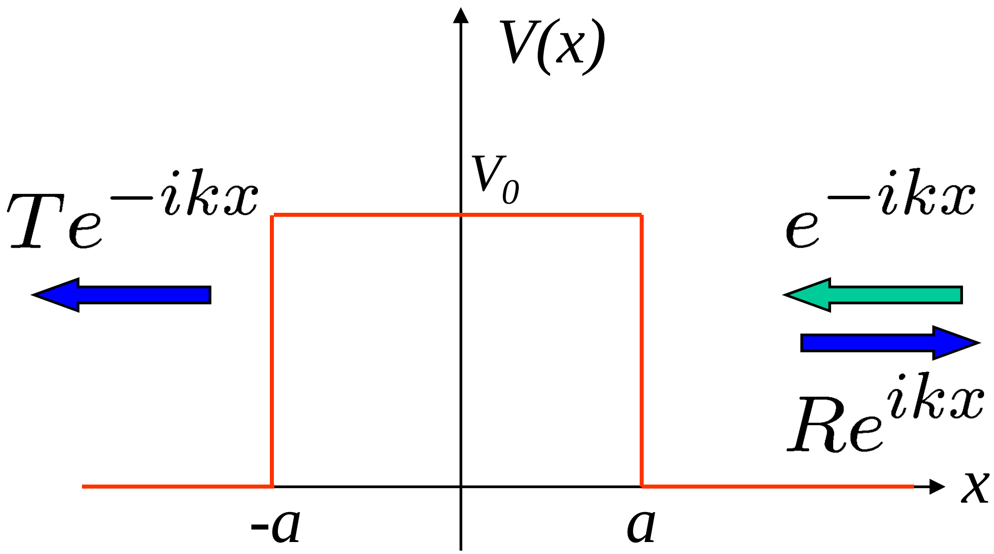

$$
\begin{aligned}
\psi(x) &= T\,e^{-ikx} && (x \le -a) \\
&= A\,e^{-\kappa x} + B\,e^{\kappa x} && (-a < x < a) \\
&= e^{-ikx} + R\,e^{ikx} && (x \ge a)
\end{aligned}
$$

$$
\begin{aligned}
k &= \sqrt{2mE/\hbar^2} \\
\kappa &= \sqrt{2m(V_0 - E)/\hbar^2}
\end{aligned}
$$

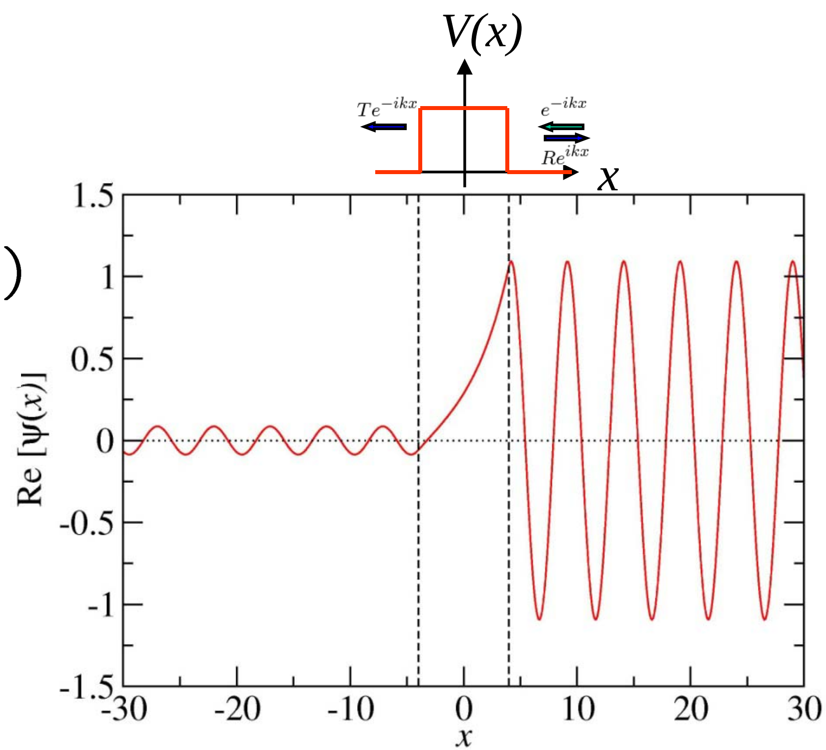

トンネル確率： $P(E) = |T|^2$

放物線障壁だと........

$$V(x) = V_b - \frac{1}{2} m \Omega^2 x^2$$

$$\boxed{P(E) = \frac{1}{1 + \exp\left[\frac{2\pi}{\hbar\Omega}(V_b - E)\right]}}$$

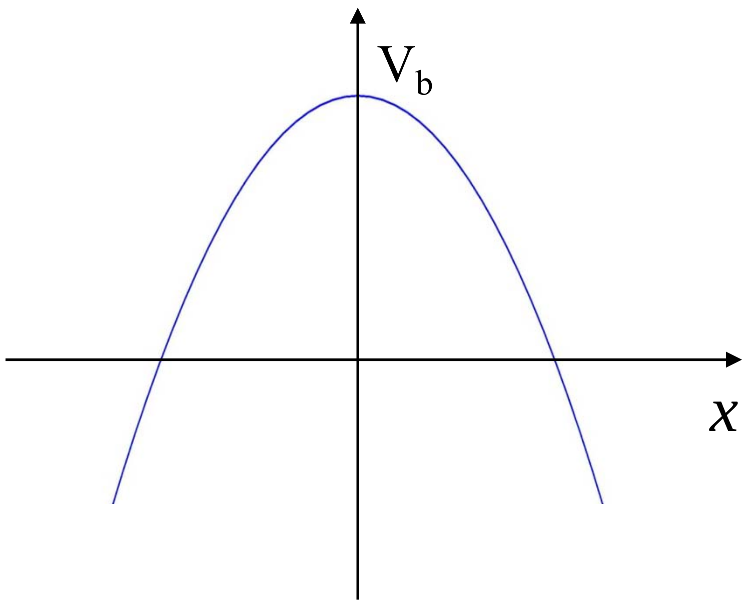

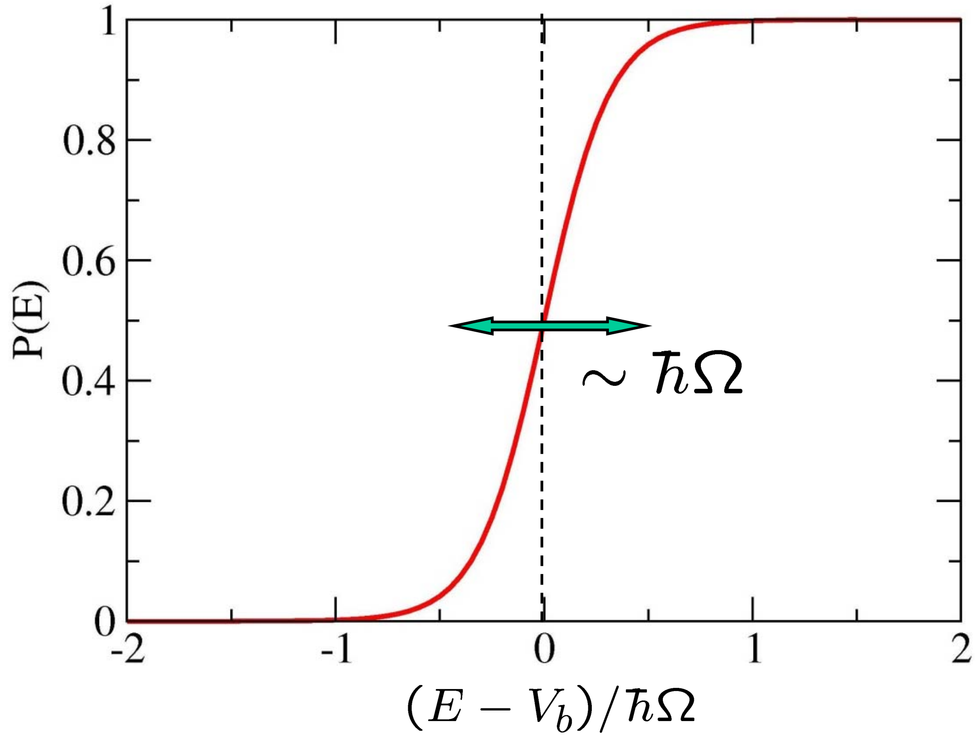

トンネル確率のエネルギー微分

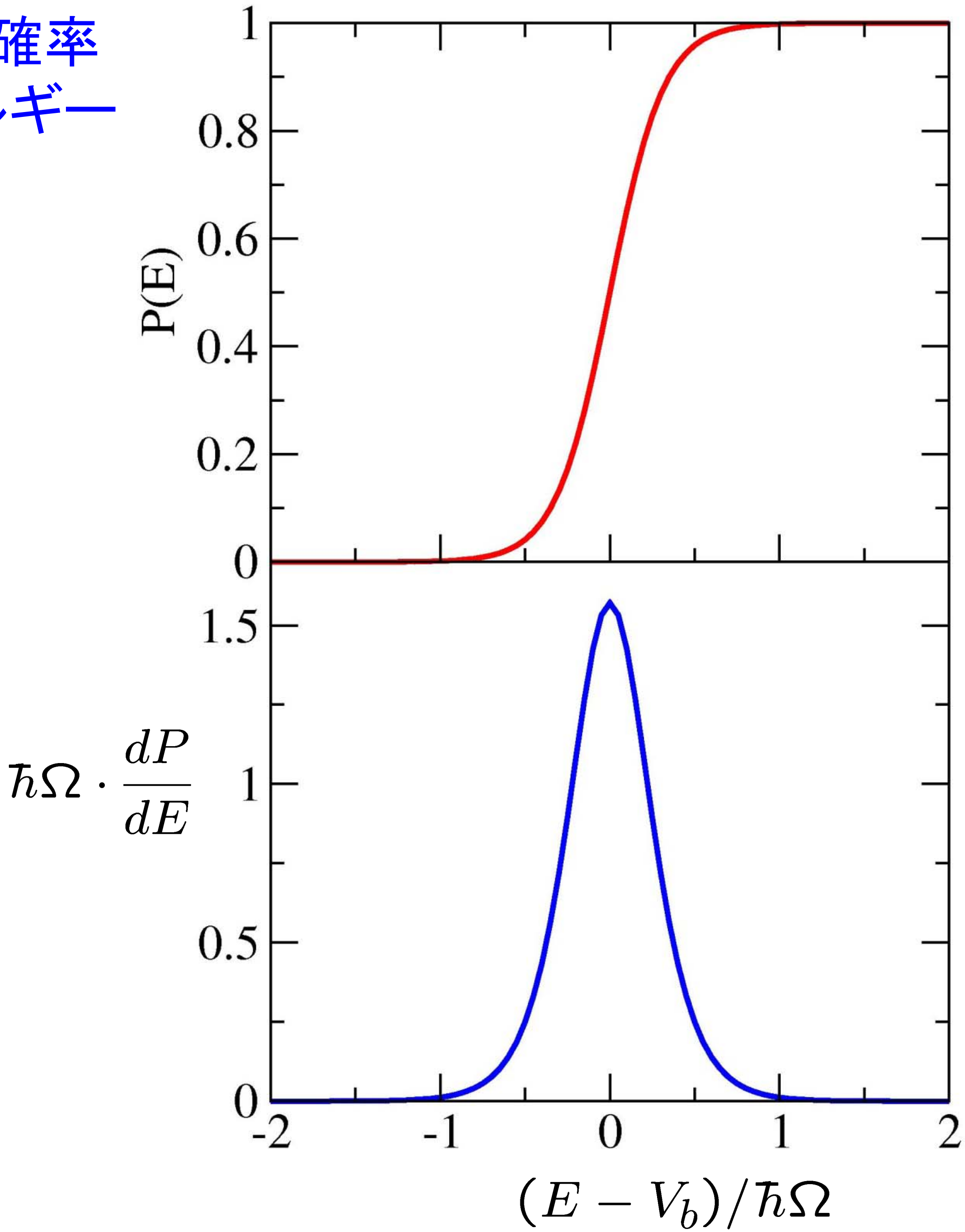

(note) 古典極限

$$
\begin{aligned}
P(E) &= \theta(E - V_b) \\
dP/dE &= \delta(E - V_b)
\end{aligned}
$$

ポテンシャル模型：成功と失敗

$$\left[-\frac{\hbar^2}{2\mu}\frac{d^2}{dr^2}+V(r)+\frac{l(l+1)^2}{2\mu r^2}-E\right]u_l(r)=0$$

遠方での境界条件:　$u_l(r) \to H_l^{(-)}(kr) - S_l\, H_l^{(+)}(kr)$

核融合反応断面積:　$\sigma_{\rm fus} = \frac{\pi}{k^2}\sum_l (2l+1)P_l$

複合核の平均角運動量:　$\langle l \rangle = \sum_l l(2l+1)P_l / \sum_l (2l+1)P_l$

$$P_l = 1 - |S_l|^2$$

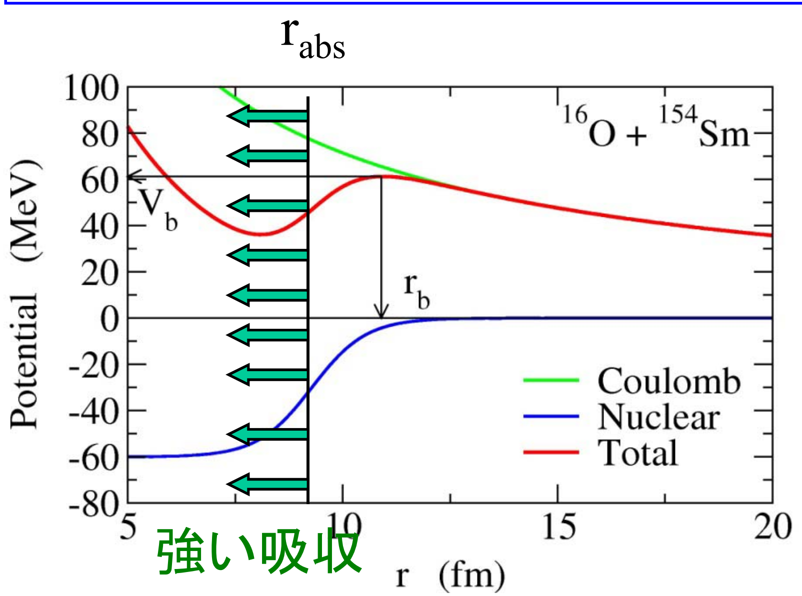

In the case of three-dimensional spherical potential:

$$\psi(\boldsymbol{r}) \to \frac{i}{2k}\sum_l (2l+1)\, i^l \,\frac{1}{r}\left[e^{-i(kr-l\pi/2)} - S_l e^{i(kr-l\pi/2)}\right] P_l(\cos\theta)$$

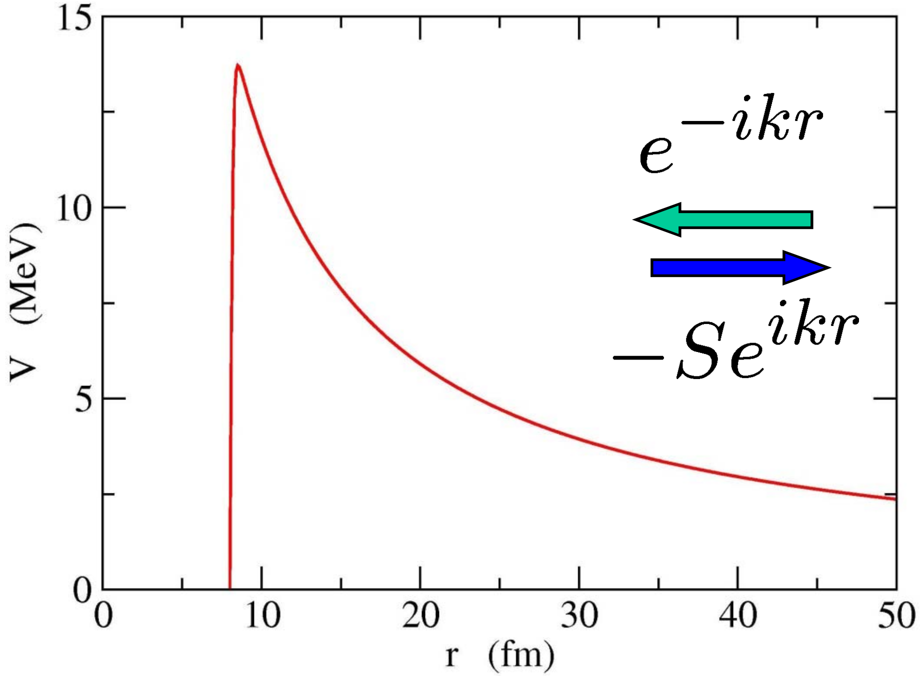

$-S_l \sim R$ (reflection coeff.) $\Longrightarrow P = |T|^2 = 1 - |S_l|^2$

$$\boxed{\sigma_{\rm abs} = \frac{\pi}{k^2}\sum_l (2l+1)(1-|S_l|^2) = \frac{\pi}{k^2}\sum_l (2l+1) P_l}$$

ポテンシャル模型と実験データの比較

エネルギーに依存しない静的なポテンシャルによる核融合反応断面積

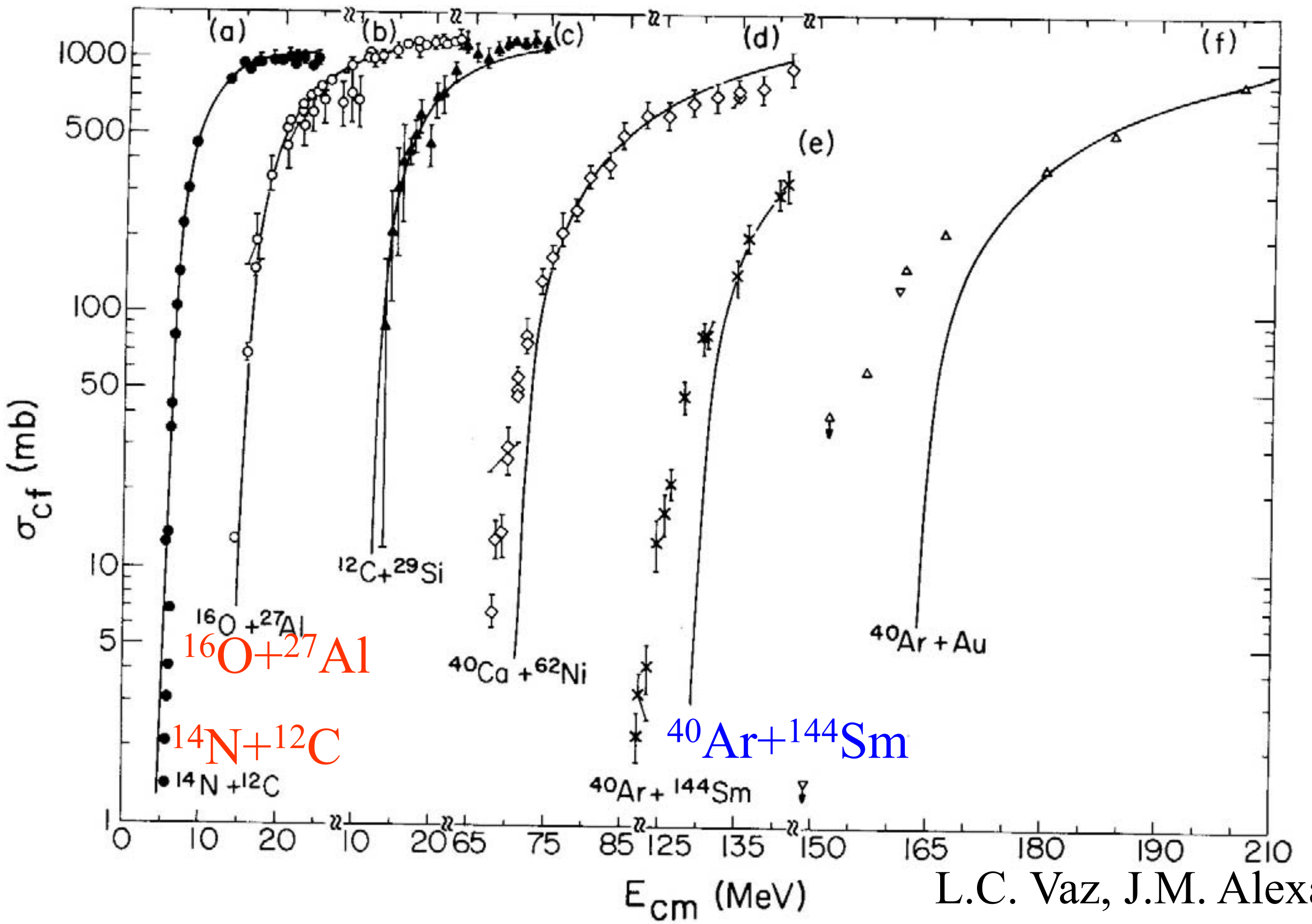

L.C. Vaz, J.M. Alexander, and G.R. Satchler, Phys. Rep. 69('81)373

- 比較的軽い系では実験データを再現
- 系が重くなると過小評価（低エネルギー）

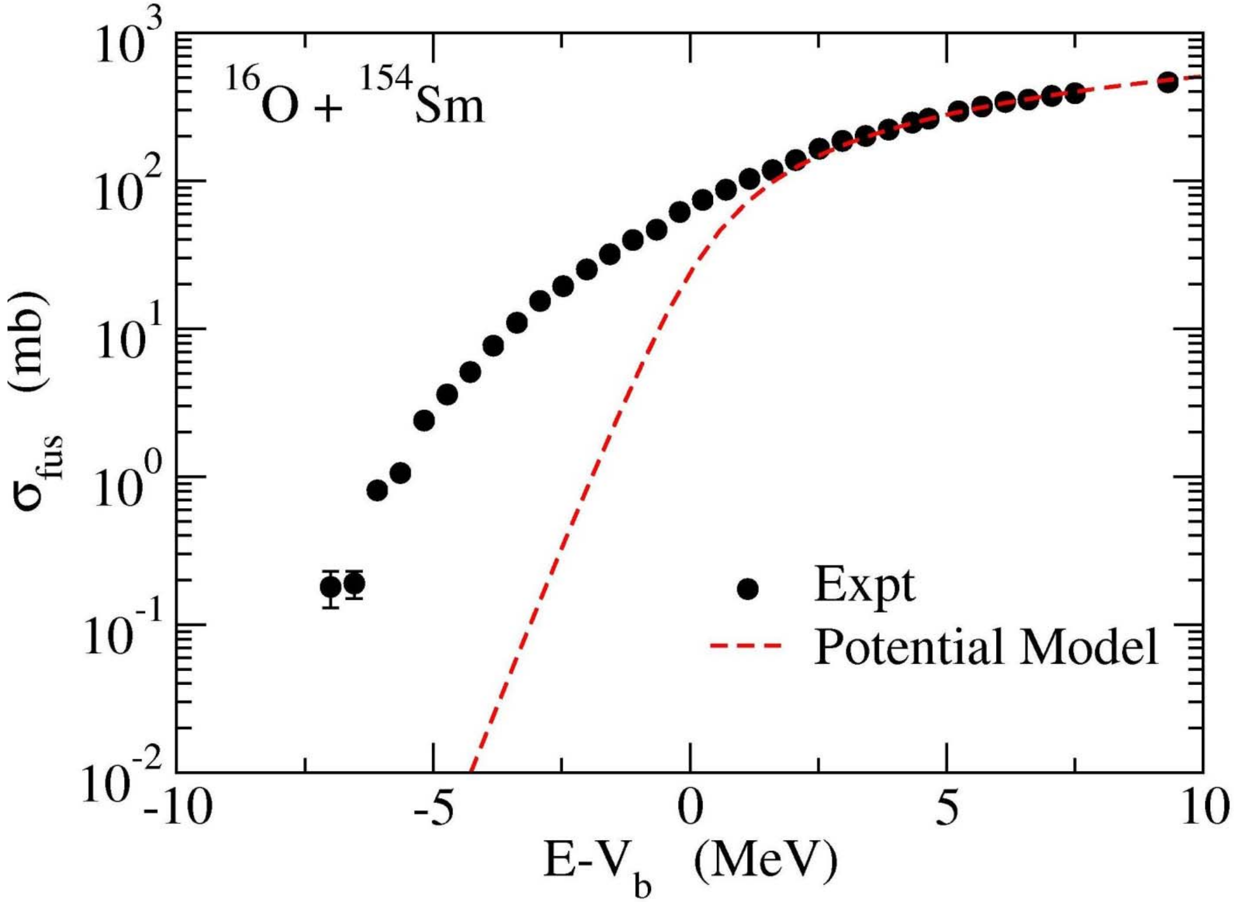

ポテンシャル模型:

$E > V_b$ では大体データを再現

$E < V_b$ では核融合断面積を過小に評価

核融合断面積の標的核依存性

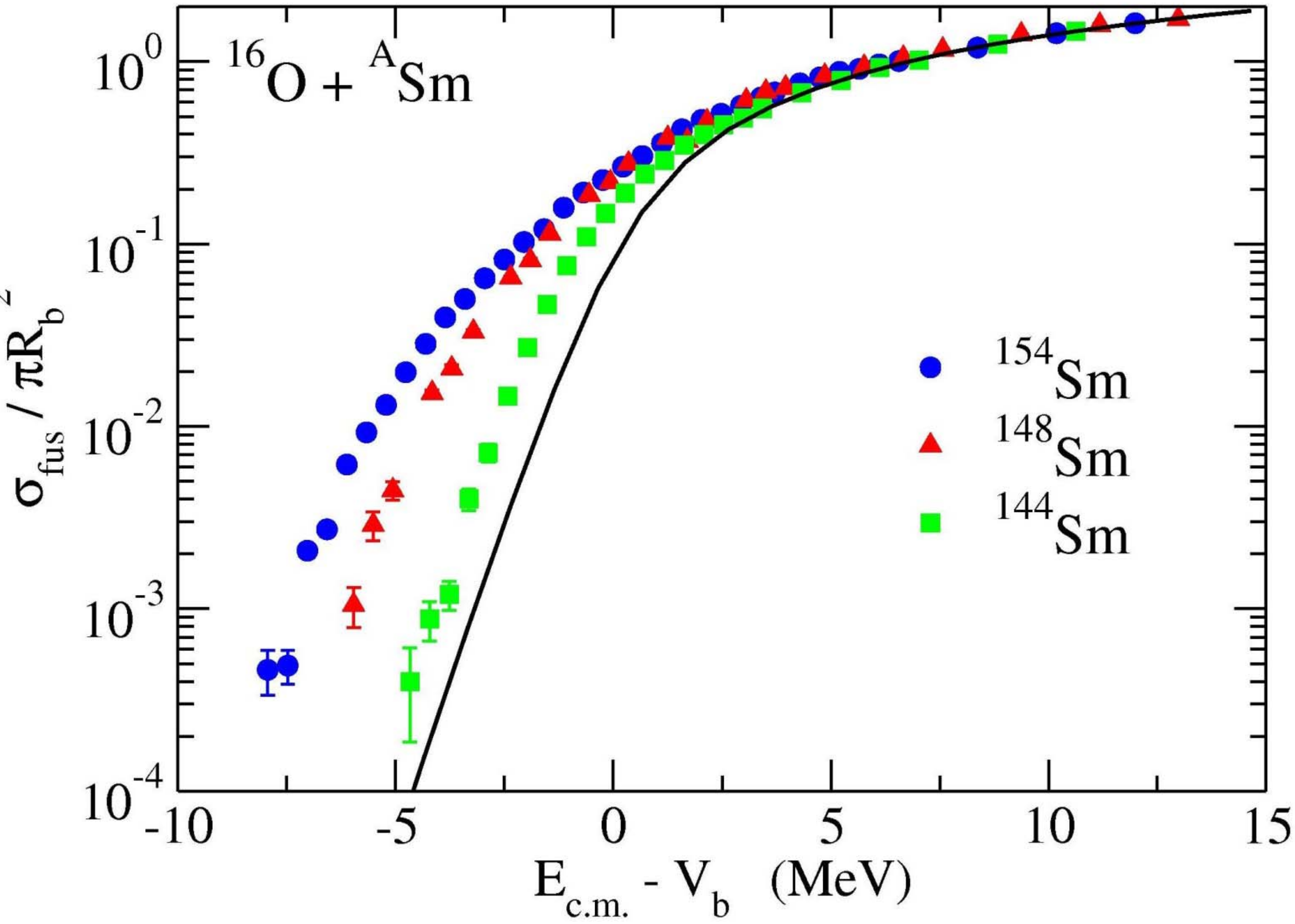

⇨ $E < V_b$ において強い標的核依存性

原子核の低励起集団運動

偶々核の低エネルギーに現れる励起状態は集団励起状態であり、対相関と殻構造を強く反映する。

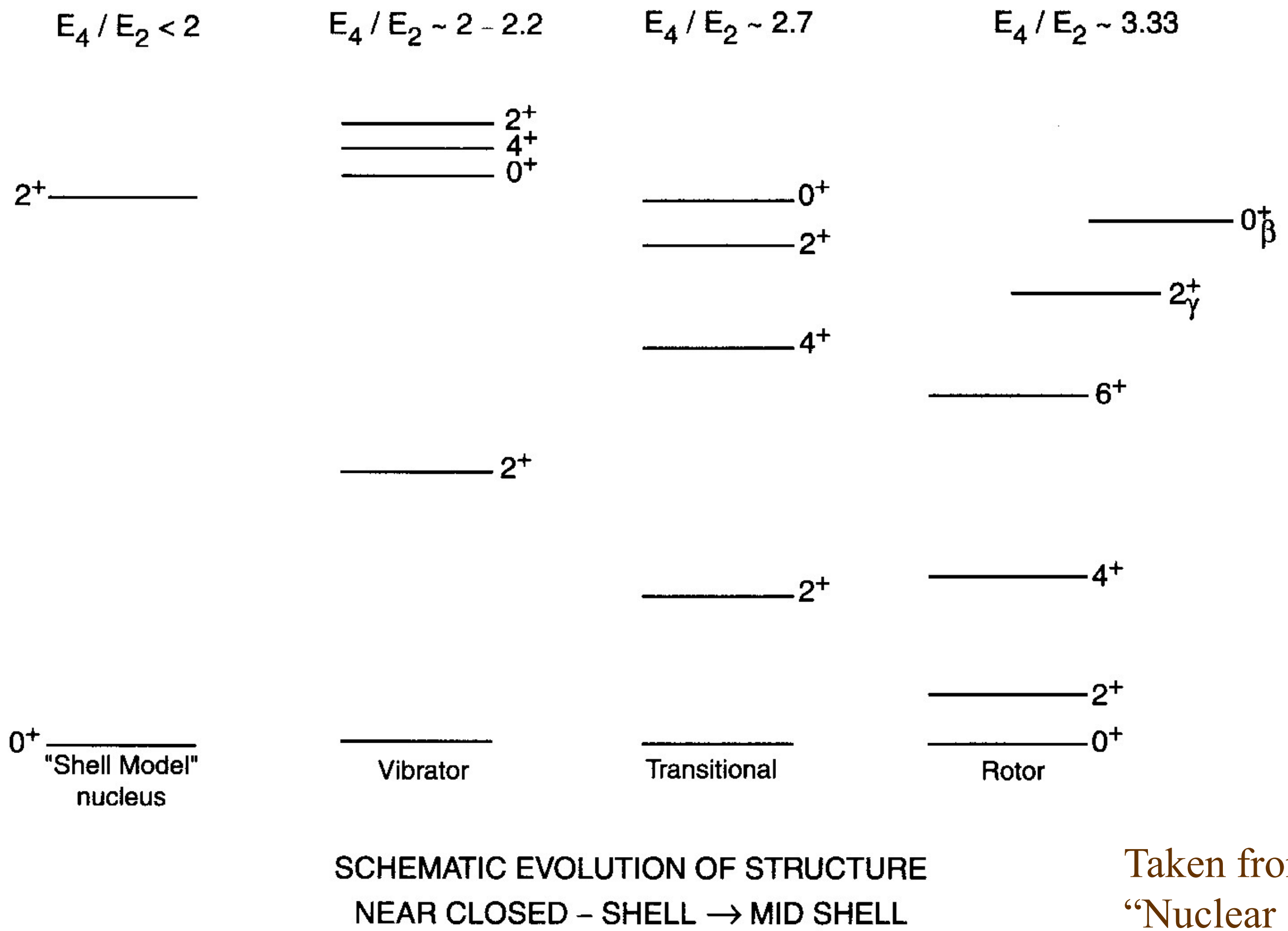

Taken from R.F. Casten, "Nuclear Structure from a Simple Perspective"

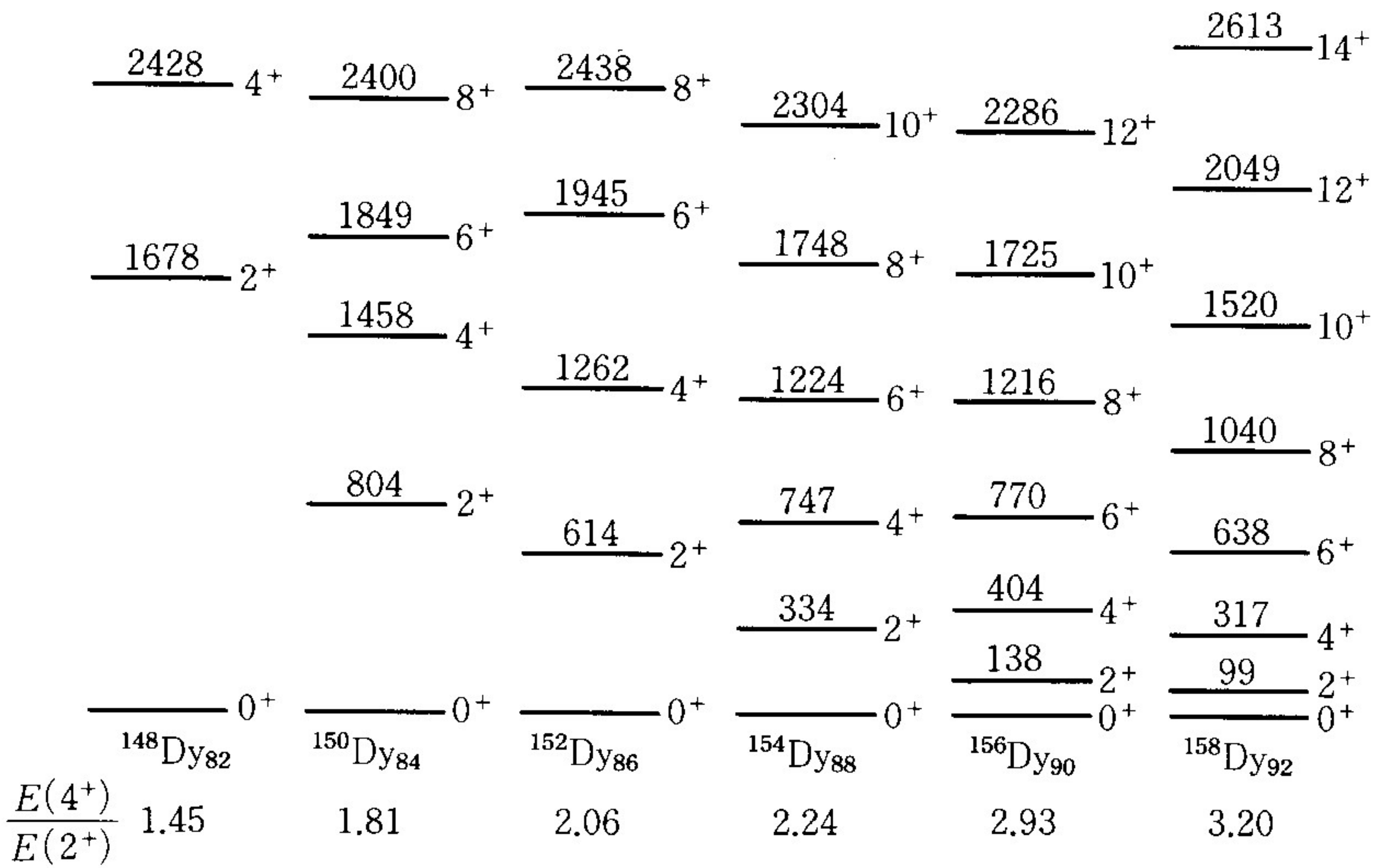

図 3-4 Dy アイソトープの低励起スペクトル．励起エネルギーの単位は keV.

市村、坂田、松柳
「原子核の理論」より

核融合反応に対する集団励起の影響: 回転の場合

エネルギー・スケールの比較

$$V(r) \sim V_b - \frac{1}{2}\mu\Omega^2 r^2$$

$$\begin{cases} \text{トンネル運動:} & E_{\text{tun}} \sim \hbar\Omega \sim 3.5\text{ MeV (クーロン障壁の曲率)} \\ \text{回転運動:} & E_{\text{rot}} \sim E_{2+} \sim 0.08\text{MeV} \end{cases}$$

$$E_{\text{tun}} \gg E_{\text{rot}} = I(I+1)\hbar^2/2\mathcal{J} \to 0$$

$$\longleftrightarrow \quad \mathcal{J} \to \infty$$

^{154}Sm の方向は反応中にほとんど変化しない

(note)
反応の初期は基底状態
(0^+ 状態)

⇨

あらゆる方向が等確率
で混ざっている

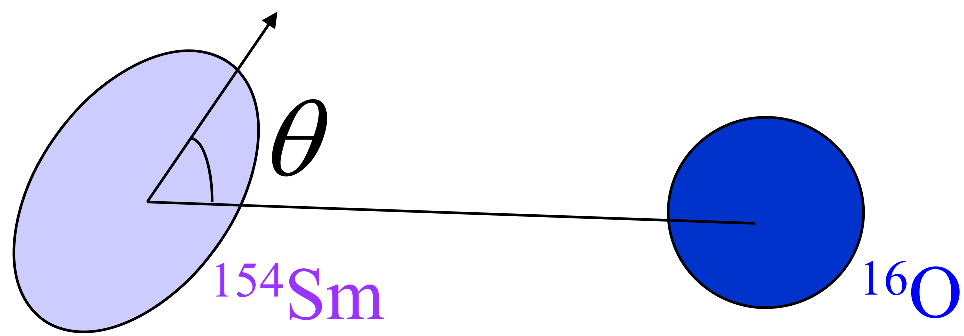

$$\boxed{\sigma_{\text{fus}}(E) = \int_0^1 d(\cos\theta)\,\sigma_{\text{fus}}(E;\theta)}$$

Effect of collective excitation on σ_{fus}: rotational case

The orientation angle of ^{154}Sm does not change much during fusion

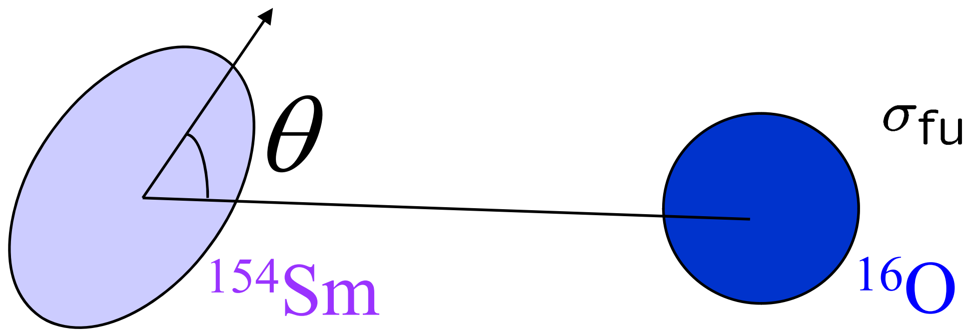

$$\sigma_{\text{fus}}(E) = \int_0^1 d(\cos\theta)\sigma_{\text{fus}}(E;\theta)$$

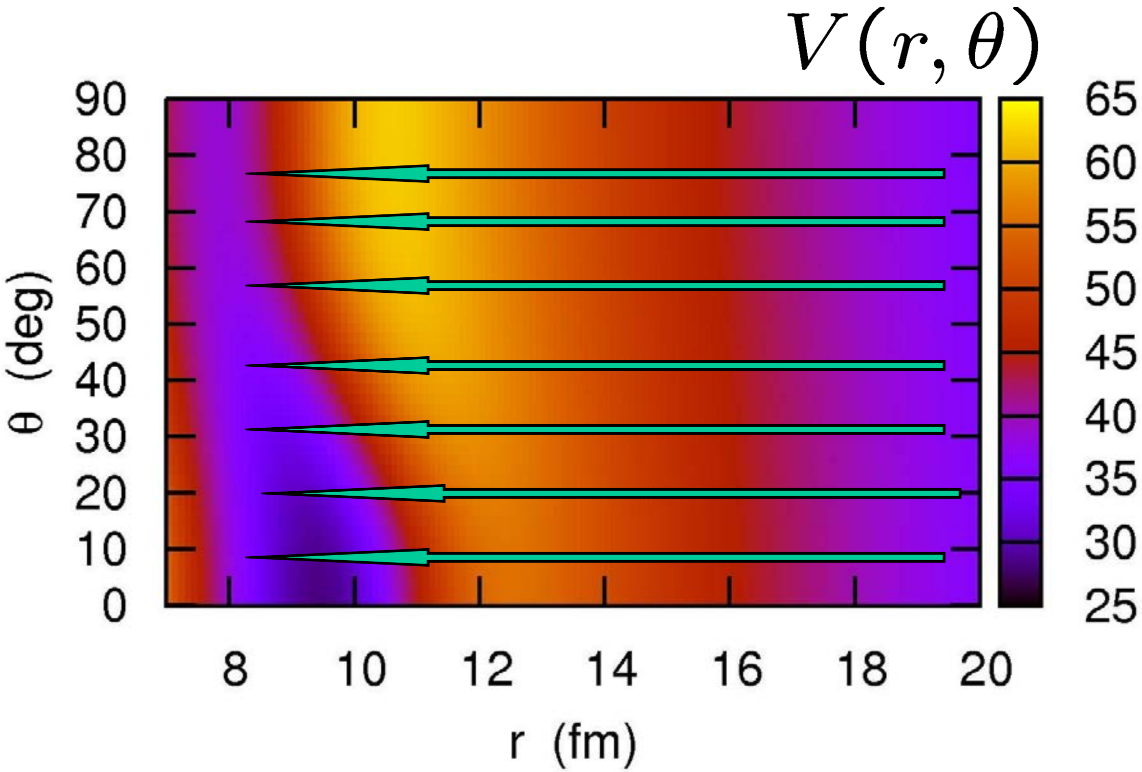

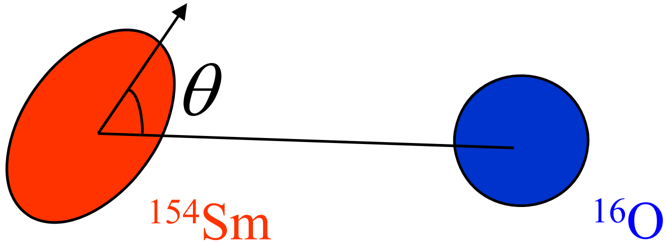

$$\sigma_{\text{fus}}(E) = \int_0^1 d(\cos\theta)\sigma_{\text{fus}}(E;\theta)$$

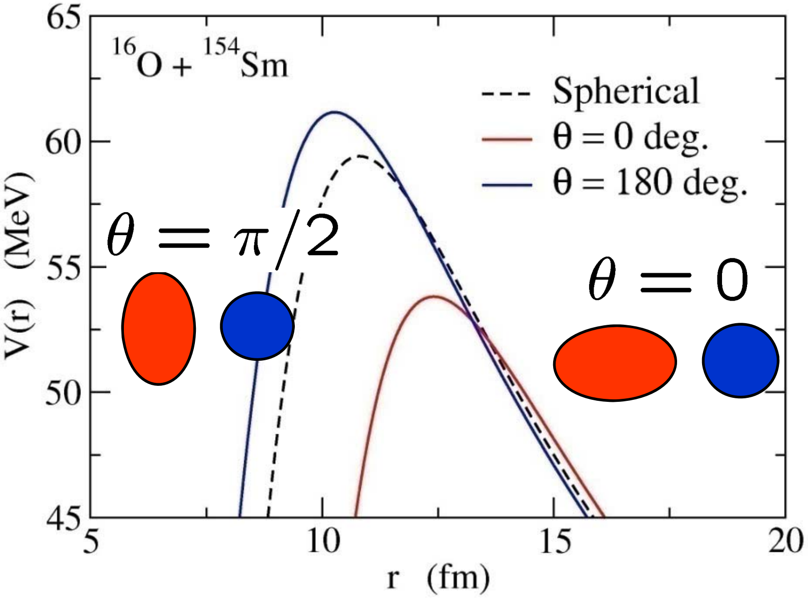

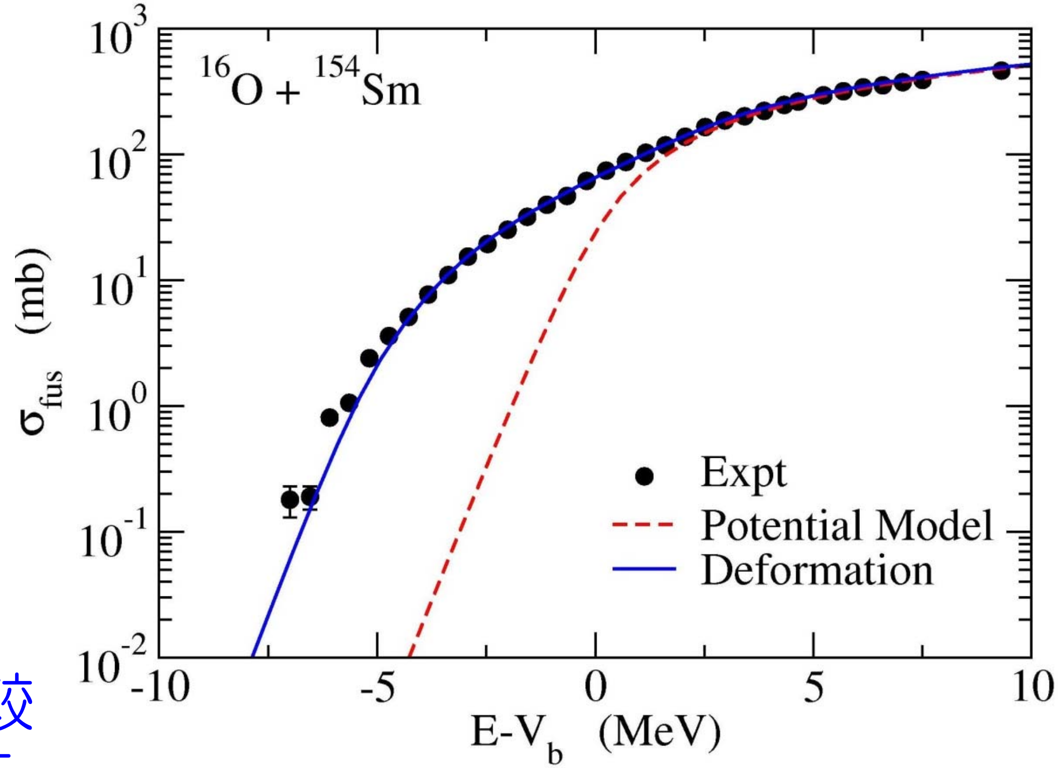

$\theta = 0$ では引力の核力が比較的遠方から働くため障壁が下がる。

$\theta = \pi/2$　はその逆。近づかないと引力が働かないため障壁は上がる。

変形の効果：核融合断面積が 10~100 倍増大

⟹ 核融合反応：核構造に対する興味深いプローブ

より量子的な取り扱い：結合チャンネル法

相対運動と内部自由度の結合

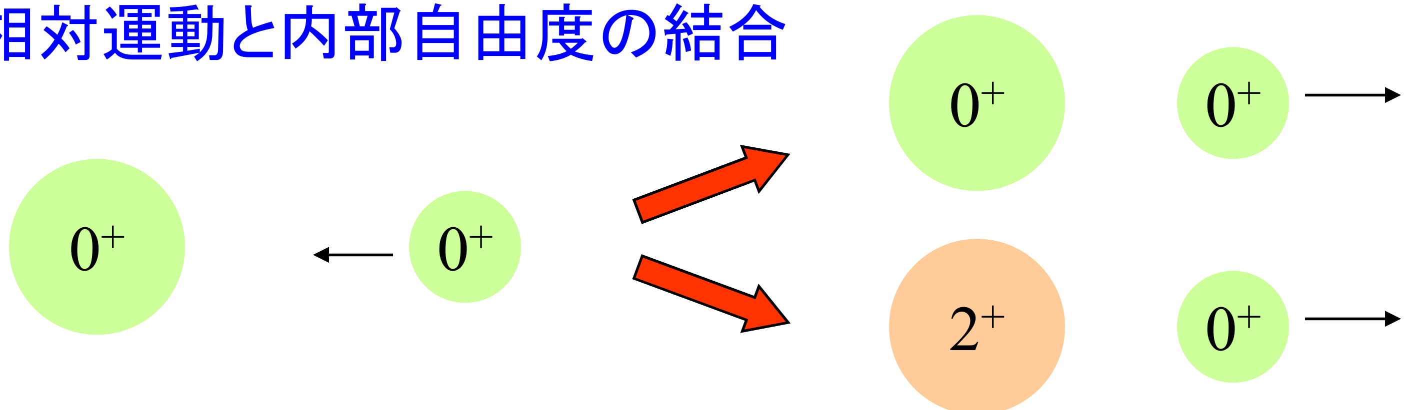

エントランス・チャンネル

励起チャンネル

$$H = -\frac{\hbar^2}{2\mu}\nabla^2 + V_0(r) + H_0(\xi) + V_{\rm coup}(\boldsymbol{r}, \xi)$$

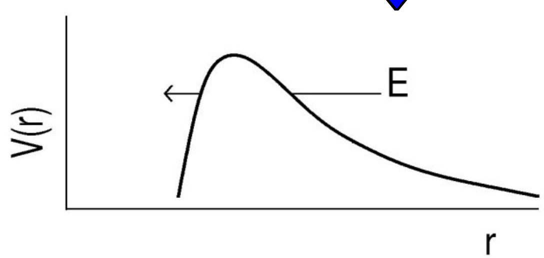

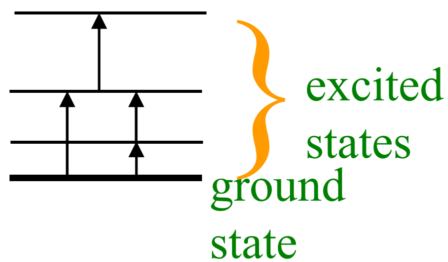

$$H_0(\xi)\phi_k(\xi) = \epsilon_k\,\phi_k(\xi)$$

$$\boxed{\Psi(\boldsymbol{r}, \xi) = \sum_k \psi_k(\boldsymbol{r})\phi_k(\xi)}$$

$$\begin{cases} H = -\dfrac{\hbar^2}{2\mu}\nabla^2 + V_0(r) + H_0(\xi) + V_{\rm coup}(\boldsymbol{r},\xi) \\ \Psi(\boldsymbol{r},\xi) = \sum_k \psi_k(\boldsymbol{r})\phi_k(\xi) \end{cases}$$

$$H_0(\xi)\phi_k(\xi) = \epsilon_k\,\phi_k(\xi)$$

Schroedinger equation: $(H-E)\Psi(\boldsymbol{r},\xi) = 0$

$\langle\phi_k| \longrightarrow$

$$\langle\phi_k|H-E|\Psi\rangle = 0$$

or

$$\boxed{\left[-\frac{\hbar^2}{2\mu}\nabla^2 + V_0(r) + \epsilon_k - E\right]\psi_k(\boldsymbol{r}) + \sum_{k'}\langle\phi_k|V_{\rm coup}|\phi_{k'}\rangle\psi_{k'}(\boldsymbol{r}) = 0}$$

結合チャンネル方程式

境界条件

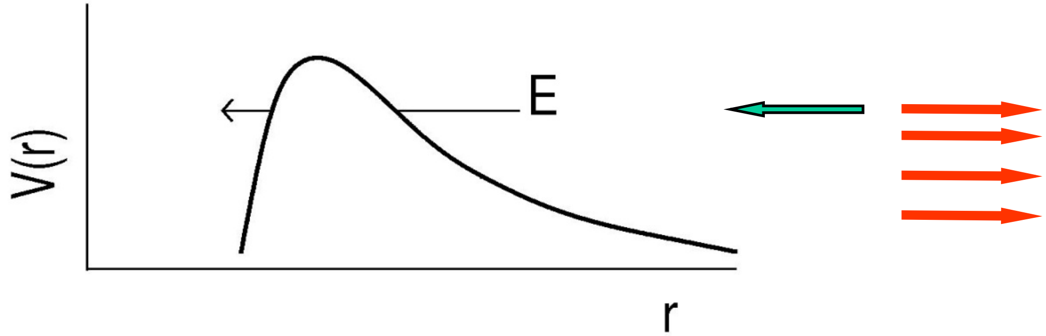

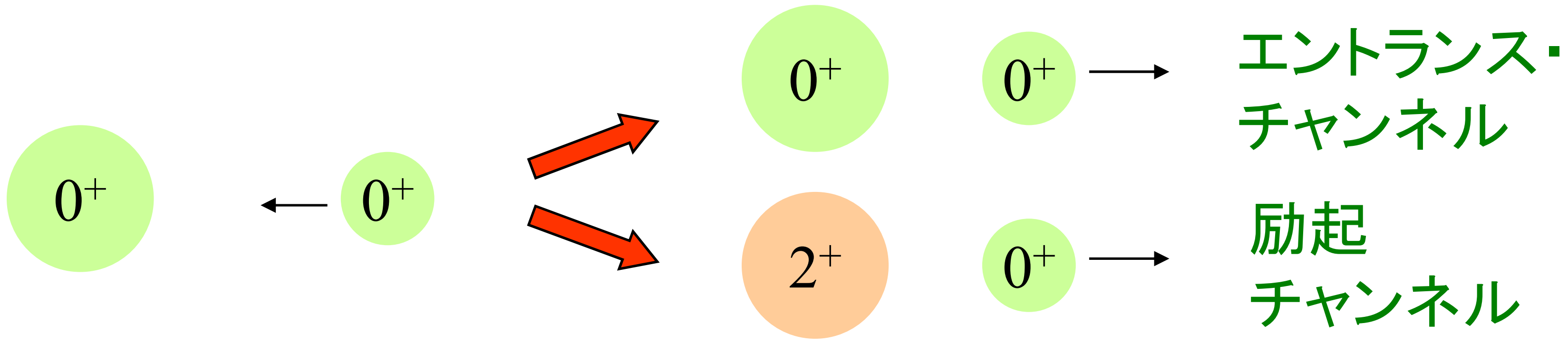

$$\Psi(\boldsymbol{r},\xi)=\sum_{n,l,I}\frac{u_{nlI}(r)}{r}[Y_l(\hat{\boldsymbol{r}})\phi_{nI}(\xi)]^{(JM)}$$

$$\boxed{u_{nlI}(r)\to H_l^{(-)}(k_{nI}r)\delta_{n,n_i}\delta_{l,l_i}\delta_{I,I_i}-\sqrt{\frac{k_0}{k_{nI}}}S_{nlI}H_l^{(+)}(k_{nI}r)}$$

$$P_l(E)=1-\sum_{nI}|S_{nlI}|^2 \qquad \sigma_{\rm fus}(E)=\frac{\pi}{k^2}\sum_l(2l+1)P_l(E)$$

結合チャンネル法のまとめ

$$\begin{cases} H = -\dfrac{\hbar^2}{2\mu}\nabla^2 + V_0(r) + H_0(\xi) + V_{\rm coup}(\boldsymbol{r},\xi) \\ \Psi(\boldsymbol{r},\xi) = \displaystyle\sum_{n,l,I} \frac{u_{nlI}(r)}{r}[Y_l(\hat{\boldsymbol{r}})\phi_{nI}(\xi)]^{(JM)} \end{cases}$$

$$H_0(\xi)\phi_{nIm_I}(\xi) = \epsilon_{nI}\,\phi_{nIm_I}(\xi)$$

$$\langle [Y_l\phi_{nI}]^{(JM)}|H-E|\Psi\rangle = 0$$

$$\boxed{\begin{aligned}&\left[-\frac{\hbar^2}{2\mu}\frac{d^2}{dr^2}+\frac{l(l+1)\hbar^2}{2\mu r^2}+V_0(r)-E+\epsilon_{nI}\right]u_{nlI}(r)\\ &\quad+\sum_{n'l'I'}\langle [Y_l\phi_{nI}]^{(JM)}|V_{\rm coup}(r)|[Y_{l'}\phi_{n'I'}]^{(JM)}\rangle\,u_{n'l'I'}(r)=0\end{aligned}}$$

$$\boxed{u_{nlI}(r) \to H_l^{(-)}(k_{nI}r)\delta_{n,n_i}\delta_{l,l_i}\delta_{I,I_i} - \sqrt{\frac{k_0}{k_{nI}}}\,S_{nlI}\,H_l^{(+)}(k_{nI}r)}$$

$$P_l(E) = 1 - \sum_{nI}|S_{nlI}|^2 \qquad \sigma_{\rm fus}(E) = \frac{\pi}{k^2}\sum_l (2l+1)P_l(E)$$

Coupling Potential: Collective Model

$$R(\theta,\phi) = R_T\left(1+\sum_\mu \alpha_{\lambda\mu}Y^*_{\lambda\mu}(\theta,\phi)\right)$$

(note) rotating frame への座標変換($\hat{\boldsymbol{r}} = 0$):

$$\sum_\mu \alpha_{\lambda\mu}Y^*_{\lambda\mu}(\theta,\phi) \to \sqrt{\frac{2\lambda+1}{4\pi}}\alpha_{\lambda 0}$$

➢振動励起の場合

$$\begin{cases} \alpha_{\lambda\mu} &= \dfrac{\beta_\lambda}{\sqrt{2\lambda+1}}(a^\dagger_{\lambda\mu}+(-)^\mu a_{\lambda\mu}) \\ H_0 &= \hbar\omega_\lambda \sum_\mu a^\dagger_{\lambda\mu}a_{\lambda\mu} \end{cases}$$

➢回転励起の場合

Body-fixed 系への座標変換:

$$\begin{cases} \alpha_{\lambda\mu} &= \sqrt{\dfrac{4\pi}{2\lambda+1}}\beta_\lambda Y_{\lambda\mu}(\theta_d,\phi_d) \quad \text{(軸対称変形の場合)} \\ H_0 &= \dfrac{I(I+1)\hbar^2}{2\mathcal{J}} \end{cases}$$

いずれの場合も $\beta_\lambda = \dfrac{4\pi}{3Z_TR_T^\lambda}\sqrt{\dfrac{B(E\lambda)\uparrow}{e^2}}$

Deformed Woods-Saxon model:

$$V_{WS}(r) = -\frac{V_0}{1+\exp[(r-R_0)/a]}$$

$$= -\frac{V_0}{1+\exp[(r-R_P-R_T)/a]}$$

$$R_T \to R_T\left(1+\sum_\mu \alpha_{\lambda\mu}Y^*_{\lambda\mu}(\theta,\phi)\right)$$

$$\boxed{V_{WS}(\boldsymbol{r}) = -\frac{V_0}{1+\exp[(r-R_0-R_T\,\alpha_\lambda\cdot Y_\lambda(\hat{\boldsymbol{r}}))/a]}}$$

Deformed Woods-Saxon model (collective model)

K.H., N. Rowley, and A.T. Kruppa,
Comp. Phys. Comm. 123('99)143

$$V_{\mathrm{coup}}(r,\hat{O}) = V^{(N)}_{\mathrm{coup}}(r,\hat{O}) + V^{(C)}_{\mathrm{coup}}(r,\hat{O})$$

Nuclear coupling:

$$V^{(N)}_{\mathrm{coup}}(r,\hat{O}) = -\frac{V_0}{1+\exp[(r-R_0-R_T\hat{O})/a]}$$

Coulomb coupling:

$$V^{(C)}_{\mathrm{coup}}(r,\hat{O}) = \frac{3}{2\lambda+1} Z_P Z_T e^2 \frac{R_T^\lambda}{r^{\lambda+1}} \hat{O}$$

Rotational coupling: $\hat{O} = \beta Y_{20}(\theta)$

Vibrational coupling: $\hat{O} = \frac{\beta}{\sqrt{4\pi}}(a+a^\dagger)$

Vibrational coupling

$$\hat{O} = \frac{\beta}{\sqrt{4\pi}}(a + a^\dagger)$$

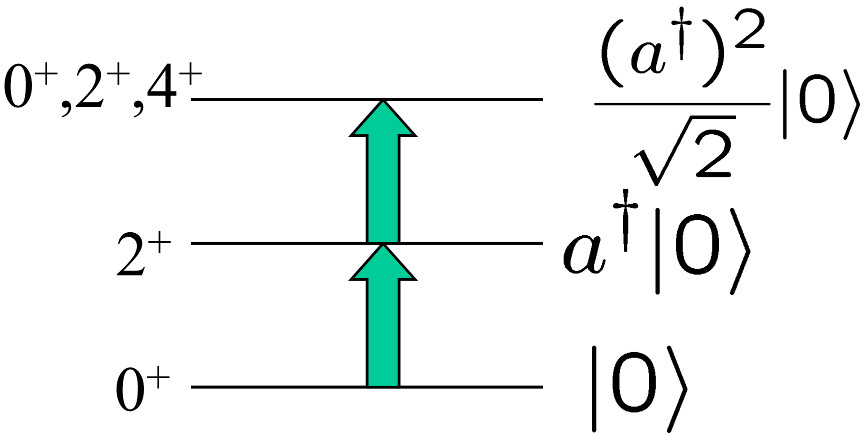

Rotational coupling

$$\hat{O} = \beta Y_{20}(\theta)$$

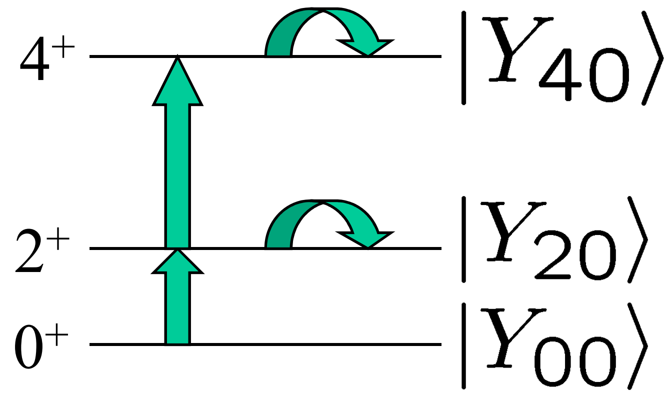

$$\begin{pmatrix} 0 & F & 0 \\ F & \epsilon & \sqrt{2}F \\ 0 & \sqrt{2}F & 2\epsilon \end{pmatrix}$$

$$\begin{pmatrix} 0 & F & 0 \\ F & \epsilon + \frac{2\sqrt{5}}{7}F & \frac{6}{7}F \\ 0 & \frac{6}{7}F & \frac{10\epsilon}{3} + \frac{20\sqrt{5}}{77}F \end{pmatrix}$$

$$F = \frac{\beta}{\sqrt{4\pi}}$$

結合チャンネル方程式の瞬間極限

$$\epsilon \to 0$$

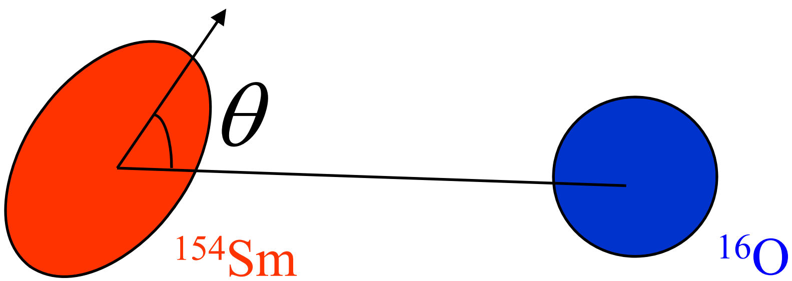

$$\epsilon_I = I(I+1)\hbar^2/2\mathcal{J}$$

$$\mathcal{J} \to \infty$$

$$\sigma_{\rm fus}(E) = \int_0^1 d(\cos\theta)\sigma_{\rm fus}(E;\theta)$$

Coupled-channels:

$$\begin{pmatrix} 0 & f(r) & 0 \\ f(r) & \frac{2\sqrt{5}}{7}f(r) & \frac{6}{7}f(r) \\ 0 & \frac{6}{7}f(r) & \frac{20\sqrt{5}}{77}f(r) \end{pmatrix} \xrightarrow{\text{diagonalize}} \begin{pmatrix} \lambda_1(r) & 0 & 0 \\ 0 & \lambda_2(r) & 0 \\ 0 & 0 & \lambda_3(r) \end{pmatrix}$$

$$P(E) = \sum_i w_i P(E; V_0(r) + \lambda_i(r))$$

Slow intrinsic motion

→ Barrier Distribution

障壁分布

$$P(E) = \sum_i w_i \, P(E; V_0(r) + \lambda_i(r))$$

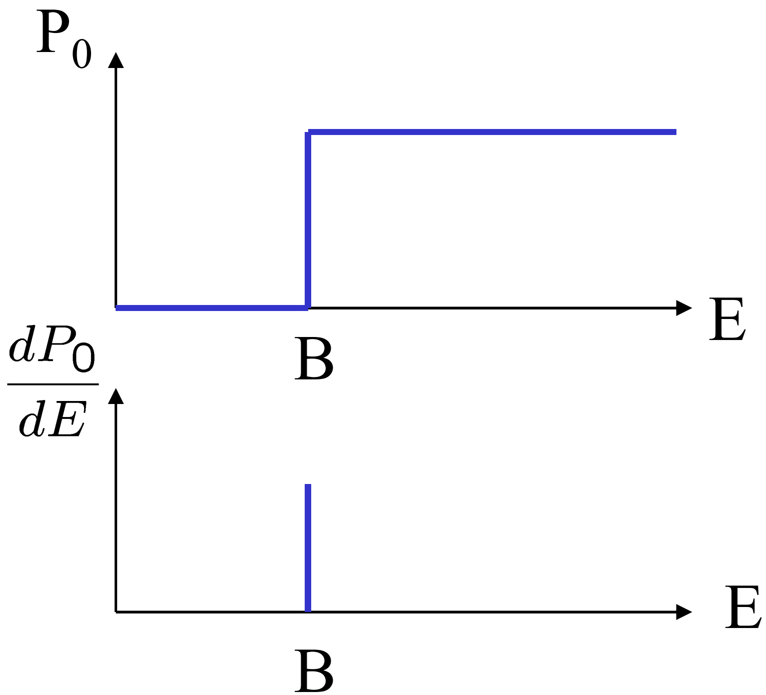

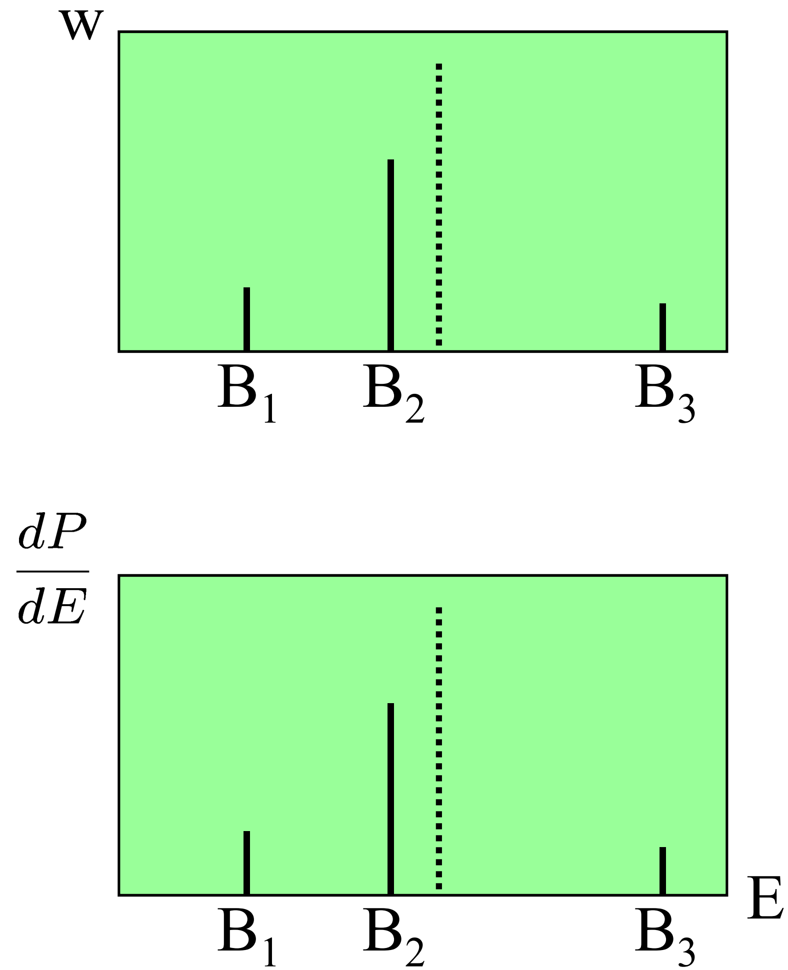

Barrier distribution: understand the concept using a spin Hamiltonian

Hamiltonian (example 1):
$$H = -\frac{\hbar^2}{2m}\frac{d^2}{dx^2} + V_0(x) + \hat{\sigma}_z \cdot V_s(x)$$

$$\hat{\sigma}_z = \begin{pmatrix} 1 & 0 \\ 0 & -1 \end{pmatrix}$$

For Spin-up

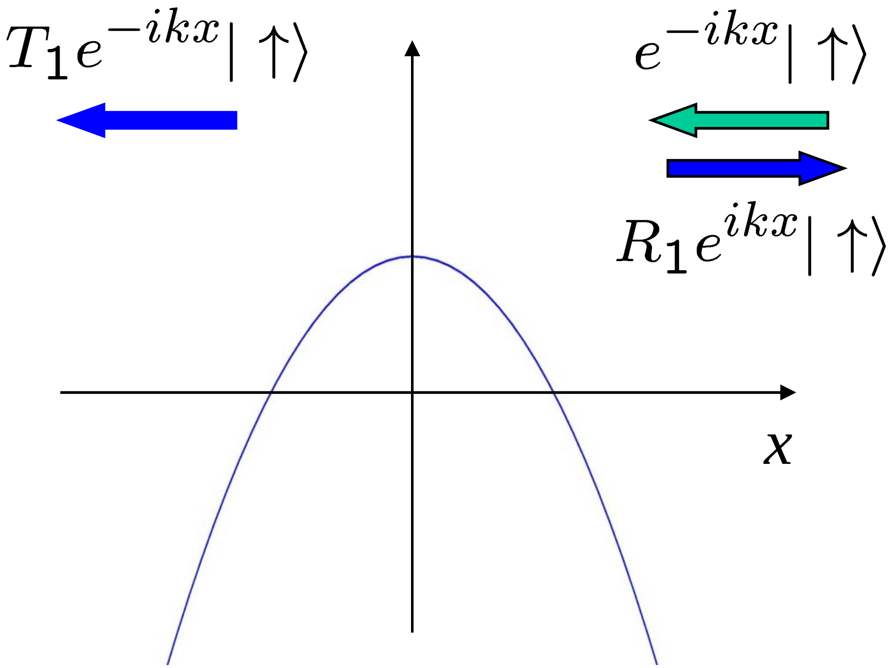

$$V_1(x) = V_0(x) + V_s(x)$$

For Spin-down

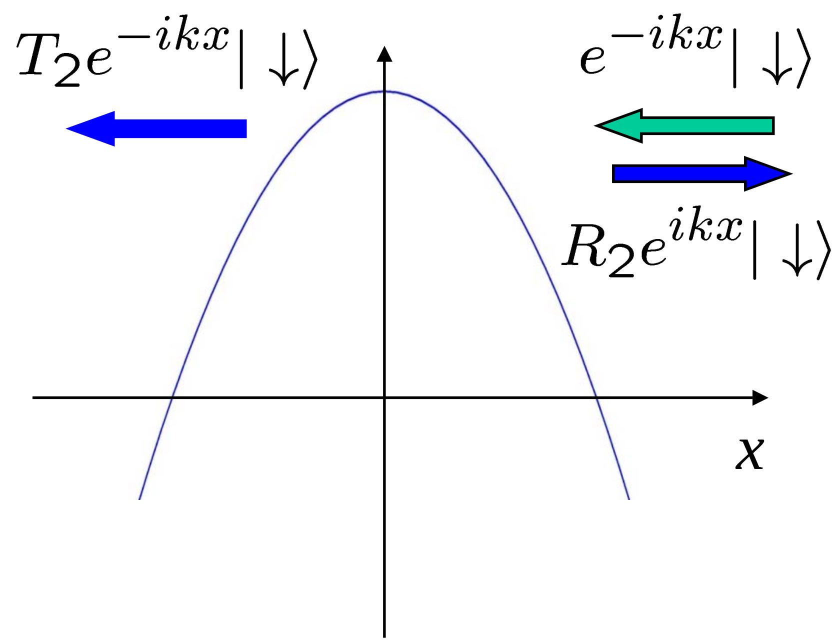

$$V_2(x) = V_0(x) - V_s(x)$$

$$H = -\frac{\hbar^2}{2m}\frac{d^2}{dx^2} + V_0(x) + \hat{\sigma}_z \cdot V_1(x)$$

→ Wave function (general form)

$$\Psi(x) = \psi_1(x)\,|\uparrow\rangle + \psi_2(x)\,|\downarrow\rangle = \begin{pmatrix} \psi_1(x) \\ \psi_2(x) \end{pmatrix}$$

Asymptotic form at $x \to \pm\infty$

$$\Psi(x) \to \begin{pmatrix} C_1(e^{-ikx} + R_1 e^{ikx}) \\ C_2(e^{-ikx} + R_2 e^{ikx}) \end{pmatrix} \quad (x \to \infty)$$

$$\to \begin{pmatrix} C_1\, T_1 e^{-ikx} \\ C_2\, T_2 e^{-ikx} \end{pmatrix} \quad (x \to -\infty)$$

$$|C_1|^2 + |C_2|^2 = 1$$

(the C_1 and C_2 are fixed according to the spin state of the system)

Tunnel probability = $\dfrac{(\text{flux at } x = -\infty)}{(\text{incoming flux at } x = \infty)}$

$$\boxed{\begin{aligned} P(E) &= \frac{|C_1 T_1|^2 + |C_2 T_2|^2}{|C_1|^2 + |C_2|^2} \\ &= |C_1|^2 P_1(E) + |C_2|^2 P_2(E) \equiv w_1 P_1(E) + w_2 P_2(E) \end{aligned}}$$

$$P(E) = w_1 P_1(E) + w_2 P_2(E)$$

$\Rightarrow$ Tunneling prob. is a weighted sum of tunnel prob. for two barriers

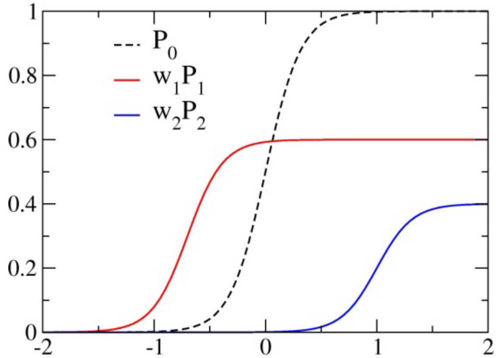

$$\begin{cases} V_1(x) = V_0(x) + V_s(x) & \Longleftarrow \quad |\uparrow\rangle \\ V_2(x) = V_0(x) - V_s(x) & \Longleftarrow \quad |\downarrow\rangle \end{cases}$$

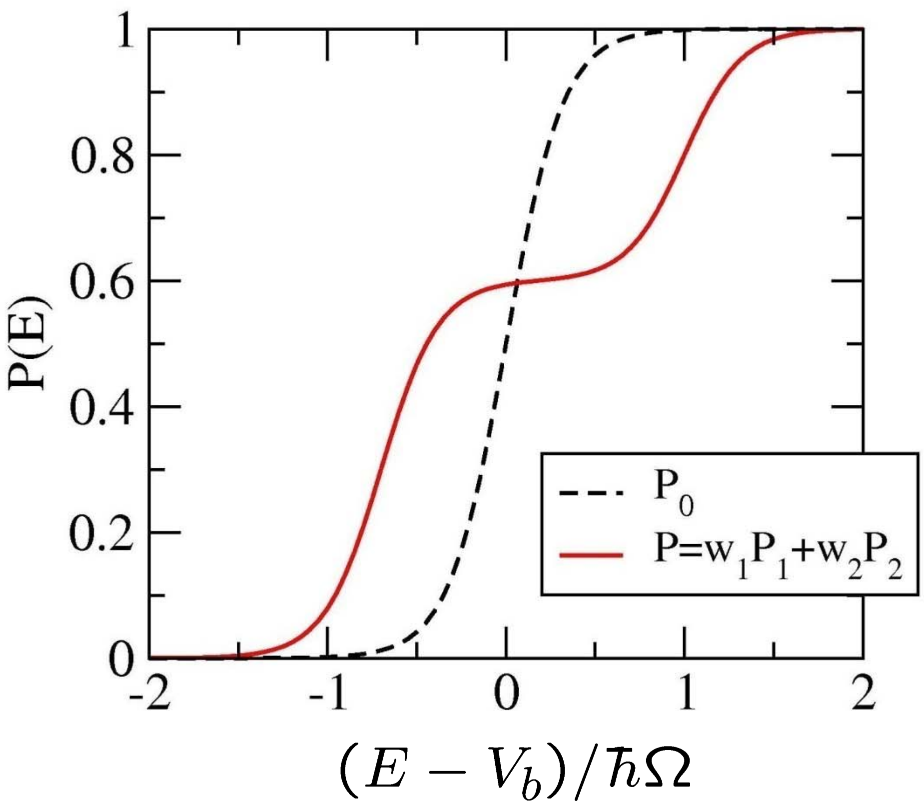

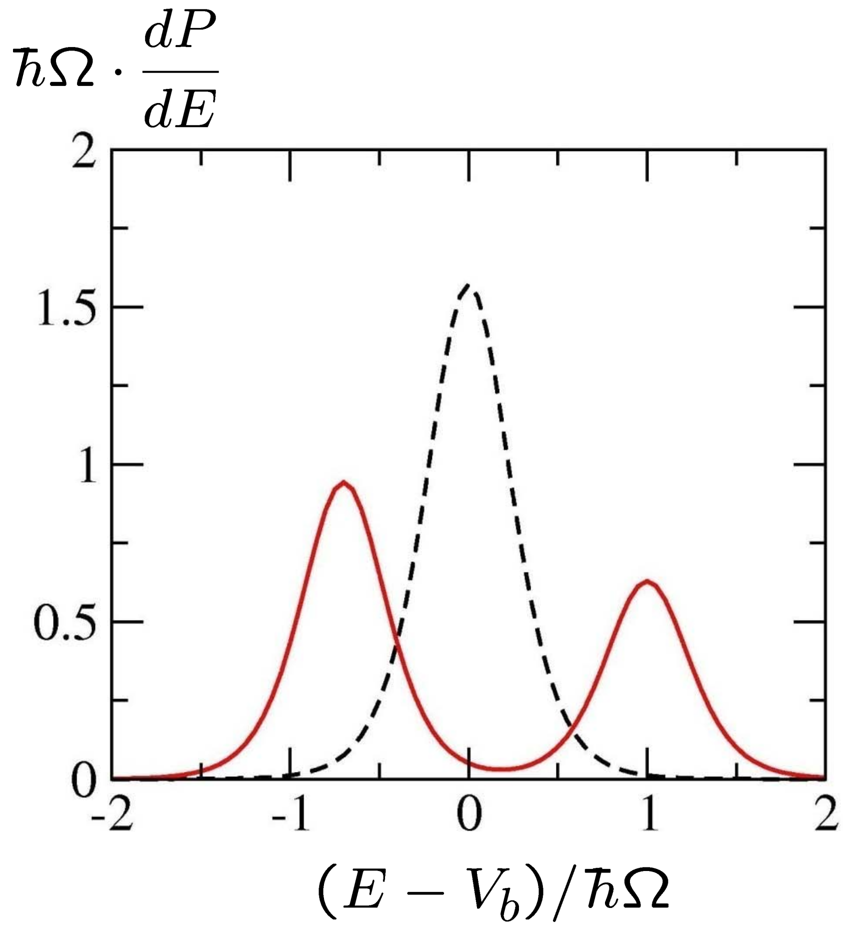

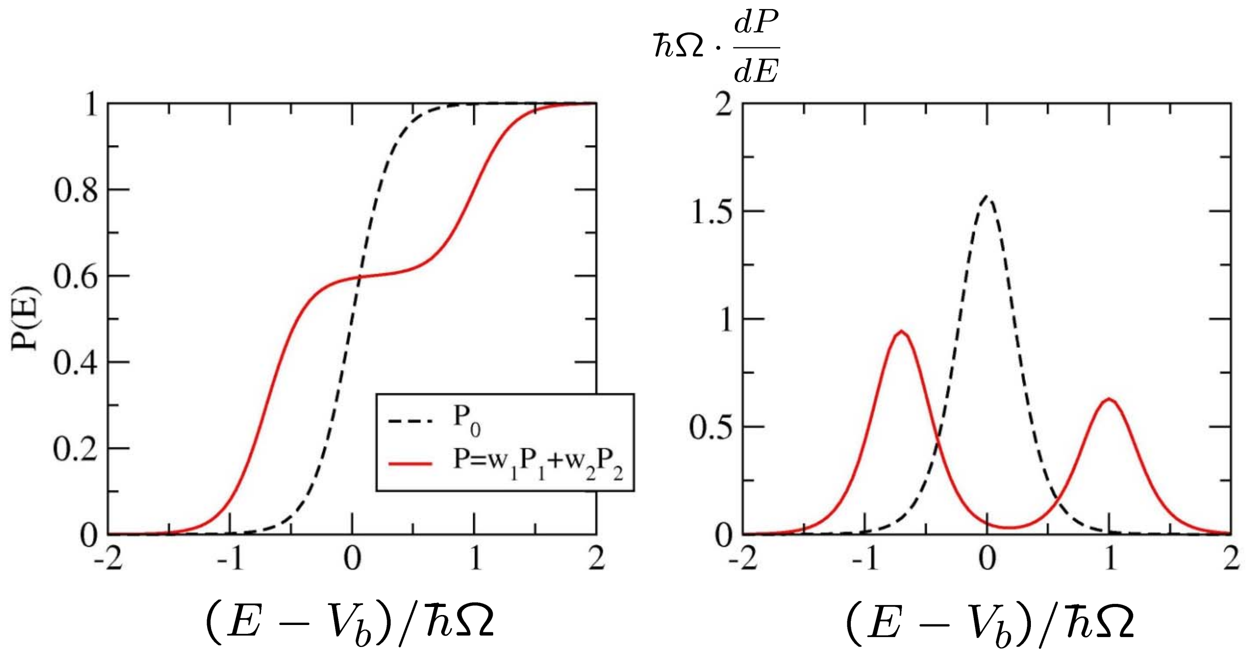

- Tunnel prob. is enhanced at $E < V_b$ and hindered $E > V_b$
- dP/dE splits to two peaks → "barrier distribution"
- The peak positions of dP/dE correspond to each barrier height
- The height of each peak is proportional to the weight factor

$$
\begin{aligned}
P(E) &= w_1 P_1(E) + w_2 P_2(E) \\
\frac{dP}{dE} &= w_1 \frac{dP_1}{dE} + w_2 \frac{dP_2}{dE}
\end{aligned}
$$

Hamiltonian (example 2): in case with off-diagonal components

$$H = -\frac{\hbar^2}{2m}\frac{d^2}{dx^2} + V_0(x) + \hat{\sigma}_x \cdot F(x) \qquad \hat{\sigma}_x = \begin{pmatrix} 0 & 1 \\ 1 & 0 \end{pmatrix}$$

$$\boxed{\begin{aligned} [\hat{t} + V_0(x)]\psi_1(x) + F(x)\psi_2(x) = E\psi_1(x) \\ [\hat{t} + V_0(x)]\psi_2(x) + F(x)\psi_1(x) = E\psi_2(x) \end{aligned}}$$

$$\phi_\pm(x) = [\psi_1(x) \pm \psi_2(x)]/\sqrt{2}$$

$$[\hat{t} + V_0(x) \pm F(x)]\phi_\pm(x) = E\phi_\pm(x)$$

If spin-up at the beginning of the reaction

$$\boxed{P(E) = \frac{1}{2}[P(E; V_0 + F) + P(E; V_0 - F)]}$$

核融合反応断面積を用いた標式

$$P_{l=0}(E) \simeq \frac{1}{\pi R_b^2} \cdot \frac{d(E\sigma_{\rm fus})}{dE}$$

$$\boxed{D_{\rm fus}(E) \equiv \frac{d^2(E\sigma_{\rm fus})}{dE^2} \simeq \pi R_b^2 \frac{dP_{l=0}}{dE}}$$

（核融合障壁分布）

N. Rowley, G.R. Satchler,
P.H. Stelson, PLB254('91)25

(note) 古典的な核融合反応断面積

$$\sigma_{\rm fus}^{cl}(E) = \pi R_b^2 \left(1 - \frac{V_b}{E}\right)\theta(E - V_b)$$

$$\frac{d}{dE}[E\sigma_{\rm fus}^{cl}(E)] = \pi R_b^2\,\theta(E-V_b) = \pi R_b^2\,P_{cl}(E)$$

$$\frac{d^2}{dE^2}[E\sigma_{\rm fus}^{cl}(E)] = \pi R_b^2\,\delta(E-V_b)$$

Fusion Test Function

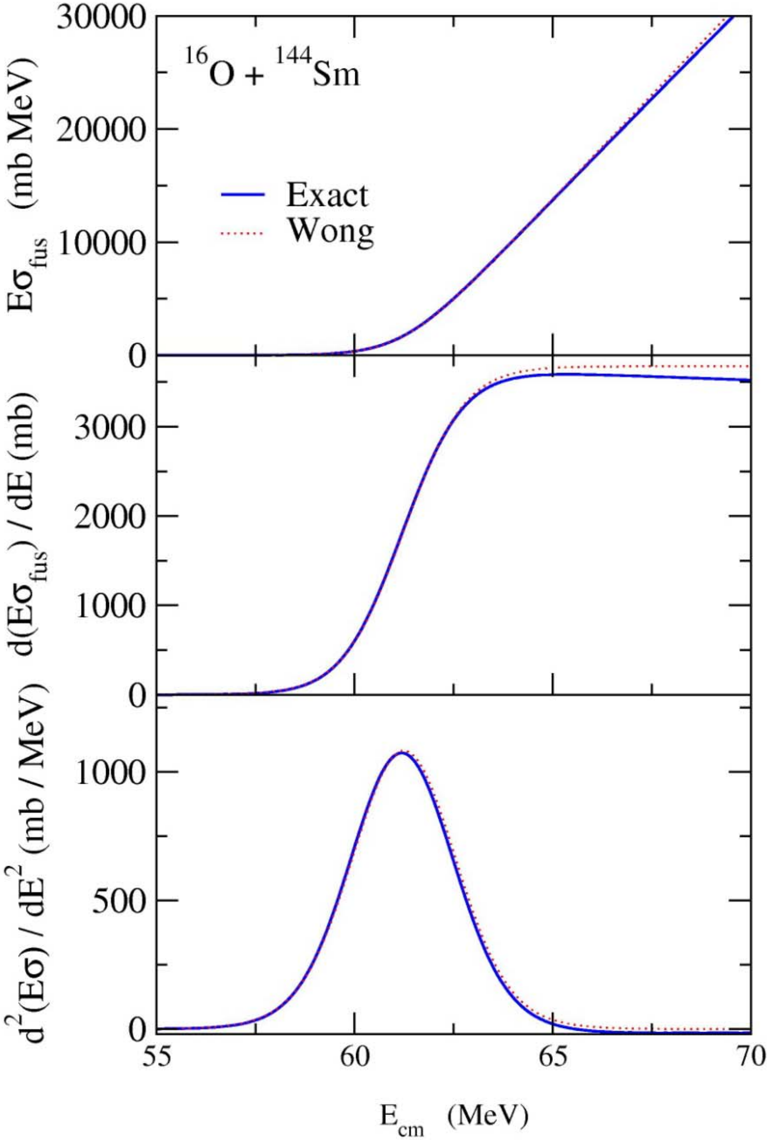

Classical fusion cross section:

$$\sigma_{\text{fus}}^{cl}(E) = \pi R_b^2 \left(1 - \frac{V_b}{E}\right) \theta(E - V_b)$$

$$\begin{aligned} \frac{d}{dE}[E\sigma_{\text{fus}}^{cl}(E)] &= \pi R_b^2\, \theta(E - V_b) \\ &= \pi R_b^2\, P_{cl}(E) \\ \frac{d^2}{dE^2}[E\sigma_{\text{fus}}^{cl}(E)] &= \pi R_b^2\, \delta(E - V_b) \end{aligned}$$

Tunneling effect

$\longrightarrow$ smears the delta function

Fusion test function:

- Symmetric around $E=V_b$
- Centered on $E=V_b$
- Its integral over E is πR_b^2
- Has a relatively narrow width $(\sim 0.56\hbar\Omega)$

障壁分布測定

核融合障壁分布 $$D_{\mathrm{fus}}(E) = \frac{d^2(E\sigma)}{dE^2}$$

2階微分をとるために非常に高精度の実験データが必要

（90年代初頭）

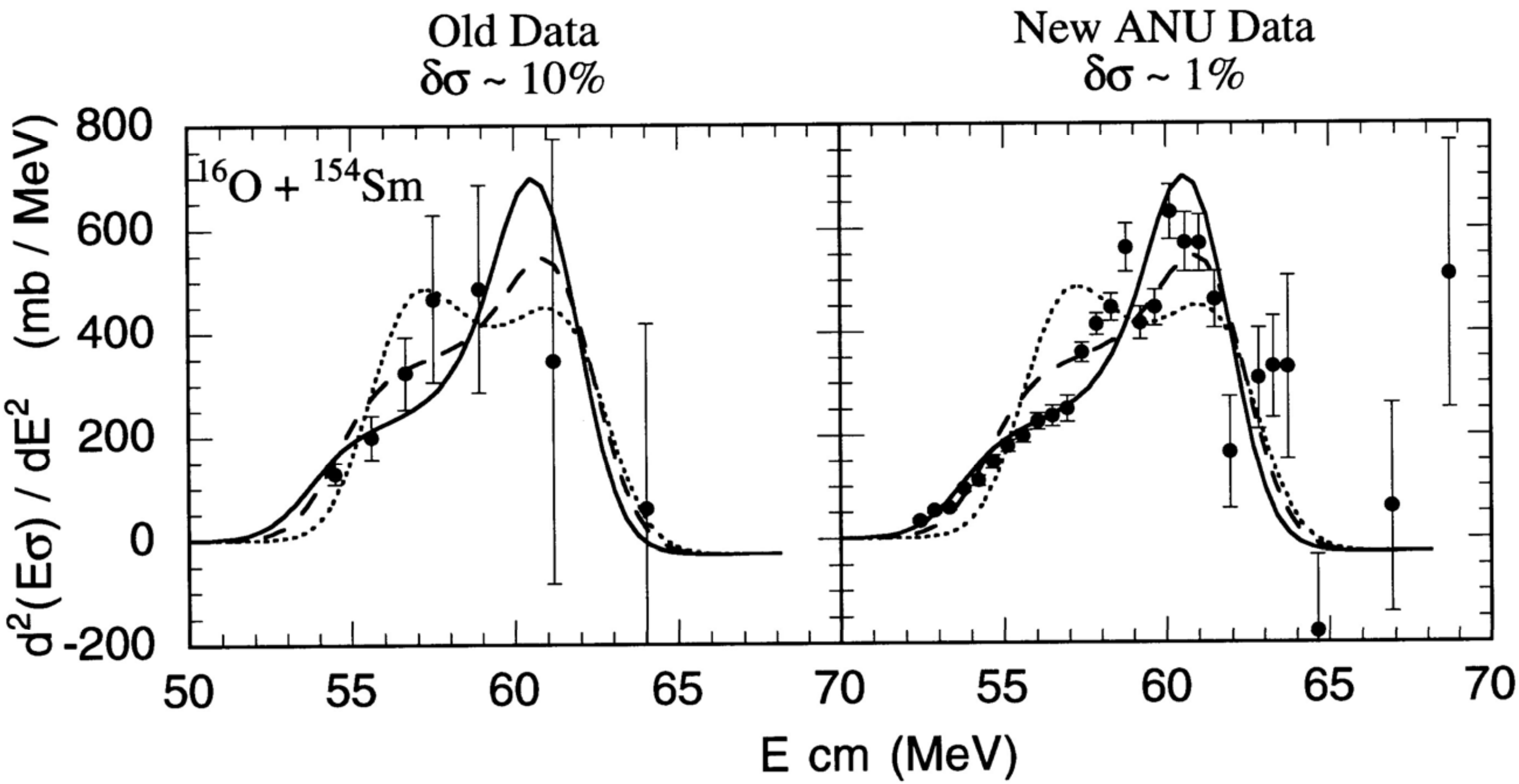

Experimental Barrier Distribution

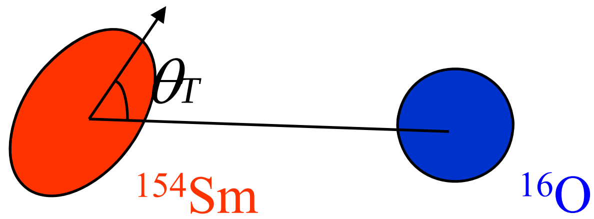

Requires high precision data

$$\sigma_{\text{fus}}(E) = \int_0^1 d(\cos\theta_T)\sigma_{\text{fus}}(E;\theta_T)$$

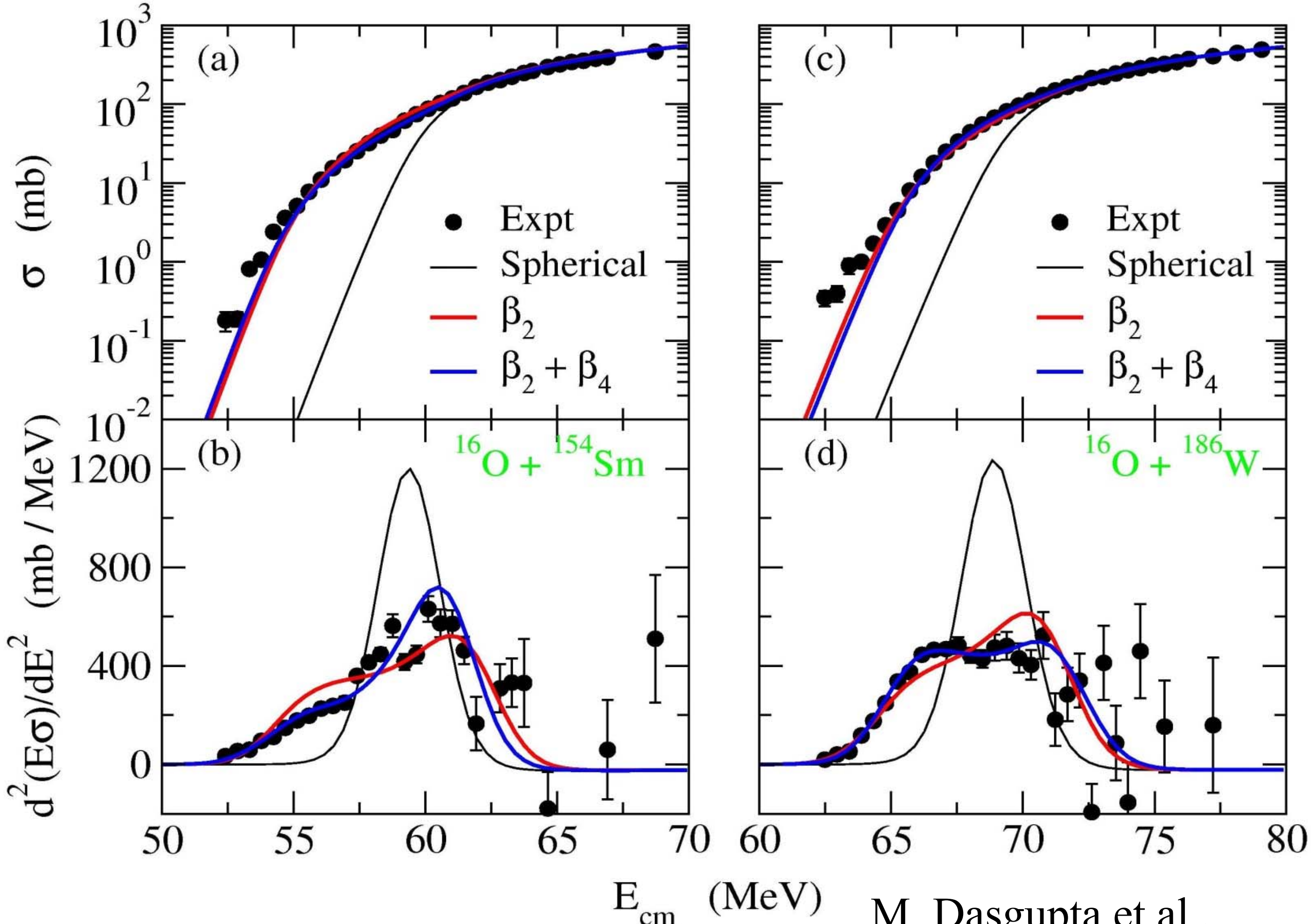

M. Dasgupta et al.,
Annu. Rev. Nucl. Part. Sci. 48('98)401

障壁分布を通じて原子核の形を視る

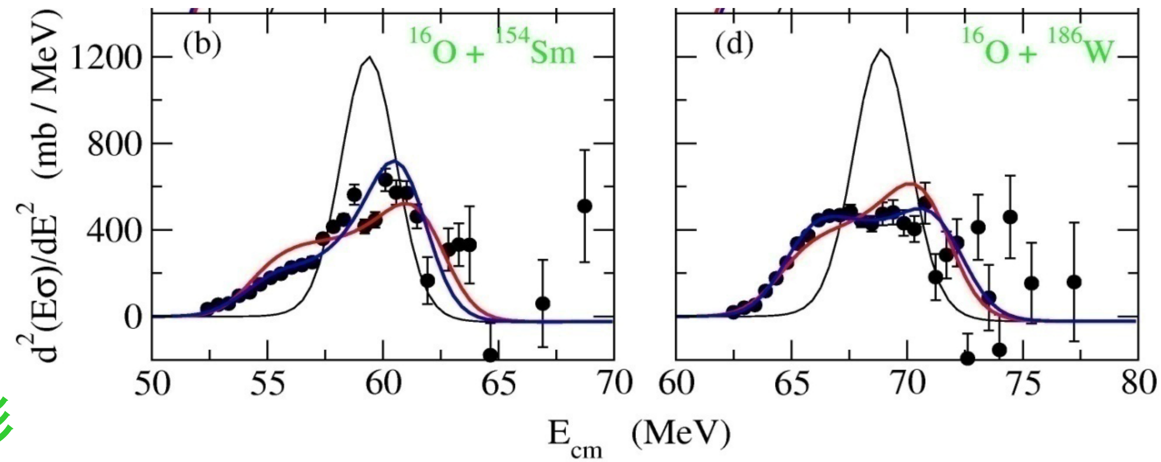

原子核の形

$$R(\theta) = R_0(1 + \beta_2 Y_{20}(\theta) + \beta_4 Y_{40}(\theta) + \cdots)$$

$$R_0 = 5.9 \text{ (fm)}, \quad \beta_2 = 0.3$$

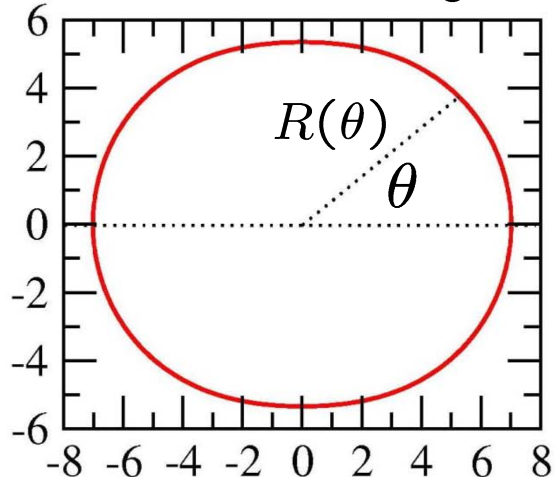

$\beta_4 = 0$

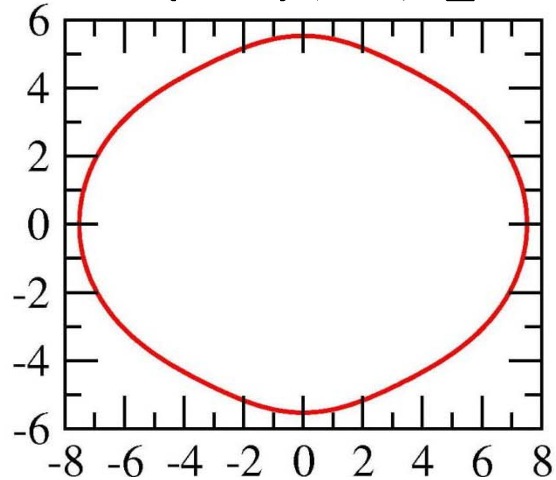

$\beta_4 = 0.1$

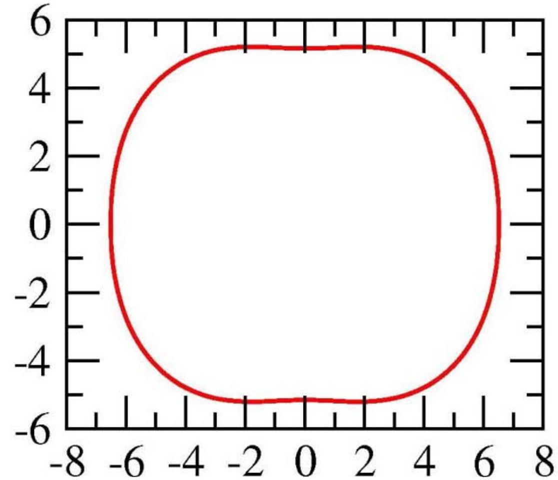

$\beta_4 = -0.1$

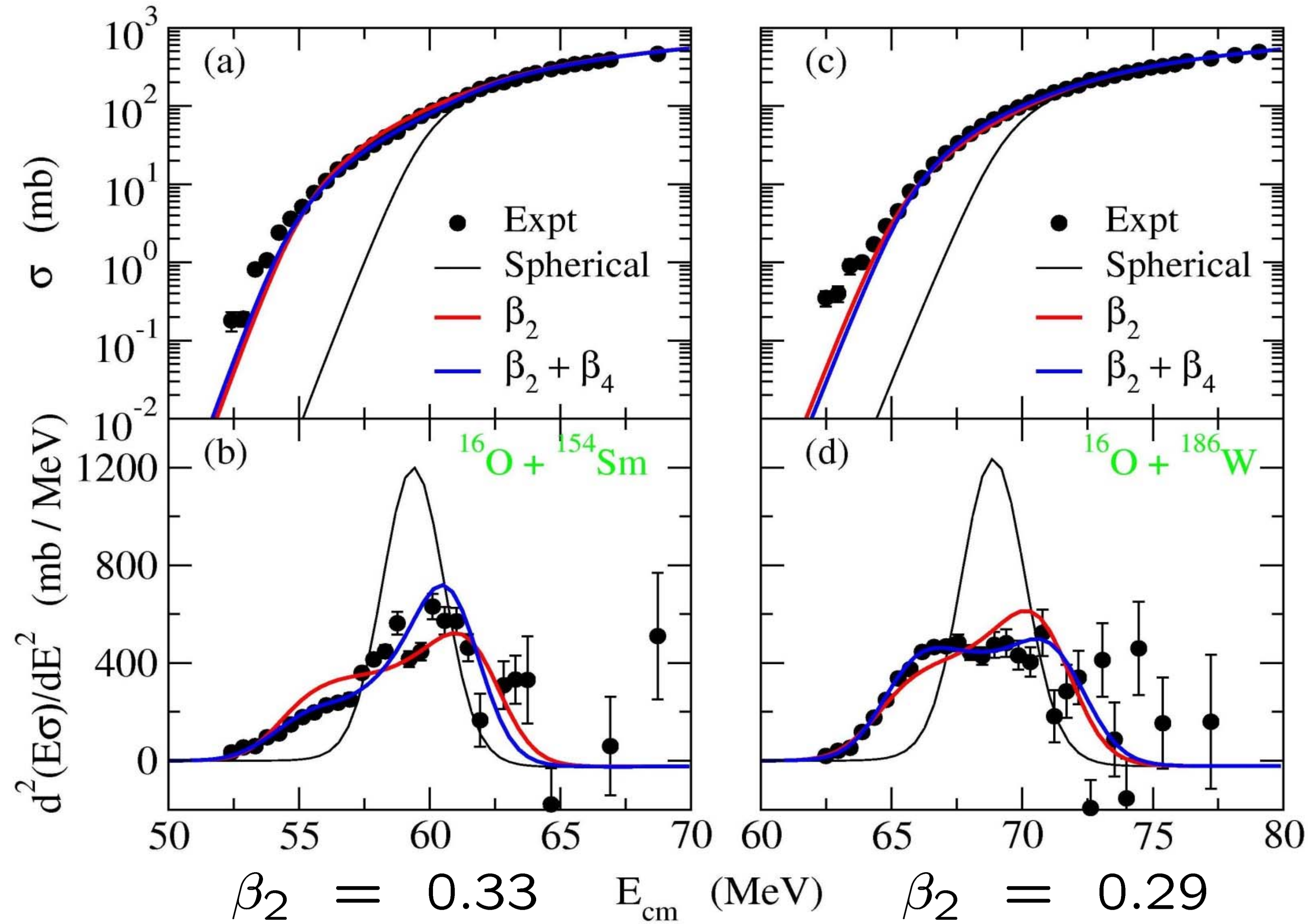

$\beta_2 = 0.33$ $\qquad$ $\beta_2 = 0.29$

$\beta_4 = +0.05$ $\qquad$ $\beta_4 = -0.03$

障壁分布をとることによって、β_4による違いがかなりはっきりと目に見える！

→ 原子核に対する量子トンネル顕微鏡としての核融合反応

Advantage of fusion barrier distribution

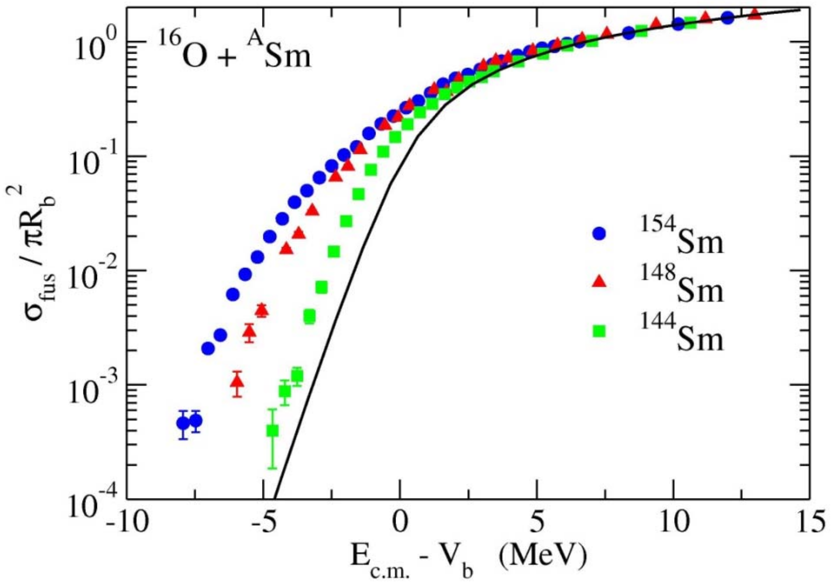

Fusion Cross sections

Very strong exponential energy dependence

Difficult to see differences due to details of nuclear structure

Plot cross sections in a different way: Fusion barrier distribution

$$\boxed{D_{\text{fus}}(E) = \frac{d^2(E\sigma)}{dE^2}}$$

N. Rowley, G.R. Satchler, P.H. Stelson, PLB254('91)25

→ Function which is sensitive to details of nuclear structure

球形振動核の例

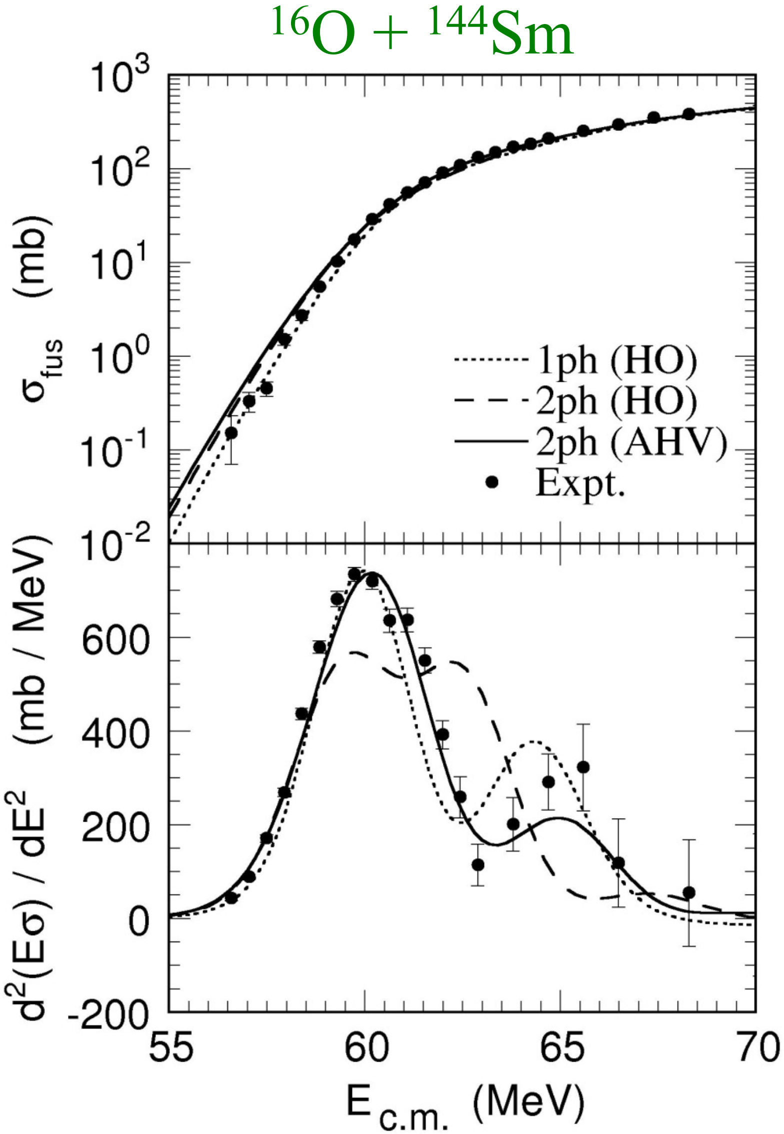

K.Hagino, N. Takigawa, and S. Kuyucak, PRL79('97)2943

Octupole 振動の非調和性

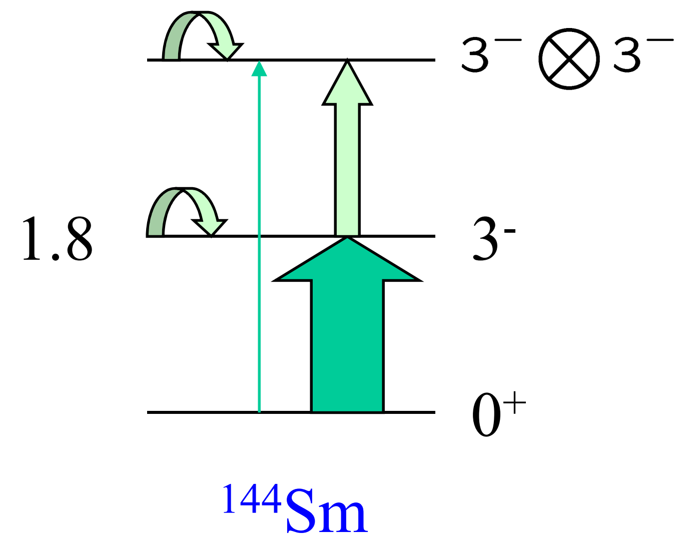

Quadrupole moment:

$$Q(3^-) = -0.70 \pm 0.02\mathrm{b}$$

Deformed Woods-Saxon model (collective model)

K.H., N. Rowley, and A.T. Kruppa,
Comp. Phys. Comm. 123('99)143

$$V_{\text{coup}}(r,\hat{O}) = V^{(N)}_{\text{coup}}(r,\hat{O}) + V^{(C)}_{\text{coup}}(r,\hat{O})$$

Nuclear coupling:

$$V^{(N)}_{\text{coup}}(r,\hat{O}) = -\frac{V_0}{1+\exp[(r-R_0-R_T\hat{O})/a]}$$

Coulomb coupling:

$$V^{(C)}_{\text{coup}}(r,\hat{O}) = \frac{3}{2\lambda+1} Z_P Z_T e^2 \frac{R_T^\lambda}{r^{\lambda+1}} \hat{O}$$

Rotational coupling: $\hat{O} = \beta Y_{20}(\theta)$

Vibrational coupling: $\hat{O} = \frac{\beta}{\sqrt{4\pi}}(a + a^\dagger)$

Vibrational coupling

$$\hat{O} = \frac{\beta}{\sqrt{4\pi}}(a + a^\dagger)$$

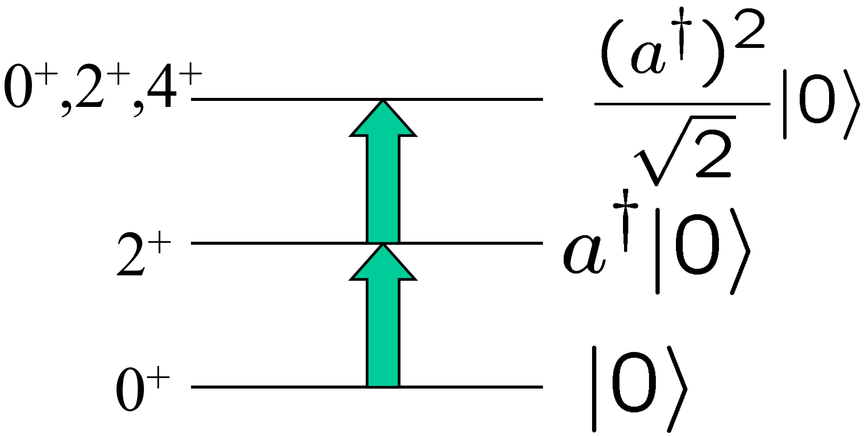

$$\begin{pmatrix} 0 & F & 0 \\ F & \epsilon & \sqrt{2}F \\ 0 & \sqrt{2}F & 2\epsilon \end{pmatrix}$$

Rotational coupling

$$\hat{O} = \beta Y_{20}(\theta)$$

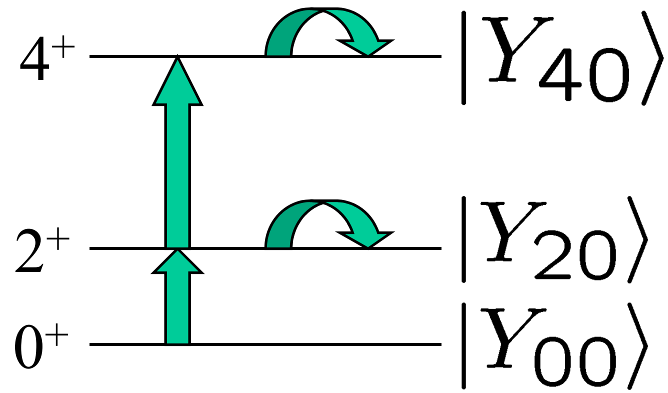

$$\begin{pmatrix} 0 & F & 0 \\ F & \epsilon + \frac{2\sqrt{5}}{7}F & \frac{6}{7}F \\ 0 & \frac{6}{7}F & \frac{10\epsilon}{3} + \frac{20\sqrt{5}}{77}F \end{pmatrix}$$

$$F = \frac{\beta}{\sqrt{4\pi}}$$

Double folding potential

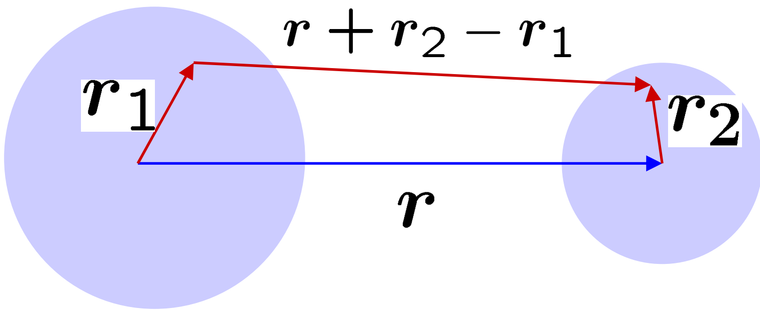

$$\boxed{\begin{aligned} V_{DF}(\boldsymbol{r}) &= \int d\boldsymbol{r}_1 d\boldsymbol{r}_2\, \rho_1(\boldsymbol{r}_1)\rho_2(\boldsymbol{r}_2) \\ &\quad \times v(\boldsymbol{r}+\boldsymbol{r}_2-\boldsymbol{r}_1) \end{aligned}}$$

cf. Michigan 3 range Yukawa (M3Y) interaction

$$\begin{aligned} v_{nn}(r) &= 7999\frac{e^{-4r}}{4r} - 2134\frac{e^{-2.5r}}{2.5r} \\ &\quad -276\,\delta(\boldsymbol{r}) \quad \text{(MeV)} \end{aligned}$$

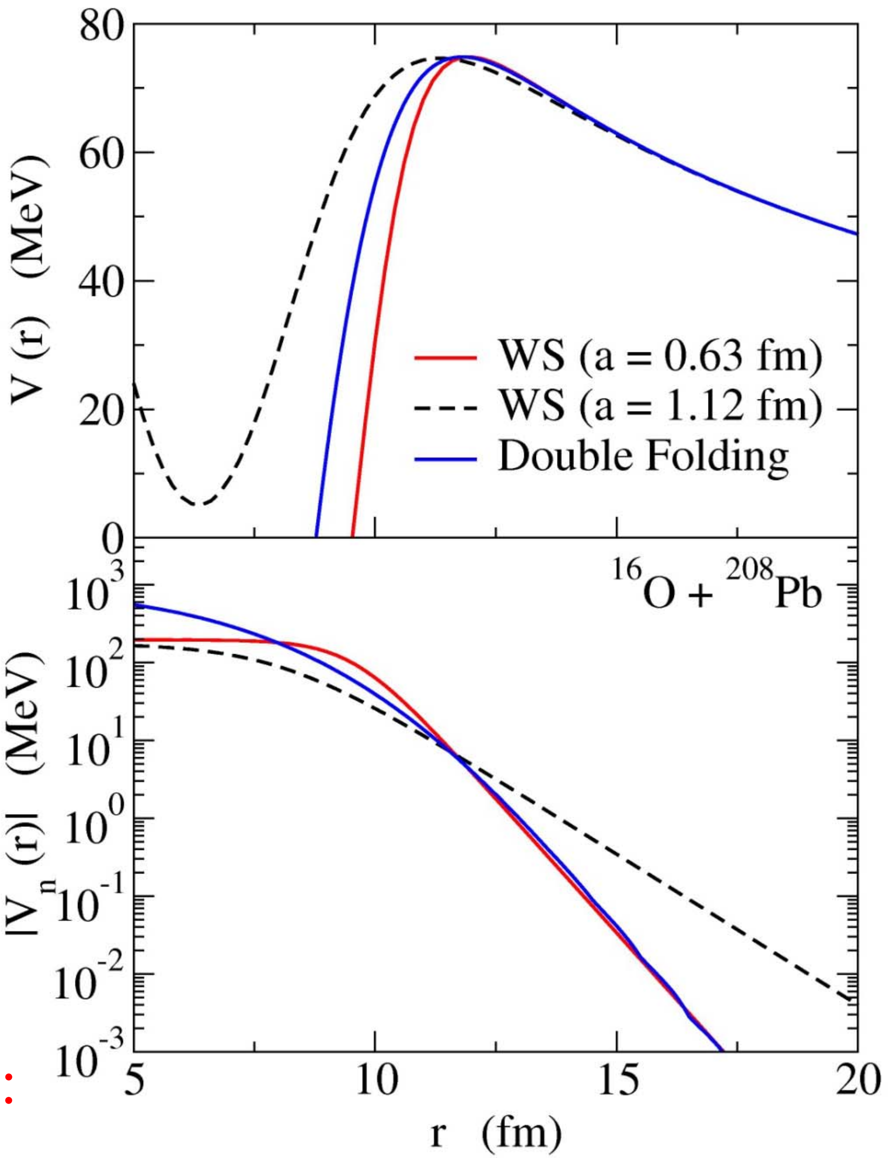

Phenomenological Woods-Saxon pot.:

$$\boxed{V_N(r) = -V_0 / [1+\exp((r-R_0)/a)]}$$